KINETICALLY MODELING TOTAL ION CHROMATOGRAMS AND EXTRACTED ION PROFILES TO IDENTIFY IGNITABLE LIQUIDS FOR FIRE DEBRIS APPLICATIONS

By

Briana Ashley Capistran

A THESIS

Submitted to
Michigan State University
in partial fulfillment for the requirements
for the degree of

Forensic Science – Master of Science

2020

ABSTRACT

KINETICALLY MODELING TOTAL ION CHROMATOGRAMS AND EXTRACTED ION PROFILES TO IDENTIFY IGNITABLE LIQUIDS FOR FIRE DEBRIS APPLICATIONS

By

Briana Ashley Capistran

Identification of ignitable liquids in fire debris samples is typically conducted *via* comparison of total ion chromatograms (TICs) of such samples to reference collections containing chromatograms of common liquids. Due to the extent of liquid evaporation in fires, reference collections often contain TICs of ignitable liquids that have been experimentally evaporated to various levels; however, such evaporations can be time intensive. A kinetic model was developed to predict evaporation rate constants of compounds as a function of GC retention index. The model can be applied to predict chromatograms of ignitable liquids at any evaporation level, alleviating the need to perform experimental evaporations. Previous work demonstrated good predictive accuracy of the model for petroleum distillate liquids and gasoline.

In this work, the kinetic model was applied to ignitable liquids of the isoparaffinic, naphthenic-paraffinic, and aromatic ASTM classes. Predicted extracted ion profiles (EIPs) were generated in addition to TICs for each liquid, and good predictive accuracy of the model was demonstrated with PPMC coefficients as high as 0.9983. Reference collections containing predicted TICs and EIPs were generated. The TICs and EIPs of single-blind samples and large-scale burn samples were compared to the reference collections; in all cases, the correct ASTM liquid class was identified. Use of the EIP reference collection for the burn samples resulted in higher correlation compared to the TIC collection due to reduced substrate interferences. Overall, this work demonstrates the utility of a kinetic model for generating predicted reference collections as a tool in the identification of ignitable liquids for fire debris applications.

ACKNOWLEDGEMENTS

First and foremost, I would like to thank my advisor, Dr. Ruth Smith, for her guidance, support, and encouragement while working on this research project. I am appreciative for all of time she has spent mentoring me, especially over the last few months. She has been incredibly supportive of me as a dual-degree student and has allowed me to grow into an independent and thoughtful scientist along the way, for which I am especially grateful. I would also like to thank Dr. Victoria McGuffin for providing thoughtful insight over the course of the project and for being such a valuable resource on the subject matter of this research and chemistry in general. I would like to thank Dr. Chris Smith for serving on my committee and for his insight on the criminal justice system in relation to my project.

I am grateful that this work was funded by the National Institute of Justice under grant number 2018-DU-BX-0225. The opinions and conclusions expressed in this work are those of the author and do not necessarily reflect the official position of the U.S. Department of Justice.

I am appreciative for all of the opportunities I have had over the course of my research career, especially for the opportunity to attend the New England Fire Investigation Seminar to collect the samples that ultimately allowed me to showcase the practical application of this project. I would like to thank those involved who were so accommodating in providing me with the assistance needed to make the experiments successful, especially Dr. Nicole Eyet and Dr. William Ryerson of Saint Anselm College, as well as Mitch Cady and John Reese of the Manchester, NH Fire Department and Andy Cox of the Bureau of Alcohol, Tobacco, Firearms and Explosives. Thank you for all the time you invested in my project and for allowing it to become part of the seminar.

Thank you to the Forensic Chemistry group members for making my time in the group so enjoyable. I would especially like to thank Amanda Setser, Hannah Clause, Becca Boyea, Emma Stuhmer, Amber Gerheart, and Otyllia Abraham for their friendship, support, and laughter that always made stressful situations better. Special thanks to Amanda Setser and Isaac Willis for preparing the blind samples that were used in this work.

I would especially like to thank Zach Capobianco for the unending amount of love and support you have shown me. Even from 800 miles away, you have managed to lift me up, encourage me, and make me laugh when I need it most. You make me a better person, and I am so blessed that you are in my life. I love you and I like you.

Finally, I would like to thank my parents, Lisa and Ray, for always supporting me in everything I have done and encouraging me to follow my heart and do what I love. Thank you for always standing by me. Special thanks to my sister, Brittany, for being my forever friend and incredible source of strength and support. The whole writing process was made better by your nightly video calls and laughter only sisters can understand, even with so many miles separating us. Lastly, to Nana, who was my biggest supporter through every chapter of my life. Though you may not be here to see me finish this chapter, you have still been with me every step of the way. This work is dedicated to you. “Lots of Love.”

TABLE OF CONTENTS

LIST OF TABLES

LIST OF FIGURES

I. Introduction

1.1 Fire Debris Analysis

Intentional fires are among the most common type of fire reported each year in the United States.[1, 2] Those intentional fires classified as arson are fires that are purposefully set with the intention of destroying property, causing harm to others, or obtaining monetary profit, among other reasons.[2, 3] Of the combined estimated 1.2 million fires reported to the U.S. Fire Administration and Federal Bureau of Investigation (FBI) in 2018, approximately 150,000 were determined to be intentional.[1, 3] According to the 2018 FBI Uniform Crime Report, intentional fires caused approximately $17,400 in damages per fire.[3] While the number of structure-related intentional fires (both residential and nonresidential) has declined over the last ten years, the number of fire-related deaths has increased.[1]

Ignitable liquids are often used in intentional fires to increase the speed and spread of the fire. In the 2018 Arson Incident Report, the Bureau of Alcohol, Tobacco, Firearms and Explosives reported that ignitable liquids were the second most common fire starter for incendiary fires.[2] Many ignitable liquids used to facilitate a fire are common products that are easily obtainable (*e.g.*, gasoline, lighter fluid, kerosene), with gasoline being the most commonly used. Because of the use of ignitable liquids for incendiary purposes, the presence of such liquids in fire debris samples could be an indication that the fire was intentionally set. Therefore, analysis of debris samples collected at the scene of a fire is important in making this determination.

1.1.1 Ignitable Liquid Classification and Identification

Ignitable liquids are divided into various classes by ASTM International according to the constituent compounds present and volatilities of the liquids. Eight classes of ignitable liquids

are defined in ASTM E1618-14, along with example products in each class (Table 1.1).[4] Within each class, liquids are characterized as light, medium, or heavy based on the corresponding carbon range. Light liquids contain compounds between $C_4 – C_9$, medium liquids contain compounds between $C_8 – C_{13}$, and heavy liquids contain compounds between $C_9 – C_{20+}$. If an ignitable liquid is determined to be present in fire debris samples, the corresponding ASTM class and carbon classification is reported. For example, according to Table 1.1, diesel fuel would be reported as a heavy petroleum distillate.

Table 1.1 Ignitable liquid classes and carbon subclasses defined in ASTM E1618-14 with example products listed for each class[4]

Class	Light ($C_4 – C_9$)	Medium ($C_8 – C_{13}$)	Heavy ($C_9 – C_{20+}$)
Gasoline	Fresh gasoline is typically in the range $C_4 – C_{12}$		
Petroleum Distillate Products	Petroleum ether Some cigarette lighter fluids	Some charcoal starters Some paint thinners	Kerosene Diesel fuel Some charcoal starters
Isoparaffinic Products	Aviation gas Some specialty solvents	Some charcoal starters Some paint thinners	Some commercial specialty solvents
Aromatic Products	Some paint and varnish removers Xylenes, toluene-based products	Some automotive parts cleaners Some insecticide vehicles	Some insecticide vehicles Industrial cleaning solvents
Naphthenic-Paraffinic Products	Cyclohexane based solvents/products	Some insecticide vehicles Some lamp oils	Some lamp oils Industrial solvents
Normal-Alkanes Products	*n*-alkane based solvents	Some candle oils Some copier toners	Some candle oils Some copier toners
Oxygenated Solvents	Alcohols Ketones Some lacquer thinners	Some industrial solvents Metal cleaners/gloss removers	N/A
Other-Miscellaneous	Single component products Some enamel reducers	Turpentine products Some blended products	Some blended products

1.1.2 Gas Chromatography-Mass Spectrometry (GC-MS) Analysis

Fire debris samples collected at fire scenes are usually packaged in paint cans and subsequently sent to forensic laboratories for analysis. At the laboratory, the samples are typically prepared *via* passive-headspace extraction followed by analysis *via* gas chromatography-mass spectrometry (GC-MS).[5] For passive-headspace extraction, an activated charcoal strip is suspended in the paint can, which is then heated, causing the volatile ignitable liquid residue (ILR) in the sample to adsorb onto the charcoal strip. The strip is then eluted with a solvent, and the resulting extract is analyzed *via* GC-MS.

Gas chromatography (GC) is a separation technique that separates compounds in a mixture according to boiling point and stationary phase interactions as the sample travels through a column.[6] In the context of ignitable liquids, the compounds in a given liquid with the highest volatilities (*i.e.*, lowest boiling points) elute from the column first, and those with lower volatilities (*i.e.*, higher boiling points) elute later. The total ion chromatogram (TIC), generated upon GC analysis, contains peaks corresponding to each compound in the mixture at corresponding retention times. Peak abundances are proportional to the concentration of compound present in the sample.[6]

The column through which the sample travels is housed inside an oven, which is typically heated according to a temperature program based on the boiling points of the sample compounds.[6] The temperature program directly affects compound retention times; thus, if different forensic laboratories use different temperature programs, compounds in the same ignitable liquid will elute at different retention times, and the TICs will not be comparable. Therefore, for the comparison of chromatograms, Kovats retention index is often used instead of retention time because it is independent of GC parameters (*e.g.*, temperature program, flow rate).[7] Retention index is a form of retention time normalization with respect to the retention

indices of normal alkanes that elute before and after an analyte. Normal alkanes have retention indices that are 100 times the corresponding carbon number. For example, *n*-hexane (C_6) and *n*-heptane (C_7) have retention indices of 600 and 700, respectively. Thus, an analyte that elutes halfway between C_6 and C_7 has a retention index of 650. To calculate retention index, an alkane ladder mixture containing consecutive normal alkanes is analyzed using the same GC program used for the sample. Retention index (I^T) is calculated for temperature-programmed conditions using Equation 1.1,[7, 8]

$$I^T = 100\left[\frac{t^T_{R,i} - t^T_{R,z}}{t^T_{R,z+1} - t^T_{R,z}} + z\right] \tag{1.1}$$

where $t^T_{R,i}$ is the retention time of the analyte, $t^T_{R,z}$ is the retention time of the normal alkane that elutes just before the analyte, $t^T_{R,z+1}$ is the retention time of the normal alkane that elutes just after the analyte, and z is the number of carbon atoms in the normal alkane that elutes before the analyte.[7, 8] The abundances for a sample are then plotted versus retention index.

Mass spectrometry (MS) is most often used as the detection method in the analysis of ILRs. Compounds in a mixture separated *via* GC elute from the column and are immediately directed to the ionization source of the mass spectrometer, in which each compound undergoes ionization and fragmentation, typically *via* electron ionization (EI).[9] This ionization technique involves bombarding sample molecules with energetic electrons to produce singly-charged fragment ions.[9] The masses and corresponding charges of the constituent fragment ions for a given compound are then detected, and the mass-to-charge (*m/z*) value for each fragment is plotted versus abundance in the resulting mass spectrum. Because the fragment ions produced using EI usually have a charge of [+1], the *m/z* axis of the mass spectrum can be read as mass.[9] The fragmentation pattern in the mass spectrum is unique to each compound under EI conditions.

Fragmentation using EI is highly reproducible, thus allowing for the development of extensive mass spectral reference libraries, which are available as tools to help with identifications. In fire debris analysis, the mass spectrum corresponding to an analyte in the chromatogram is compared to reference spectra in such mass spectral libraries to identify the compound.

In forensic laboratories, in-house reference collections are often generated and contain chromatograms of common ignitable liquids of various ASTM classes. Once the major compounds present in a sample chromatogram are identified *via* mass spectral comparisons, the chromatogram is compared to the reference collection to identify the ignitable liquid class present. However, the chromatogram of a fire debris sample often contains compounds associated with the substrate in addition to the ignitable liquid, which can interfere with liquid class identification. Extracted ion profiles (EIPs) are often generated from the TICs of debris samples to minimize these interferences. The profiles are generated for specific compound classes and only contain compounds that have mass spectral fragment ions at certain *m/z* values indicative of that class. For example, abundant ions at *m/z* 57, 71, 85, and 99 are characteristic to alkane compounds and are thus used to generate the alkane EIP.[4] The reference collections used in forensic laboratories often contain EIPs for major compound classes (*e.g.*, alkane, cycloalkane, aromatic, indane, polynuclear aromatic), to which sample EIPs can be compared to more easily identify the ignitable liquid class present, with minimal substrate interferences.

1.2 Ignitable Liquid Evaporation

Identification of ignitable liquids in fire debris samples becomes difficult if the ignitable liquid has undergone evaporation. The volatile compounds present in such liquids are highly dependent on the degree of evaporation. Compounds with high volatilities are likely to evaporate quickly under ambient conditions, and the temperature of a fire can accelerate the evaporation

process immensely. As a result, the compounds that have evaporated during a fire will not appear in the chromatogram of the debris sample, and the composition of the liquid will vary at different levels of evaporation. Therefore, the resulting chromatogram will look markedly different than that of the same unevaporated liquid (Figure 1.1).[10] The difference in chromatographic profiles becomes problematic when the chromatogram of a sample is compared to a reference collection containing chromatograms of unevaporated ignitable liquids. Even though an ignitable liquid may be present, it might not be identified due to the absence of compounds that have evaporated.

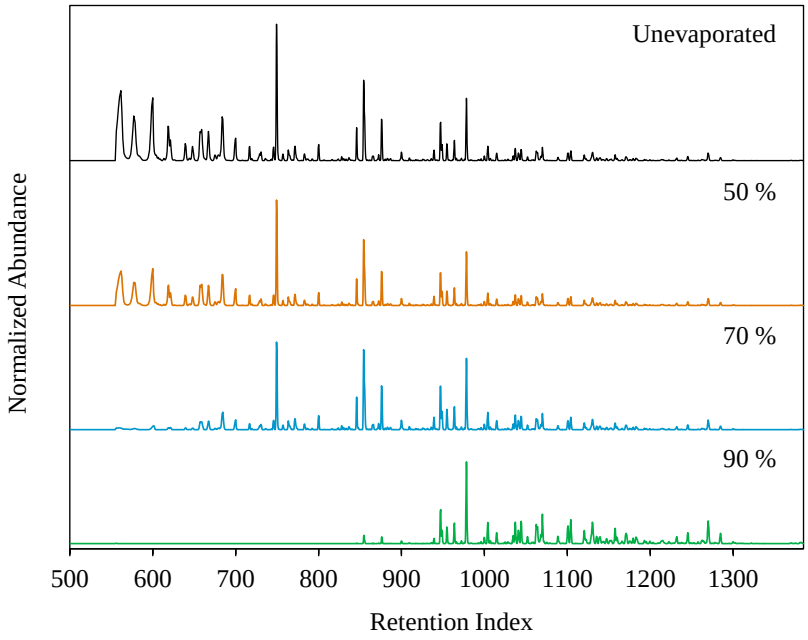

Figure 1.1 TICs of unevaporated gasoline (black) and gasoline evaporated to 50% (orange), 70% (blue), and 90% (green) evaporated by volume

To address the problem of ignitable liquid evaporation, reference collections often include chromatograms of liquids that have been evaporated to various levels. Building these collections is typically achieved by experimentally evaporating the liquids to various levels at room temperature followed by GC-MS analysis to obtain the corresponding chromatograms. While the experimental chromatograms give accurate representations of liquid compositions at

given evaporation levels, the evaporations and analyses can be time- and resource-intensive, and thus not every liquid is evaporated to every level. For example, it was previously determined that it took an average of 130 days to experimentally evaporate gasoline to 93 – 95% evaporated at room temperature.[11] Consequently, it is not ideal for a forensic laboratory to conduct these time-consuming evaporations in addition to ongoing casework.

The Ignitable Liquids Database and Reference Collection (ILRC) developed by the Technical and Scientific Working Group for Fire and Explosions (T/SWGFEX) and the National Center for Forensic Science (NCFS) is a database containing chromatograms of ignitable liquids at various evaporation levels.[12] The database serves as a reference library which can be used to search for chromatograms of ignitable liquids for comparison to the chromatogram of a fire debris sample. Ignitable liquids of the eight ASTM liquid classes were experimentally evaporated to five evaporation levels (*i.e.*, 25%, 50%, 75%, 90%, and 95%) and analyzed by GC-MS. The resulting TICs and EIPs, as well as the TICs of the unevaporated liquids, are included in the reference collection. While the collection contains chromatographic data for a vast number of ignitable liquids at different evaporation levels, it can be time consuming to search through the entire collection or a particular subclass of chromatograms. This time-intensive process highlights the need for a more efficient way to build such reference collections.

Bruno *et al.* reported a method to predict the compositions of ignitable liquids at various evaporation levels without performing actual evaporations.[13, 14] This method, known as the advanced distillation curve method, requires distillation of an ignitable liquid of interest and analysis of the distillate volume fractions at various temperatures during the distillation. For each ignitable liquid studied, the chemical composition of the distillate fractions could be used to predict the composition of the remaining liquid in the distillate flask. This composition was

comparable to corresponding compositions of the liquid at different experimental evaporation levels.[13, 14] Whereas experimental evaporations can take days or weeks, especially for heavy liquids, the distillations take only several hours, thus alleviating the need to perform time-consuming evaporations. The energy released by an ignitable liquid (proportional to liquid evaporation) can be determined by calculating the enthalpy of combustion for each distillate fraction; however, this calculation requires the identities of compounds and corresponding pure component enthalpies of combustion in each fraction to be known. Additionally, predicting the composition of liquids at low evaporation levels can be difficult due to the elevated temperatures necessary for the distillation process.

1.3 Modeling Ignitable Liquid Evaporation

To eliminate the need for experimental evaporations, mathematical models have been developed to predict the composition of volatile liquids at different evaporation levels, mainly for environmental applications. Butler developed a semi-quantitative kinetic model to predict the evaporation rate constants of normal alkanes in crude oil as a function of vapor pressure for application to the evaporation of oil residues.[15] The relationship between vapor pressure and carbon number was established for compounds of various chemical classes (*e.g.*, *n*-alkanes, branched alkanes, cycloalkanes, alkylbenzenes). Given that evaporation is proportional to the vapor pressure and fraction remaining of each compound, the corresponding evaporation rate constants were predicted.[15] Similarly, Regnier and Scott developed a kinetic model to determine the evaporation rate constants of *n*-alkanes in diesel fuel to predict the amount of fuel remaining for applications in cleaning oil spills on water.[16] The semi-empirical model was based on the vapor pressures of the compounds of interest and mathematically related vapor pressure to evaporation rate constant following experimental evaporations. Using this relationship, the vapor

pressure was used to determine the fraction remaining of a given *n*-alkane in a diesel mixture, which was then used to predict the composition of the overall mixture at various times.[16]

Whereas Regnier and Scott's model focused on predicting the evaporation of a single compound, Okamoto *et al.* developed a kinetic model to predict the total amount of bulk fuel remaining at a given time.[17, 18] The work focused on gasoline due to its high volatility that leads to significant compositional changes depending on the extent of evaporation. The vapor pressures of evaporated gasoline samples were calculated based on the weight loss of the mixture at a given time, which was then used to calculate the evaporation rate constant for gasoline. This process was repeated at various temperatures to evaluate the change in evaporation rate with increasing temperature. Based on the evaporation rate constant, the amount of gasoline vapor remaining at a given time could be calculated.[17, 18] While successful performance of the model was demonstrated, the application was geared towards gasoline evaporation in fuel spills rather than in fire debris samples.

Birks *et al.* developed a thermodynamic model to predict the weathering, or evaporation, of individual compounds in a simulated gasoline mixture for fire debris applications.[19, 20] The partial and total vapor pressures of a seven-component mixture were calculated upon varying degrees of weathering at different temperatures. Weathering was simulated by subtracting vapor losses from the original partial and total vapor pressures in a stepwise fashion, and the fractional composition of each component was calculated at each simulated weathering level. Upon experimentally weathering the simulated gasoline mixture, the model was determined to accurately predict the fractional composition of each component. Additionally, higher concentrations of volatile components (*e.g.*, toluene, ethylbenzene) were observed at higher temperatures (above 90 °C) compared to lower temperatures (*e.g.*, 25 °C). This unexpected

phenomenon was attributed to the smaller difference in vapor pressures for compounds of varying volatilities at high temperatures, which leads to more uniform evaporation at elevated temperatures.[19, 20] While the model was demonstrated to accurately predict fractional composition as a function of temperature, further work is necessary for the application to a complete gasoline mixture rather than individual components in a simulated mixture.

The models described thus far are useful to predict the evaporation of fuels and single components; however, predictions are difficult if compound identities, and thus the corresponding vapor pressures or boiling points, are unknown. To alleviate the requirement of compound-specific knowledge such as vapor pressure or boiling point, McIlroy *et al*. developed a mathematical model employing retention index (I^T) to predict evaporation rate constants for compounds in petroleum distillates.[21] Retention index, which does not require the identity of a compound to be known, was used as a substitute for boiling point due to the close relationship between the two properties.

To develop the model, diesel fuel was evaporated and analyzed by GC-MS at various time points up to 300 h. First-order decay curves were generated for individual compounds of characteristic classes within the mixture (*e.g.*, normal alkanes, branched and cycloalkanes, alkyl aromatics, polynuclear aromatics). Normalized abundances of individual compounds were plotted versus time and fit to the first-order kinetic rate equation (Equation 1.2) to determine the evaporation rate constant for the compound (Figure 1.2). For example, the evaporation rate constant determined from the first-order rate equation for the decay curve of *n*-octane was determined to be 0.226 h^{-1}. For each compound studied, the natural logarithm of the rate constant was plotted as a function of I^T (Figure 1.3). Using linear regression, the relationship between I^T and evaporation rate constant (k) was established (Equation 1.3).

$$C_t = C_0 \times \exp(-k \times t) \tag{1.2}$$

$$\ln(k) = -1.05 \times 10^{-2} I^T + 6.71 \tag{1.3}$$

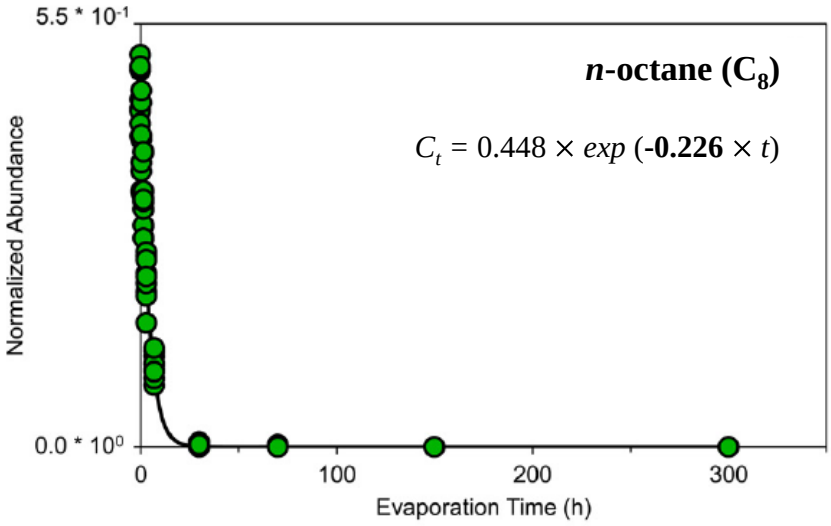

Figure 1.2 Example decay curve for *n*-octane (C_8) generated from experimentally evaporating diesel fuel, plotting the normalized chromatographic abundance versus evaporation time, and fitting the curve to a first-order rate equation[21]

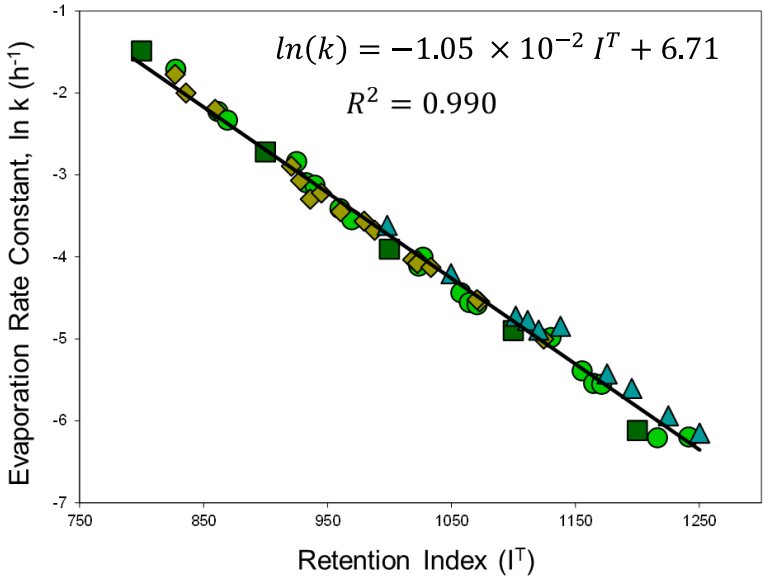

Figure 1.3 Plot of natural log of the evaporation rate constant (ln(*k*)) versus retention index (I^T) for compounds used for development of the kinetic model: *n*-alkanes (squares), branched alkanes (circles), alkylbenzenes (diamonds) and polynuclear aromatics (triangles)[21]

The first-order rate equation (Equation 1.2) was then rearranged to solve for the fractional amount of a compound present at a particular I^T (F_{I^T}) (Equation 1.4), where $C_{I,t}$ is the concentration of the compound at time t, $C_{I,0}$ is the initial concentration of the compound, k is the compound-specific evaporation rate constant, and t is time in hours.

$$F_{I^T} = \frac{C_{I,t}}{C_{I,0}} = \exp(-k \times t) \tag{1.4}$$

Solving Equation 1.3 for k and substituting this form of k into the rearranged first-order rate equation (Equation 1.4), the fraction remaining at an individual I^T can be calculated (Equation 1.5), which eliminates the need to know the identity of a given compound.

$$F_{I^T} = \exp\left(-\left(\exp\left(-1.05 \times 10^{-2} I^T + 6.71\right) \times t\right)\right) \tag{1.5}$$

For a certain fuel, plotting the fraction remaining of individual components as a function of I^T results in an S-shaped curve representing the total fraction remaining of the fuel as a function of I^T (Figure 1.4). By summing the individual fractions remaining along a given curve, the total fraction remaining (F_{Total}) of the mixture at a given time can be calculated using Equation 1.6, where F_j is the fraction of a given compound remaining and C_j is the concentration (or chromatographic abundance) of that compound.

$$F_{Total} = \frac{\sum_{j=I_i^T}^{I_f^T} F_j C_j}{\sum_{j=I_i^T}^{I_f^T} C_j} \tag{1.6}$$

Each S-shaped curve is unique to a specific fuel and time. By varying t in Equation 1.5, the curve shifts to reflect the total fraction remaining of a mixture as a function of time (Figure 1.4). The S-shaped curve corresponding to a calculated total fraction remaining of the fuel can then be multiplied by the chromatogram of the unevaporated fuel, which generates a predicted

chromatogram of the fuel at that specific F_{Total}.[22] This process can be repeated for multiple F_{Total} levels for various liquids, resulting in an extensive collection of predicted chromatograms.

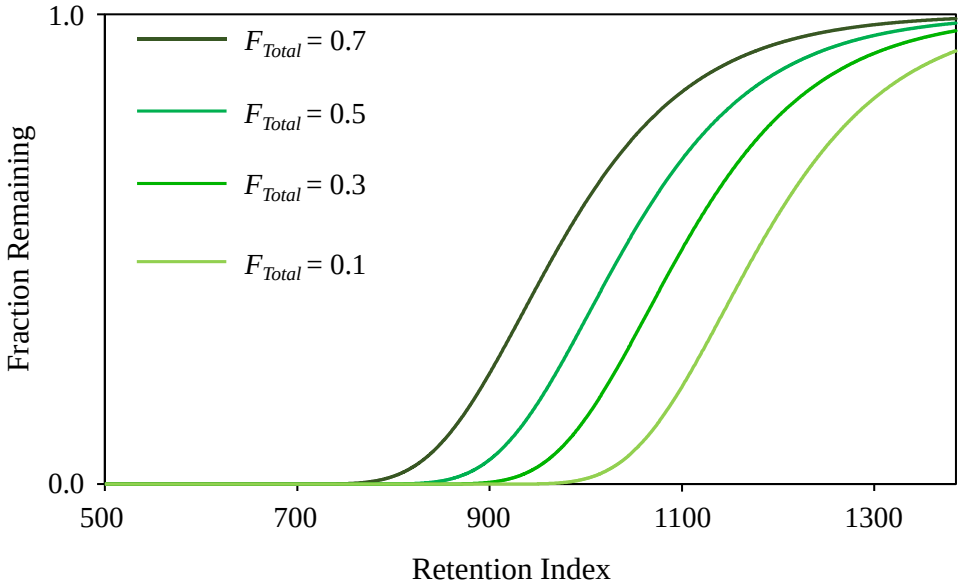

Figure 1.4 Example S-shaped curves representing the total fraction remaining of a given liquid generated by plotting the individual fraction remaining calculated at each I^T. Each curve was generated by changing t in Equation 1.5.

To determine the prediction accuracy of the model, petroleum distillates were experimentally evaporated to various F_{Total} levels, and the predicted chromatograms at such levels were generated. The corresponding experimental and predicted chromatograms were compared by calculating Pearson product-moment correlation (PPMC) coefficients (r) using Equation 1.7,

$$r_{xy} = \frac{\sum_{j=I_i^T}^{I_f^T} \left\{ \left(A_{I^T x} - \overline{A_x} \right) \left(A_{I^T y} - \overline{A_y} \right) \right\}}{\sqrt{\left\{ \left[\sum_{j=I_i^T}^{I_f^T} \left(A_{I^T x} - \overline{A_x} \right)^2 \right] \left[\sum_{j=I_i^T}^{I_f^T} \left(A_{I^T y} - \overline{A_y} \right)^2 \right] \right\}}} \tag{1.7}$$

where I_i^T and I_f^T are the initial and final retention indices of the chromatograms of interest, $A_{I^T x}$ and $A_{I^T y}$ are the individual abundances in chromatograms x and y, respectively, and $\overline{A_x}$ and $\overline{A_y}$

are the average abundance in chromatograms *x* and *y*, respectively. Coefficients greater than ± 0.8 indicate strong correlation, coefficients between $\pm 0.5 \leq r \leq \pm 0.79$ indicate moderate correlation, and coefficients less than ± 0.5 indicate weak correlation. Overall, the comparisons resulted in strong correlation, and good predictive accuracy of the model was demonstrated.[22] Based on these findings, the kinetic model is directly applicable to fire debris scenarios and is especially useful in a forensic setting when comparing chromatograms of liquids with unknown properties and evaporation levels.

While the kinetic model developed by McIlroy *et al.* was determined to perform well for petroleum distillates, limitations arose when applied for the prediction of gasoline. When used to predict chromatograms of gasoline at various F_{Total} levels, the model appeared to overestimate the extent of evaporation, resulting in decreased PPMC coefficients ($r < 0.8$) compared to those observed for petroleum distillates. Subsequent work by Eklund *et al.* focused on modifying instrument parameters for GC-MS analysis of the experimentally evaporated liquids and refining the method by which predicted chromatograms are generated.[23] Modifications to the instrumental analysis method included removal of the solvent delay and subtraction of solvent peaks in the experimental chromatograms. By removing the solvent delay from the original GC program and instead turning the detector off only during solvent elution, compounds that eluted during the delay time were detected. Background subtraction was also performed to subtract peaks associated with residual solvent or solvent impurities, neither of which were present in the predicted chromatograms.[23, 24] By performing these modifications, improvements in the prediction accuracy of the model were made.

Lastly, the method by which F_{Total} was calculated was modified to more accurately represent the fraction of liquid remaining at a given evaporation level. The F_{Total} level was

previously determined by calculating the mass loss of a liquid during evaporation, referred to as F_{Total} by mass. The calculation method was modified, and F_{Total} was instead calculated by dividing the area under the curve in the chromatogram of the experimentally evaporated liquid by the area under the chromatogram of the corresponding unevaporated liquid. This calculation method is the method by which F_{Total} is calculated in the kinetic model (Equation 1.6); thus, the calculation of the experimental F_{Total} was modified such that it was consistent with the method of F_{Total} calculation in the model. When the corresponding predicted chromatogram was modeled to this newly calculated F_{Total} level, referred to as F_{Total} by area, the prediction accuracy increased. When all three methods of optimization (*i.e.*, solvent delay, background subtraction, F_{Total} calculation) were employed, the correlation between the experimental and predicted chromatograms of gasoline improved. Specifically, in the most illustrative examples, the PPMC coefficients increased from approximately 0.7 (moderate correlation) to ≥ 0.93 (strong correlation) at F_{Total} = 0.5 and 0.3.[23, 24] Thus, the prediction accuracy of the model for gasoline was improved by modifying the instrument and prediction method parameters.

Another limitation previously mentioned in the identification of ignitable liquids in fire debris samples is the presence of substrate interferences in the sample chromatogram. Debris samples are typically submitted to a forensic laboratory as burned substrates, such as carpet, wood, cloth, or laminate. Numerous compounds present in unburned substrates, as well as those produced by thermal degradation or pyrolysis of the substrate during a fire, are similar to those present in many ignitable liquids.[25-28] As a result, corresponding compounds in the chromatogram of a fire debris sample have the potential to interfere with the compounds associated with the ignitable liquid so much so that the liquid is unidentifiable when compared to reference chromatograms. Research has been conducted to determine alternative methods for the

identification of ignitable liquids in the presence of substrate interferences, including using chemometric procedures and isotope-ratio mass spectrometry.[29-31] However, further work is necessary to assess the application of these techniques.

While EIPs are currently used to minimize substrate interferences in the identification of ignitable liquids, their inclusion in reference collections still requires evaporations of such liquids to be performed. As previously discussed, modeling the evaporation of ignitable liquids alleviates the need for time-consuming experimental evaporations and allows reference collections to be generated in a time- and cost-efficient manner. However, the application of these predicted reference collections to realistic samples in the presence of ignitable liquid evaporation and substrate interferences is still necessary. Thus, building such reference collections with demonstrated application to burn samples is an important step in advancing the field of forensic fire debris analysis.

1.4 Research Objectives

The first part of this work focuses on applying the kinetic model developed by McIlroy *et al.* to ignitable liquids of other ASTM classes (*i.e.*, isoparaffinic, naphthenic-paraffinic, and aromatic classes) to assess the predictive accuracy of the model for such liquids.[21, 22] Application to TICs of experimentally evaporated petroleum distillate and gasoline liquids was previously demonstrated.[21-24] In addition to TICs, the model will be applied to corresponding EIPs of liquids from the other ASTM classes studied to assess the ability of the model to accurately predict profiles of different chemical classes. The utility of the kinetic model to generate predicted reference collections using both TICs and EIPs is also investigated. Model validation is performed by comparing the experimental TICs and EIPs of the evaporated liquids to the

predicted reference collections to assess the utility of the collections to aid in ignitable liquid identifications.

The second part of this work focuses on demonstrating the practical application of the kinetic model for the identification of ignitable liquids in blind samples and large-scale burn samples. The utility of the TIC and EIP reference collections is investigated through comparisons of TICs and EIPs of blind samples of unknown liquid classes and evaporation levels. Practical application of the model is assessed through the collection of large-scale burn samples and subsequent comparisons of the corresponding TICs and EIPs to the reference collections. The utility of the reference collections as a tool to aid in the identification of ignitable liquid class is ultimately assessed for the large-scale burn samples. These samples, which contain ignitable liquid evaporation and substrate interferences, most closely resemble those submitted to forensic laboratories for analysis.

REFERENCES

REFERENCES

1. U.S. Fire Administration. U.S. Fire Statistics. https://www.usfa.fema.gov/data/statistics/#causesNR (accessed 05/15/20).

2. United States Bomb Data Center. *Arson Incident Report*. Technical Report for Bomb Arson Tracking System, 2018.

3. Federal Bureau of Investigation. 2018 Uniform Crime Report. (accessed 05/15/20).

4. ASTM E1618-14 Standard Test Method for Ignitable Liquid Residues in Extracts from Fire Debris Samples by Gas Chromatography-Mass Spectrometry. A. International, West Conshohocken, PA, 2014.

5. ASTM E1412-16 Standard Practice for Separation of Ignitable Liquid Residues from Fire Debris Samples by Passive Headspace Concentration with Activated Charcoal. A. International, West Conshohocken, PA, 2016.

6. D. Skoog, F. Holler and S. Crouch. Principles of Instrumental Analysis. 6th ed. Belmont, CA: Thomson Books/Cole, 2007.

7. E. Kovats, Gas-Chromatographische Charakterisierung Organischer Verbindungen. Teil 1: Retentionsindices Aliphatischer Halogenide, Alkohole, Aldehyde Und Ketone, Helv. Chim. Acta 41 (1958) 1915-1932.

8. H. Van Den Dool and P.D. Kratz, A Generalization of the Retention Index System Including Linear Temperature Programmed Gas-Liquid Partition Chromatography, J. Chromatogr. 11 (1963) 463-471.

9. E. Hoffmann and V. Stroobant. Mass Spectrometry: Principles and Applications. 3rd ed. Somerset: Wiley, 2013.

10. D.A. Turner and J.V. Goodpaster, Comparing the Effects of Weathering and Microbial Degradation on Gasoline Using Principal Components Analysis, J Forensic Sci 57 (2012) 64-9.

11. S.S. Hetzel, Survey of American (USA) Gasolines (2008), J Forensic Sci 60 Suppl 1 (2015) S197-206.

12. Ignitable Liquids Reference Collection Database [internet]. National Center for Forensic Science, University of Central Florida. [cited 04/03/20], Available from: http://ilrc.ucf.edu/.

13. T.J. Bruno, T.M. Lovestead and M.L. Huber, Prediction and Preliminary Standardization of Fire Debris Constituents with the Advanced Distillation Curve Method, J Forensic Sci 56 Suppl 1 (2011) S192-202.

14. T.J. Bruno and S. Allen, Weathering Patterns of Ignitable Liquids with the Advanced Distillation Curve Method, J. Res. Natl. Inst. Stand. Technol. 118 (2013) 29-51.

15. J.N. Butler, Evaporative Weathering of Petroleum Residues: The Age of Pelagic Tar, Mar. Chem. 3 (1975) 9-21.

16. Z.R. Regnier and B.F. Scott, Evaporation Rates of Oil Components, Environ. Sci. Technol. 9 (1975) 469-472.

17. K. Okamoto, N. Watanabe, Y. Hagimoto, K. Miwa and H. Ohtani, Changes in Evaporation Rate and Vapor Pressure of Gasoline with Progress of Evaporation, Fire Saf. J. 44 (2009) 756-763.

18. K. Okamoto, et al., Evaporation and Diffusion Behavior of Fuel Mixtures of Gasoline and Kerosene, Fire Saf. J. 49 (2012) 47-61.

19. H.L. Birks, A.R. Cochran, T.J. Williams and G.P. Jackson, The Surprising Effect of Temperature on the Weathering of Gasoline, Forensic Chem. 4 (2017) 32-40.

20. I.C. Willis, Z. Fan, J.T. Davidson and G.P. Jackson, Weathering of Ignitable Liquids at Elevated Temperatures: A Thermodynamic Model, Based on Laws of Ideal Solutions, to Predict Weathering in Structure Fires, Forensic Chem. 18 (2020) 100215.

21. J.W. McIlroy, A.D. Jones and V.L. McGuffin, Gas Chromatographic Retention Index as a Basis for Predicting Evaporation Rates of Complex Mixtures, Anal. Chim. Acta 852 (2014) 257-266.

22. R. Waddell Smith, R.J. Brehe, J.W. McIlroy and V.L. McGuffin, Mathematically Modeling Chromatograms of Evaporated Ignitable Liquids for Fire Debris Applications, Forensic Chem. 2 (2016) 37-45.

23. N.K. Eklund, B.A. Capistran, V.L. McGuffin and R. Waddell Smith, Improvements in a Kinetic-Based Model to Predict Evaporation of Gasoline, Forensic Chemistry 17 (2020) 100194.

24. N.K. Eklund, Further Investigation of a Kinetic Model to Accurately Predict Evaporation of Gasoline. Michigan State University, 2019.

25. J.J. Lentini, J.A. Dolan and C. Cherry, The Petroleum-Laced Background, J. Forensic Sci. 45 (2000) 968-989.

26. J.R. Almirall and K.G. Furton, Characterization of Background and Pyrolysis Products That May Interfere with the Forensic Analysis of Fire Debris, J. Anal. Appl. Pyrolysis 71 (2004) 51-67.

27. E. Stauffer, J.A. Dolan and R. Newman. Fire Debris Analysis. Burlington, MA: Academic Press, 2008.

28. E. Stauffer, Identification and Characterization of Interfering Products in Fire Debris Analysis. Florida International University, 2001.

29. J.M. Baerncopf, V.L. McGuffin and R. Waddell Smith, Association of Ignitable Liquid Residues to Neat Ignitable Liquids in the Presence of Matrix Interferences Using Chemometric Procedures, J Forensic Sci 56 (2011) 70-81.

30. K.R. Prather, V.L. McGuffin and R. Waddell Smith, Effect of Evaporation and Matrix Interferences on the Association of Simulated Ignitable Liquid Residues to the Corresponding Liquid Standard, Forensic Sci Int 222 (2012) 242-251.

31. Z. Schwartz, Y. An, K.I. Konstantynova and G.P. Jackson, Analysis of Household Ignitable Liquids and Their Post-Combustion Weathered Residues Using Compound-Specific Gas Chromatography-Combustion-Isotope Ratio Mass Spectrometry, Forensic Sci. Int. 233 (2013) 365-373.

II. Materials and Methods

2.1 Experimental Evaporation of Ignitable Liquids

Experimental evaporations were performed for 16 ignitable liquids representing five different ASTM classes: isoparaffinic, naphthenic-paraffinic, aromatic, petroleum distillate, and gasoline (Table 2.1). Liquids were either selected from an in-house collection or were purchased from local hardware stores. Naphthenic-paraffinic liquids were difficult to obtain; thus, only two liquids from this class were used. Petroleum distillate liquids were very common, and seven liquids of this class were used for the reference collections (five for experimental evaporations and two additional liquids for validation).

Table 2.1 Identities, brands, and carbon classifications of ignitable liquids used for experimental evaporations and model validation

ASTM Class	Ignitable Liquid (Brand)	Carbon Range & Classification
Isoparaffinic	Fabric and Upholstery Protector (ScotchGard™)	$C_5 – C_9$ (light)
Isoparaffinic	Lighter Fluid (Zippo®)	$C_5 – C_9$ (light)
Isoparaffinic	Paint Thinner (Crown®)	$C_9 – C_{13}$ (medium)
Isoparaffinic	Paint Thinner (Sunnyside)	$C_9 – C_{13}$ (medium)
Naphthenic-Paraffinic	Paint and Varnish Thinner (Sunnyside)	$C_5 – C_9$ (light)
Naphthenic-Paraffinic	Marine Fuel Stabilizer (Pennzoil®)	$C_9 – C_{14}$ (medium)
Aromatic	Adhesive Remover (Goof-Off®)	$C_5 – C_9$ (light)
Aromatic	Paint Remover (Sunnyside)	$C_5 – C_9$ (light)
Aromatic	Lacquer Thinner (Sunnyside)	$C_5 – C_9$ (light)
Aromatic	Fruit Tree Spray (Bonide®)	$C_6 – C_{10}$ (medium)
Petroleum Distillate	Charcoal Lighter Fluid (Ace)	$C_8 – C_{12}$ (medium)
Petroleum Distillate	Paint Thinner (MI KleanStrip®)	$C_8 – C_{12}$ (medium)
Petroleum Distillate	Paint Thinner (NH KleanStrip®)	$C_{11} – C_{15}$ (heavy)
Petroleum Distillate	Torch Fuel (Tiki®)	$C_{10} – C_{15}$ (heavy)
Petroleum Distillate	Lamp Oil (Medallion®)	$C_9 – C_{19}$ (heavy)
Gasoline	Gasoline (Speedway®; Jolly Rd, Lansing, MI)	$C_5 – C_{13}$

Each ignitable liquid was prepared in its unevaporated state at the start of the evaporation. The unevaporated liquid was prepared at a 1:200 dilution factor (10 μL) and

combined with an appropriate internal standard at a 1:100 dilution factor (20 μL) in a 2-mL volumetric flask. For light and most medium liquids, *n*-tetradecane (C_{14}, 0.051 M, Sigma-Aldrich, St. Louis, MO, USA) was used as the internal standard, whereas *n*-heptadecane (C_{17}, 0.020 M, Sigma Aldrich) was used as the internal standard for medium and heavy liquids with wider carbon ranges. The samples were brought to volume with dichloromethane (ACS grade, Macron Fine Chemicals, Darmstadt, Germany). Samples were divided among three amber gas chromatography (GC) vials for instrument replicates to minimize evaporation of volatile compounds.

All experimental evaporations were conducted in a 10-mL graduated cylinder. A micro stir bar was placed inside the graduated cylinder and aluminum foil was placed on top of the cylinder and a total weight was recorded. A 10 mL aliquot of the liquid being evaporated was added, and the total mass was again recorded. The cylinder was placed on a magnetic stir plate to maintain liquid homogeneity, and the liquid was then evaporated with a nitrogen line positioned above the meniscus. When the liquid reached the desired volume (5, 3, or 1 mL, corresponding to nominal F_{Total} levels of 0.5, 0.3, and 0.1, respectively), the mass of the liquid, cylinder, stir bar, and foil was again recorded. The mass of the evaporated liquid was subtracted from the mass of the liquid prior to evaporation to calculate F_{Total} by mass. The evaporated liquid was diluted to 10 mL with dichloromethane, and this solution was prepared at a 1:200 dilution factor, to which the appropriate internal standard was added (1:100). The sample was brought to volume with dichloromethane. Aliquots of the evaporated sample were divided among three amber GC vials for gas chromatography-mass spectrometry (GC-MS) analysis.

The blind samples were prepared by analysts other than the original analyst in a similar manner. The liquid identities and evaporation levels remained unknown to the original analyst.

Liquids were evaporated to pre-selected F_{Total} levels and diluted to 10 mL with dichloromethane. Each sample was then prepared for GC-MS analysis by the original analyst following the same method described above.

Retention index was determined by analyzing an alkane ladder mixture at the beginning of each instrument sequence. The mixture consisted of gasoline and diesel fuel (1:5 gasoline:diesel fuel) and was diluted 1:50 with dichloromethane (40 μL in 2 mL). Retention times for the normal alkanes from *n*-pentane (C_5) to *n*-tetracosane (C_{24}) were used to calculate retention index using Equation 1.1.

2.2 Collection, Preparation, and Analysis of Large-Scale Burn Samples

The large-scale burn samples were collected from burns conducted at the New England Fire Investigation Seminar at Saint Anselm College in Manchester, NH. Three burn cells (A – C) (2.4 m x 4.9 m) were built with lumber frames and drywall interiors. Example photographs of the burn cells are included in the Appendix. The floors were covered with olefin carpet (#563752, Lowe's Home Improvement, Bedford, NH), and the cells were fully furnished and decorated with common furniture items (*e.g.*, couch, love seat, coffee/end tables, curtains) to resemble common living spaces in an apartment. In each cell, aliquots (approximately 5 mL) of a selected ignitable liquid were poured on various parts of the floor (Figure 2.1). Paint thinner (NH KleanStrip®) was used as the ignitable liquid for burn cell A, and gasoline (Irving Oil, Hooksett, NH) was used as the ignitable liquid for burn cells B and C. The gasoline used was different from that used for the experimental evaporations and generation of the predicted reference collections.

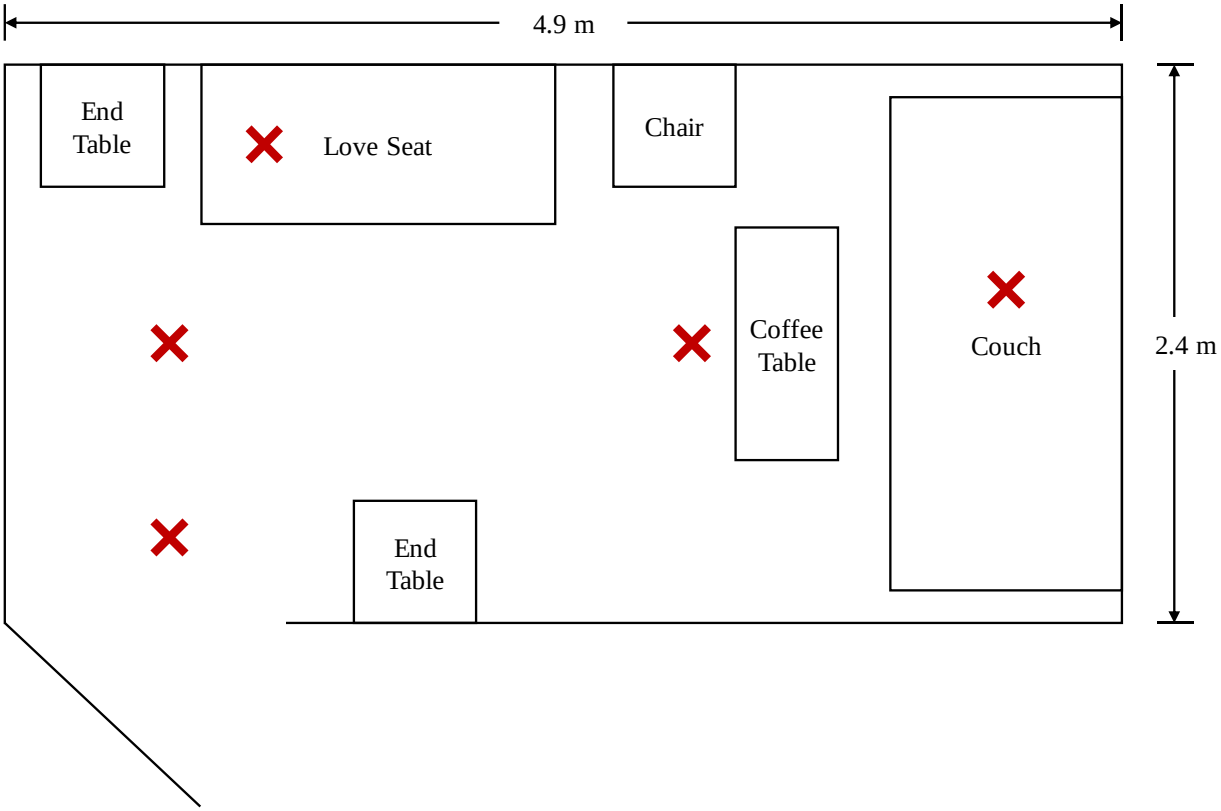

Figure 2.1 Sketch of burn cell layout (not to scale) with red x's indicating areas where ignitable liquid was poured. For marks on the love seat and couch, the liquid was poured on the floor underneath the furniture.

Following the deposition of ignitable liquids, each cell was ignited with a blow torch and allowed to burn until past flashover (approximately 10 minutes); the flames were extinguished with water. Samples of flooring where the ignitable liquids were poured were collected and stored in evidence paint cans (EVIDENT, Inc., Union Hall, VA). Floor samples were also collected in areas where ignitable liquid was not poured. Samples were analyzed following the passive-headspace extraction procedure outlined in ASTM E1412-16.[1] A third of an activated charcoal strip (Albrayco Technologies Inc., Cromwell, CT) was suspended above the debris sample in each paint can and the cans were resealed and heated in an oven at 80 °C for 4 hours. After this time, the cans were removed from the oven and allowed to reach room temperature.

For each sample, the charcoal strip was rinsed with 300 μL of dichloromethane. The internal standards listed in Section 2.1 were further diluted (1:50 v/v), and 50 μL of the appropriate internal standard was added to the samples (C_{17} was used for burn sample A and C_{14} was used for burn samples B and C). The final solutions for each sample were divided among three amber GC vials with vial inserts for instrumental analysis. Samples of the unburned carpet and wood subfloor used in the burn cells were also collected, prepared, and analyzed in the same manner as the burn samples.

2.3 GC-MS Analysis

All unevaporated liquids, evaporated liquids, blind samples, and burn samples were analyzed by GC-MS. In addition, unevaporated samples of kerosene (KleanStrip®) and diesel (Sunoco®) prepared as described in Section 2.1 were also analyzed and used for model validation. The GC-MS instrument consisted of an Agilent 6890N gas chromatograph and Agilent 5975C mass spectrometer, equipped with an Agilent 7683B autosampler (all Agilent Technologies, Santa Clara, CA). A 100% polydimethylsiloxane column (DB-1, 30-m x 0.25 mm x 0.25 μm i.d., Agilent Technologies) was used for all analyses. Ultra-high purity helium (Airgas, Independence, OH) was used as the carrier gas at a nominal flow rate of 1 mL/min. A 1-μL injection volume was used for all samples, which were injected in pulsed, splitless mode with a pulse pressure of 15 psi for 0.25 min (gas saver off). The injection port was set to 250 °C. The temperature program used for sample analysis was adapted from the program used by the National Center for Forensic Science (NCFS): initial temperature of 40 °C, hold for 3 min, ramp at 10 °C/min to 280 °C, hold for 4 min.[2] The transfer line was set to 280 °C, with the 70-eV electron ionization source set at 230 °C and the quadrupole mass analyzer at 150 °C. A scan range of *m/z* 40 – 550 was used with a scan rate of 2.86 scans/second. The detector was turned

off between 1.56 – 1.80 minutes during solvent elution. For the alkane ladder mixture, the detector was turned off between 1.58 – 1.80 minutes to allow for elution of pentane. All samples were analyzed in triplicate.

2.4 Data Analysis

Data from the GC-MS analyses were gathered using ChemStation (Enhanced ChemStation, MSD ChemStation E.01.00.237, Copyright 1989-2007, Agilent Technologies Inc.). Compound identifications, background subtraction, and extracted ion profile (EIP) generation were conducted using this software. The raw data were exported into Microsoft Excel (Microsoft Office 365, Microsoft Corporation, Redmond, WA) for further processing.

For the total ion chromatograms (TICs), background subtraction was performed to remove interferences from residual solvent and solvent impurities.[3] These interferences were present at retention times of 1.830 (dichloromethane), 2.034 (trichloromethane), 2.483 (cyclohexene), and 4.773 minutes. The mass spectrum corresponding to the compound at 4.773 minutes did not have many ions present and thus the identity could not be determined.

The EIPs were generated manually by first generating extracted ion chromatograms (EICs) for the TIC of the sample of interest in ChemStation using characteristic *m/z* values for five compound classes defined by ASTM 1618-14.[1, 4] The EICs for each compound class were generated for the following individual *m/z* values: alkane (*m/z* 57, 71, 85, 99); cycloalkane (*m/z* 55, 69, 83, 97); aromatic (*m/z* 91, 105, 119, 133); indane (*m/z* 117, 131, 145, 159); polynuclear aromatic (PNA) (*m/z* 128, 142, 156). Raw data were exported into Excel. To generate the compound class EIP, the relevant EICs were summed and normalized to the abundance of the internal standard in the TIC. Additional EIPs for blind samples and large-scale burn samples were generated using OpenChrom (Lablicate Edition 1.4.0.202004162337) using the same *m/z*

values for each compound class. The EICs were treated in the same way as described above to generate the relevant EIPs.

Retention-time alignment was performed as necessary to align peak apices in the chromatograms of evaporated liquids with those in the chromatogram of the corresponding unevaporated liquid. All alignment was conducted in Unscrambler (Version 11, Camo Analytics, Montclair, NJ). For each alignment, the chromatogram of the unevaporated liquid was used as the target, with segment sizes ranging from 5 – 10 and warp sizes ranging from 1 – 5.

2.4.1 Generation of Predicted Chromatograms

To generate the predicted chromatograms, retention indices were first calculated as described in Section 2.1 for each experimental chromatogram analyzed on the same instrument sequence. The normalized data for each unevaporated sample were truncated according to the carbon range of the liquid. For most liquids, the range used was I^T = 500 – 1385. For one medium liquid and all heavy liquids, this range was extended: marine fuel stabilizer (I^T = 500 – 1500), NH KleanStrip® paint thinner (I^T = 500 – 1685), torch fuel (I^T = 500 – 1685), and lamp oil (I^T = 500 – 2000).

The kinetic model was applied to the chromatogram of the unevaporated liquid to predict chromatograms using the corresponding F_{Total} by mass and F_{Total} by area levels for the given liquid and evaporation level. To calculate F_{Total} by area for an evaporated liquid, the area under the corresponding experimental chromatogram was divided by the area under the experimental chromatogram of the unevaporated liquid. To generate a given predicted chromatogram, t in Equation 1.5 was varied until the F_{Total} value was equal to the corresponding F_{Total} by mass or area value for the particular evaporated liquid. For a given sample, the predicted chromatogram and corresponding experimental chromatogram were compared using Pearson product-moment

correlation (PPMC) coefficients (Equation 1.7). Mean PPMC coefficients and associated standard deviations were calculated for the comparison of the experimental and predicted chromatograms at each F_{Total} level (n = 3).

APPENDIX

Figure A.1 Example burn cell built and used for large-scale burns

Figure A.2 Furnishings inside burn cell, including couches, curtains, coffee tables, and clothes

Figure A.3 Burned couch and debris inside burn cell post-burn

Figure A.4 Example sampling spots, circled in orange, from floor of burn cell B from which large-scale burn samples were collected

REFERENCES

REFERENCES

1. ASTM E1412-16 Standard Practice for Separation of Ignitable Liquid Residues from Fire Debris Samples by Passive Headspace Concentration with Activated Charcoal. ASTM International, West Conshohocken, PA, 2016.

2. Ignitable Liquids Reference Collection Database [internet]. N. C. f. F. Science, University of Central Florida. [cited 04/03/20], Available from: http://ilrc.ucf.edu/.

3. N. K. Eklund, Further Investigation of a Kinetic Model to Accurately Predict Evaporation of Gasoline. Michigan State University, 2019.

4. ASTM E1618-14 Standard Test Method for Ignitable Liquid Residues in Extracts from Fire Debris Samples by Gas Chromatography-Mass Spectrometry. ASTM International, West Conshohocken, PA, 2014.

III. Validation of a Kinetic Model to Predict Total Ion Chromatogram (TIC) Reference Collections for Ignitable Liquids from Different ASTM Classes

The chromatographic data generated by gas chromatography-mass spectrometry (GC-MS) analysis of fire debris samples are usually compared to an in-house reference collection developed in the forensic laboratory at which the analysis is performed. The kinetic model previously developed allows for similar reference collections to be generated by predicting chromatograms of ignitable liquids at various evaporation levels using only the chromatogram of the unevaporated liquid. This alleviates the need for experimental evaporations to be performed. Previous work demonstrated the performance and predictive accuracy of the model for liquids of the petroleum distillate class, and subsequent work reported improvements to the model for application to gasoline.[1-4] The work in this chapter focused on validating the predictive accuracy of the kinetic model for application to ignitable liquids of other ASTM classes, specifically the isoparaffinic, naphthenic-paraffinic, and aromatic classes. The model was then applied to generate a predicted reference collection using the total ion chromatograms (TICs) of the liquids studied. Model validation was performed by comparing the TICs of the experimentally evaporated liquids to the TIC reference collection to assess the ability to properly identify the ignitable liquid class present in the samples.

3.1 Comparison of TICs of Experimentally Evaporated Liquids to Predicted TICs

3.1.1 Isoparaffinic Liquids

Isoparaffinic liquids primarily consist of branched alkanes and some normal alkanes.[5] Four isoparaffinic liquids were investigated in this work: fabric and upholstery protector (C_5 – C_9), lighter fluid (C_5 – C_9), and two paint thinners (C_9 – C_{13}). The paint thinners were of different brands (Crown® and Sunnyside) but had similar chromatographic profiles and contained similar

compounds. Figure 3.1A illustrates the chromatogram of unevaporated lighter fluid as a representative liquid from this class. Chromatograms of the three additional unevaporated isoparaffinic liquids are included in Appendix 3A in Figures A.5 – A.16.

The majority of compounds in the lighter fluid eluted between retention indices I^T = 600 – 900 (Figure 3.1A). The compounds included branched alkanes, normal alkanes, and some cycloalkanes. Because this was a light liquid containing C_5 – C_9, the early-eluting compounds, especially those between I^T = 500 – 800, were most affected by evaporation. At F_{Total} = 0.1, compounds below I^T = 750 completely evaporated (Figure 3.1B), and peaks above I^T = 750 were significantly less abundant when compared to the chromatogram of the unevaporated liquid.

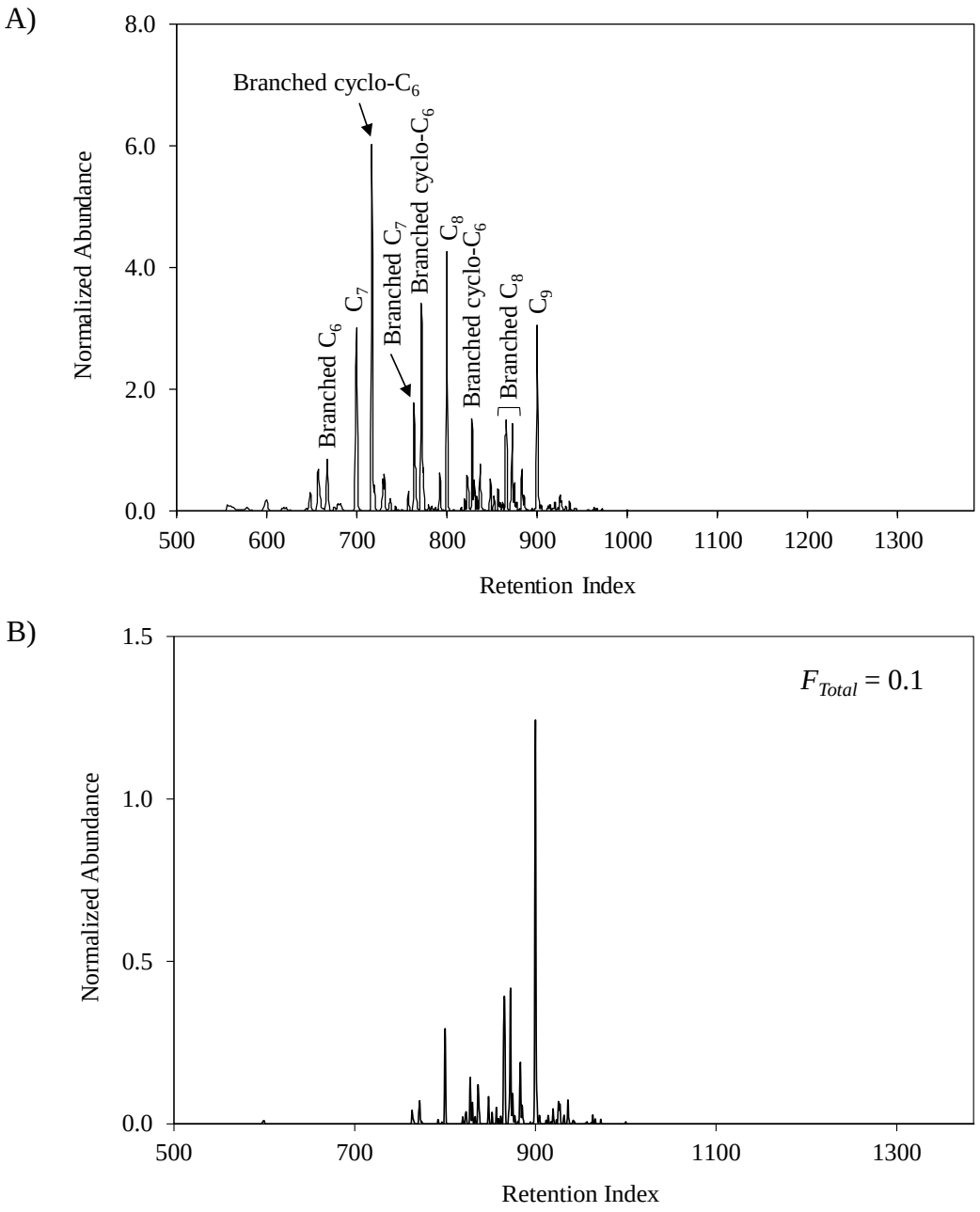

Figure 3.1 TICs of (A) unevaporated lighter fluid and (B) lighter fluid experimentally evaporated to F_{Total} = 0.1

For all four isoparaffinic liquids, comparisons between experimental and predicted chromatograms resulted in mean PPMC coefficients greater than 0.933 across all evaporation levels and for F_{Total} by mass (mass lost) and F_{Total} by area (area under the chromatogram) (Table

3.1). Coefficients above 0.99 were observed for many comparisons, including those at low F_{Total} levels. This was the case for the lighter fluid, for which a mean PPMC coefficient of 0.9914 was observed for the comparison at F_{Total} = 0.1 by area. The abundances in the predicted chromatogram agreed well with those in the experimental chromatogram (Figure 3.2). While it appeared that the model overpredicted the extent of evaporation for some compounds, this did not affect the overall correlation, evidenced by the high PPMC coefficient. The slight abundance differences were likely exaggerated by the low abundance scale. The strong correlation observed was expected given the modifications made to the prediction method in previous work, which resulted in increased correlation at low retention indices.[3, 4] As a whole, the liquids in the isoparaffinic class contained compounds of similar volatilities to those in gasoline; thus, it was reasonable that the model accurately predicted evaporations of these compounds.

Table 3.1 Mean PPMC coefficients for comparisons of experimental and predicted chromatograms of isoparaffinic liquids using F_{Total} by mass and area, as well as difference between F_{Total} by mass and area numerical values

Ignitable Liquid	Nominal F_{Total}	Mean PPMC Coefficient		$\lvert F_{Total}$ by area – F_{Total} by mass$\rvert$
		F_{Total} by Mass	F_{Total} by Area	
Fabric and Upholstery Protector *(Light)*	0.5	0.992 ± 0.004	0.994 ± 0.004	0.107 ± 0.006
	0.3	0.9932 ± 0.0004	0.9948 ± 0.0005	0.025 ± 0.003
	0.1	0.966 ± 0.003	0.960 ± 0.002	0.0338 ± 0.0006
Lighter Fluid *(Light)*	0.5	0.9887 ± 0.0009	0.995 ± 0.002	0.07 ± 0.02
	0.3	0.989 ± 0.002	0.992 ± 0.002	0.058 ± 0.006
	0.1	0.9915 ± 0.0008	0.9914 ± 0.0007	0.002 ± 0.003
Crown® Paint Thinner *(Medium)*	0.5	0.985 ± 0.003	0.986 ± 0.003	0.015 ± 0.006
	0.3	0.9915 ± 0.0002	0.9904 ± 0.0005	0.014 ± 0.005
	0.1	0.983 ± 0.003*	0.966 ± 0.005*	0.0224 ± 0.0006
Sunnyside Paint Thinner *(Medium)*	0.5	0.984 ± 0.006	0.984 ± 0.006	0.01 ± 0.02
	0.3	0.9900 ± 0.0004	0.9886 ± 0.0002	0.022 ± 0.003
	0.1	0.971 ± 0.006*	0.933 ± 0.008*	0.024 ± 0.002

*PPMC coefficients reported were calculated after retention time alignment

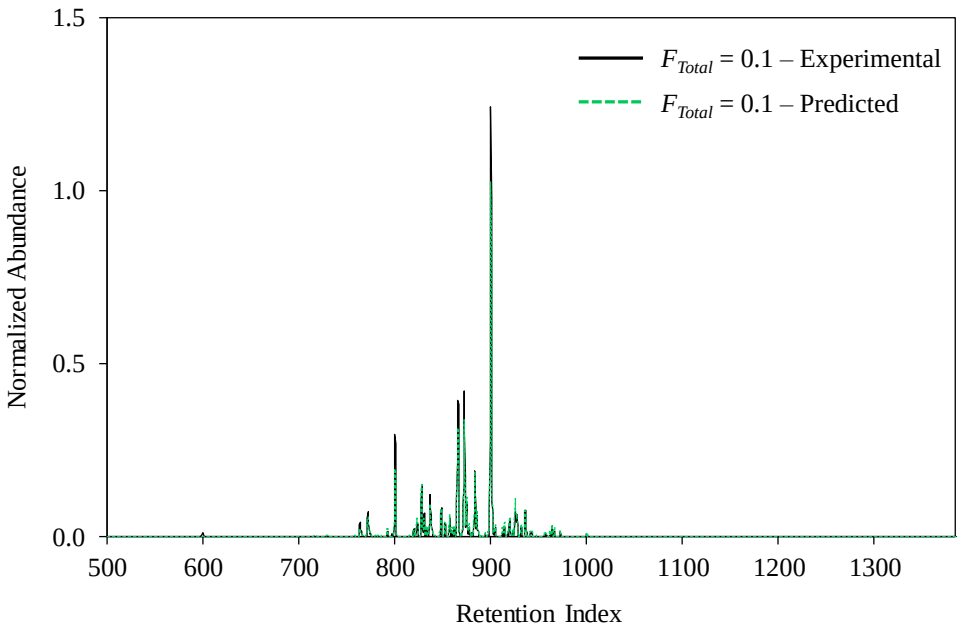

Figure 3.2 Overlay of experimental and predicted chromatograms for isoparaffinic lighter fluid at F_{Total} = 0.1. The predicted chromatogram was generated using F_{Total} by area.

The range of PPMC coefficients was generally similar irrespective of the method by which F_{Total} was calculated (Table 3.1). For the lighter fluid and fabric and upholstery protector, the PPMC coefficients were similar for all evaporation levels. Likewise, for the two paint thinners, the method of F_{Total} calculation had little effect on PPMC coefficients at F_{Total} = 0.5 and 0.3. However, at F_{Total} = 0.1, the PPMC coefficients were higher when calculated using F_{Total} by mass compared to F_{Total} by area for both liquids.

The larger difference in PPMC coefficients was due to discrepancies in peak alignment between the experimental and predicted chromatograms. Retention-time alignment for both evaporated liquid chromatograms was performed to optimize correlation. For example, improved alignment was visually noticeable in the experimental chromatogram for the Sunnyside paint thinner for peaks at I^T = 1038 and 1057, corresponding to branched C_9 and branched C_{10} compounds, respectively (Figure 3.3). Despite the improved correlation, the PPMC coefficient

after alignment for the Sunnyside paint thinner comparison using F_{Total} by area (r = 0.933) was the lowest for this class, which was attributed to the misalignment issue. While correlation was improved upon retention-time alignment, it could not be improved with further alignment without causing misalignment of other peaks.

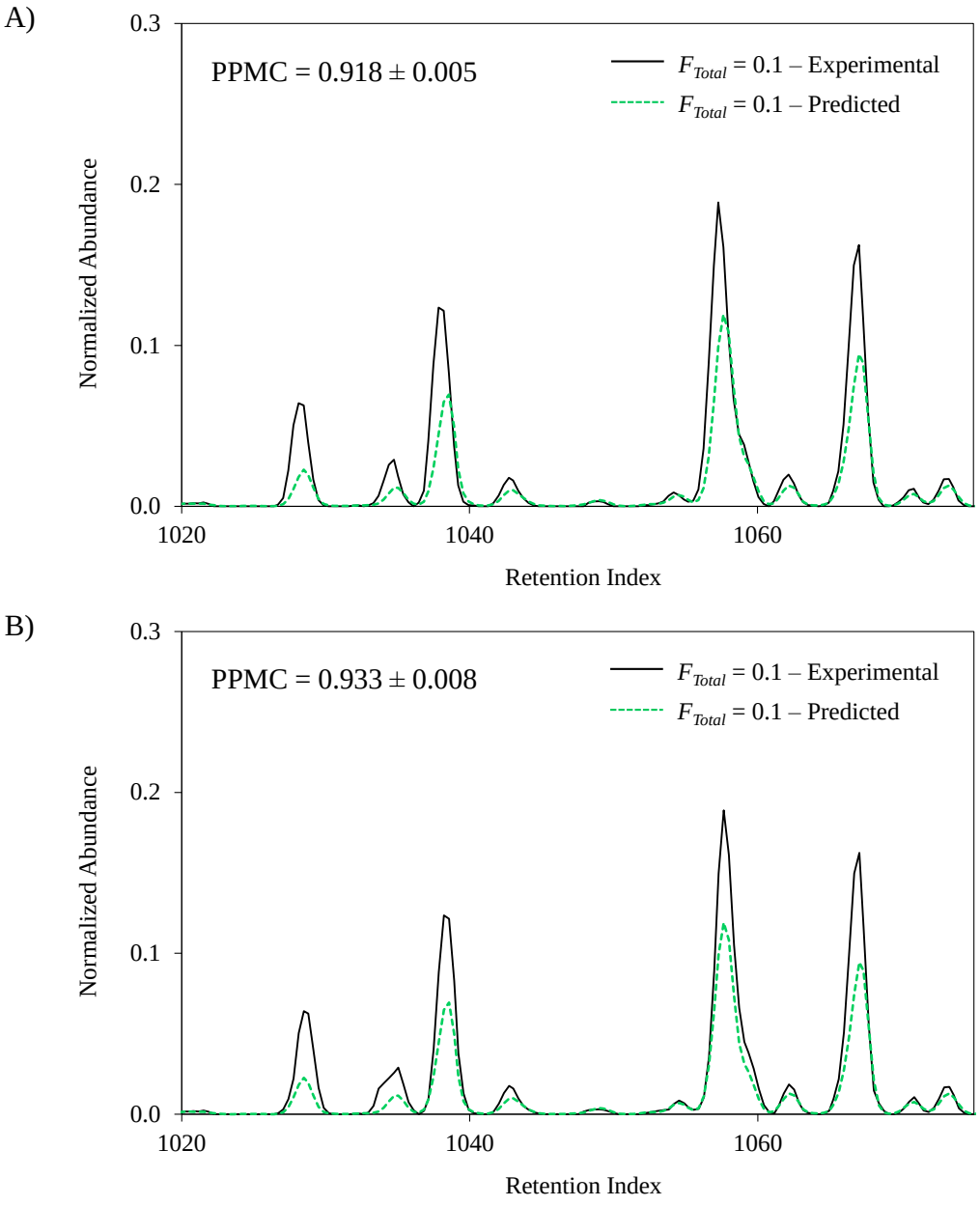

Figure 3.3 Overlays of experimental and predicted chromatograms for Sunnyside paint thinner at F_{Total} = 0.1 across the reduced range I^T = 1020 – 1075 (A) before peak alignment and (B) after peak alignment. Predicted chromatograms were generated using F_{Total} by area.

The misalignments for the Crown® and Sunnyside paint thinners at F_{Total} = 0.1 were likely due to the behavior of the samples through the GC column. For samples at low F_{Total} levels, the concentration of ignitable liquid was low due to experimental evaporation. More solvent was therefore present in these samples compared to those at higher F_{Total} levels. During splitless injections, it is common for the solvent to recondense in the column if the column temperature is below the boiling point of the solvent (by approximately 20 °C).[6-8] As the sample flows through the column, later eluting compounds with lower volatilities likely interact with the solvent until the solvent fully evaporates. Depending on the amount of solvent interactions for individual compounds, slight shifts in retention times could result. Hence, retention-time alignment served as a remedy to this problem.

The differences in the numerical F_{Total} values when calculated by mass versus area were consistent for three out of the four liquids and evaporation levels (Table 3.2, column 5). The greatest difference occurred for the fabric and upholstery protector at F_{Total} = 0.5, for which the F_{Total} by area was 0.107 greater than F_{Total} by mass. Compared to the other liquids in this class, the most abundant compounds (branched alkanes) in the fabric and upholstery protector eluted between I^T = 500 – 800, whereas compounds at I^T > 800 were present at lower abundances. The larger difference observed in F_{Total} by mass and area at F_{Total} = 0.5 was likely due to the effect of detector response factor: similar results were observed in previous work for gasoline.[3] Molar response, or sensitivity, of the mass spectrometer detector has been demonstrated to increase linearly with carbon number and exhibit a structure dependence (*e.g.*, straight-chain versus aromatic hydrocarbon).[9] For the fabric and upholstery protector, volatile compounds (I^T < 800) were more affected by evaporation than less volatile compounds (I^T > 800). However, at F_{Total} = 0.5 and 0.3, the volatile compounds were still present albeit at lower abundances. Compared to

the chromatogram of the unevaporated liquid, the abundance ratio for compounds present at these F_{Total} levels was greater in favor of compounds at higher retention indices ($I^T > 800$) that preconcentrate as the highly volatile compounds evaporate. Therefore, the area under the chromatogram was more heavily weighted by the larger proportionality constants for these lesser volatile compounds. This resulted in a larger F_{Total} by area compared to F_{Total} by mass, which does not take into account response factor.

3.1.2 Naphthenic-Paraffinic Liquids

Naphthenic-paraffinic liquids mainly consist of cycloalkanes and aromatic compounds but can also include several *n*-alkanes or branched alkanes.[5] Two naphthenic-paraffinic liquids were investigated in this work: paint and varnish thinner ($C_5 – C_9$) and marine fuel stabilizer ($C_9 – C_{14}$). The chromatogram of unevaporated marine fuel stabilizer is shown in Figure 3.4A and the chromatogram of unevaporated paint and varnish thinner is shown in Appendix 3A.

The marine fuel stabilizer consisted of substituted naphthalenes, cycloalkanes, and branched alkanes, which eluted over the range $I^T = 800 – 1500$. Because this was a medium liquid containing compounds between $C_8 – C_{15}$, the effect of evaporation was not as great as for light liquids with compounds at low retention indices ($I^T < 800$). At $F_{Total} = 0.1$, the majority of compounds that eluted at $I^T < 1200$ evaporated (Figure 3.4B) and the abundances of compounds with $I^T > 1200$ decreased when compared to those in the chromatogram of the unevaporated liquid (Figure 3.4B compared to Figure 3.4A).

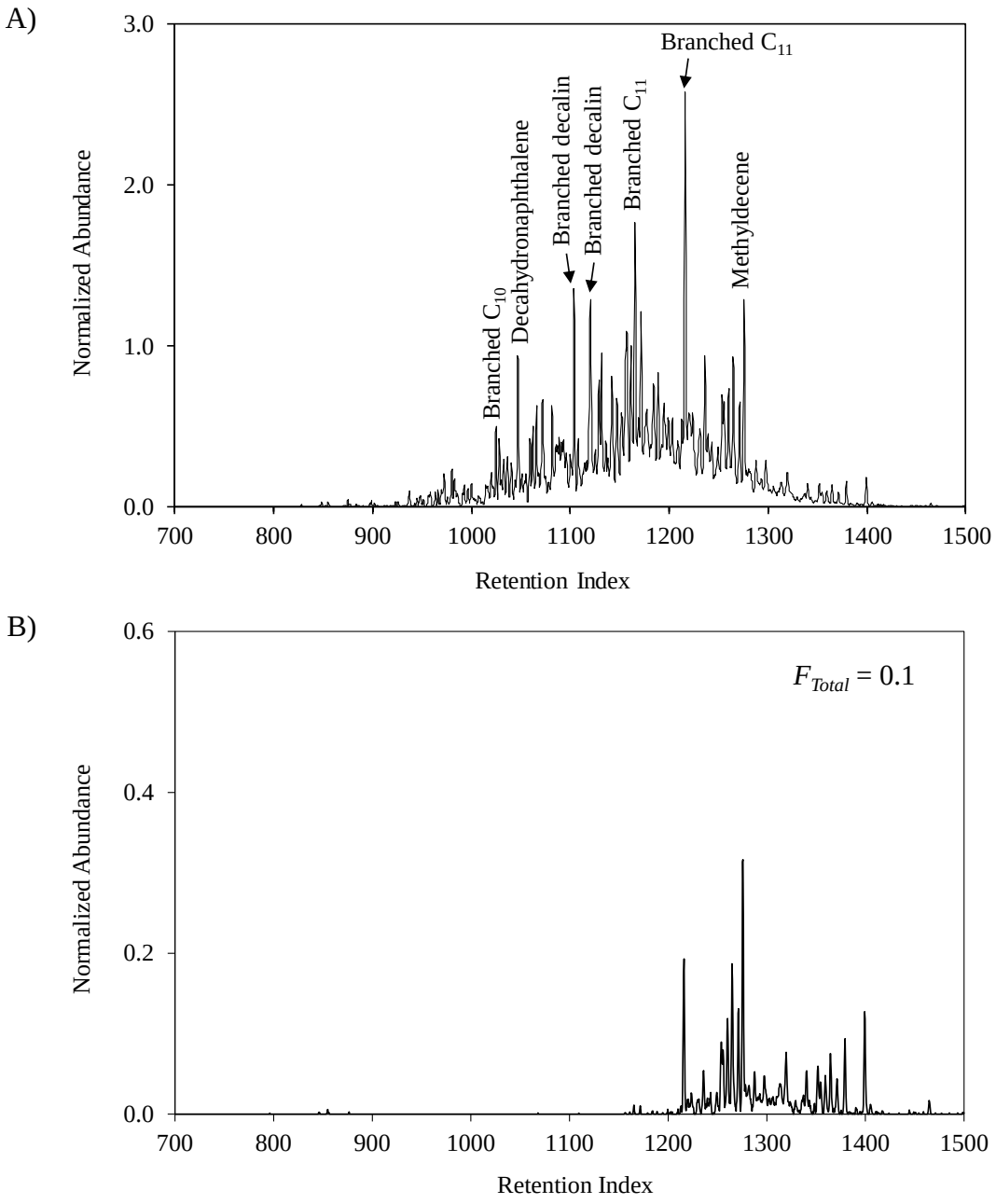

Figure 3.4 TICs of (A) unevaporated marine fuel stabilizer and (B) marine fuel stabilizer experimentally evaporated to F_{Total} = 0.1 across the reduced range I^T = 700 – 1500

In general, for the naphthenic-paraffinic class, strong correlation was observed for all liquids across all evaporation levels and for both methods of F_{Total} calculation (Table 3.2). For all comparisons, PPMC coefficients above 0.91 were observed, and for all but two comparisons,

coefficients were above 0.96. While still indicating strong correlation, the PPMC coefficients for the marine fuel stabilizer at F_{Total} = 0.1 were lower than those at F_{Total} = 0.5 and 0.3 for both methods of F_{Total} calculation. Visually, the model appeared to slightly overpredict the extent of evaporation at F_{Total} = 0.1 (Figure 3.5); however, this was likely exaggerated by the low abundance scale. The mean PPMC coefficient for this comparison (r = 0.91) still indicated strong correlation, demonstrating good predictive accuracy of the model.

Table 3.2 Mean PPMC coefficients for comparisons of experimental and predicted chromatograms of naphthenic-paraffinic liquids using F_{Total} by mass and area, as well as difference between F_{Total} by mass and area numerical values

Ignitable Liquid	**Nominal F_{Total}**	**Mean PPMC Coefficient**		**$\lvert F_{Total}$ by area – F_{Total} by mass$\rvert$**
		F_{Total} by Mass	**F_{Total} by Area**	
Paint and Varnish Thinner *(Light)*	0.5	0.99 ± 0.01	0.99 ± 0.02	0.045 ± 0.004
	0.3	0.97 ± 0.02	0.97 ± 0.02	0.036 ± 0.004
	0.1	0.974 ± 0.004	0.974 ± 0.005	0.019 ± 0.002
Marine Fuel Stabilizer *(Medium)*	0.5	0.9906 ± 0.0008	0.9947 ± 0.0003	0.027 ± 0.009
	0.3	0.981 ± 0.001	0.983 ± 0.001	0.057 ± 0.002
	0.1	0.918 ± 0.002	0.91 ± 0.01	0.048 ± 0.003

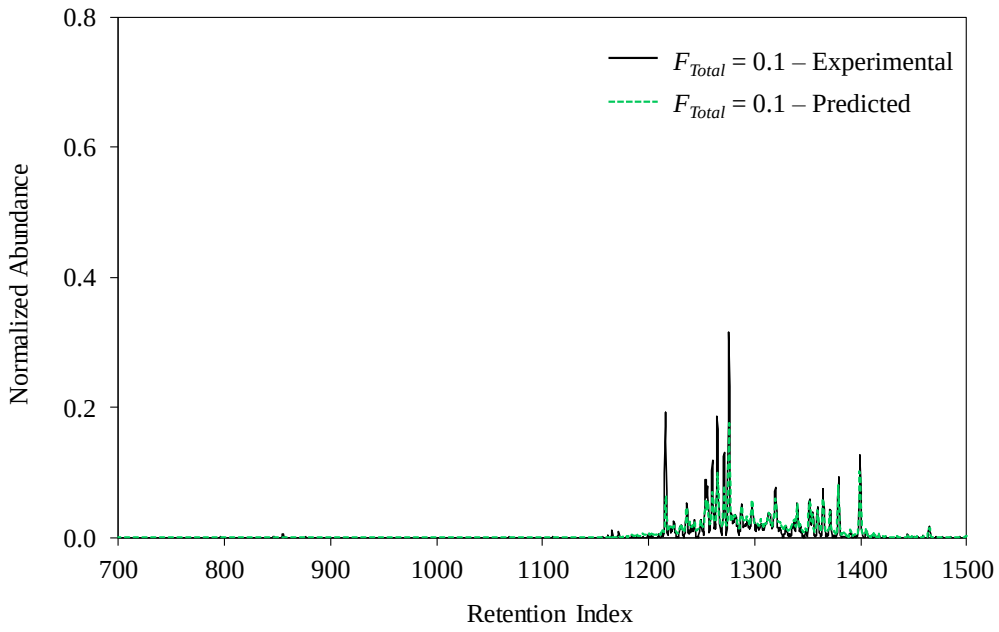

Figure 3.5 Overlay of experimental and predicted chromatograms for marine fuel stabilizer at F_{Total} = 0.1 over the reduced range I^T = 700 – 1500. The predicted chromatogram was generated using F_{Total} by area.

There were several cases where differences in PPMC coefficients were observed based on the method by which F_{Total} was calculated (Table 3.2). For example, the PPMC coefficient for the marine fuel stabilizer at F_{Total} = 0.5 increased slightly when F_{Total} by area was used. At this F_{Total}, the difference in numerical F_{Total} values was not as large compared to other liquids and evaporation levels in this class (Table 3.2, column 5). However, the F_{Total} by area value was likely a more accurate representation of the experimental chromatogram rather than F_{Total} by mass, due to the effect of the detector response factor discussed previously.

3.1.3 Aromatic Liquids

Aromatic liquids consist of aromatic compounds, mainly substituted benzenes.[5] Four aromatic liquids were studied in this work: adhesive remover (C_5 – C_9), paint remover (C_5 – C_9), lacquer thinner (C_5 – C_9), and fruit tree spray (C_6 – C_{10}). A visual example of an aromatic profile

is illustrated by the TIC of unevaporated lacquer thinner (Figure 3.6A). Chromatograms of additional unevaporated aromatic liquids are in Appendix 3A.

The lacquer thinner contained compounds between retention indices I^T = 500 – 900, and most compounds were substituted benzenes (Figure 3.6A). Two non-aromatic compounds were also present and eluted before the substituted benzenes (2-butanone and ethyl acetate at I^T = 572 and 601, respectively). Given the retention index range of the liquid, the volatile compounds were greatly affected by evaporation, especially the most volatile compounds at I^T < 800. At F_{Total} = 0.1, the abundances of all compounds decreased, especially those eluting with I^T < 800 (Figure 3.6B), when compared to the chromatogram of the unevaporated liquid (Figure 3.6B compared to Figure 3.6A)).

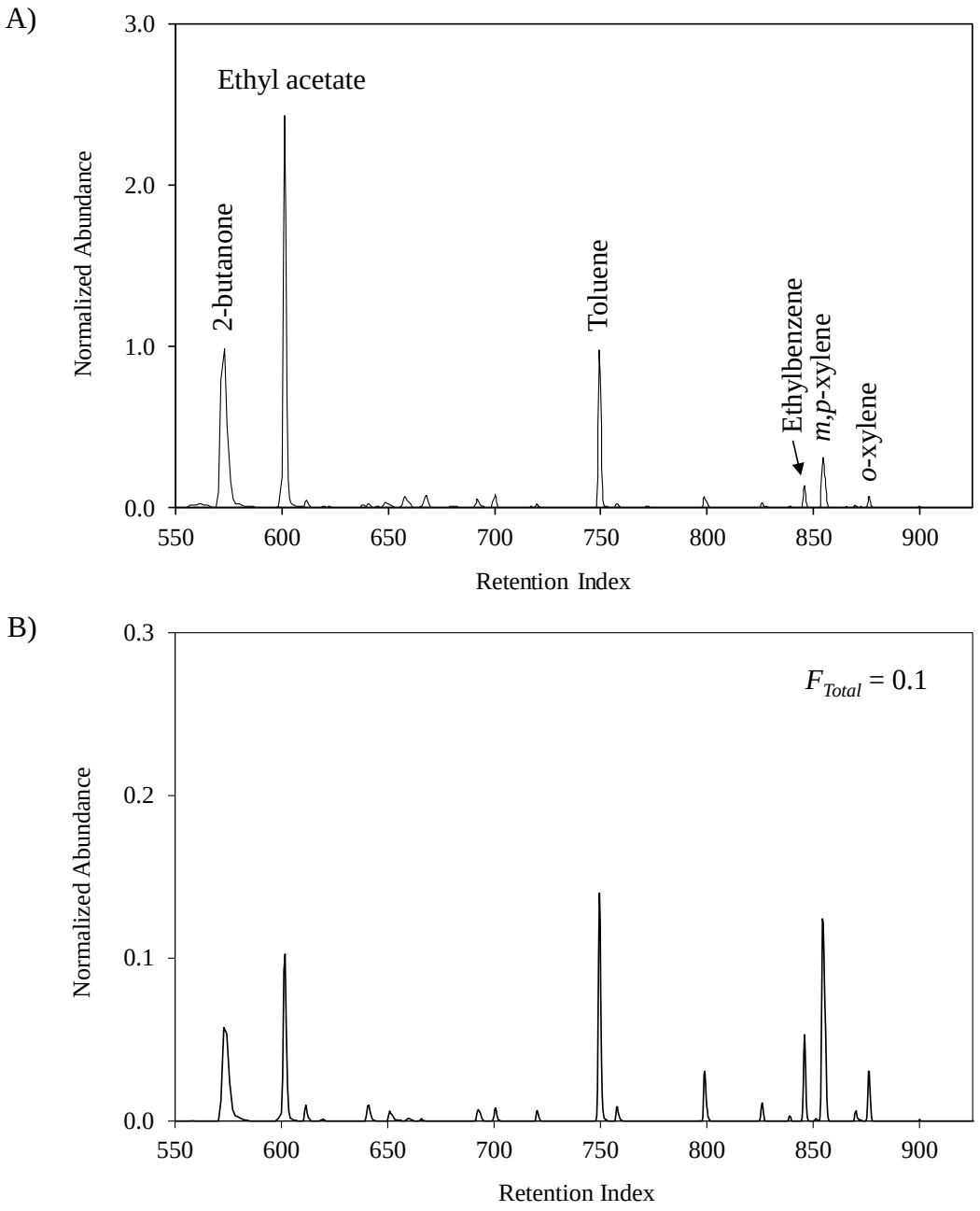

Figure 3.6 TICs of (A) unevaporated lacquer thinner and (B) lacquer thinner experimentally evaporated to F_{Total} = 0.1 across the reduced range I^T = 500 – 950

For the four aromatic liquids, comparisons of the experimental and predicted chromatograms resulted in strong correlation at each evaporation level and method of F_{Total} calculation, with the exception of the lacquer thinner at F_{Total} = 0.3 by mass (Table 3.3). The

PPMC coefficients for this class overall were lower compared to those for the isoparaffinic and naphthenic-paraffinic liquids discussed previously. In general, the aromatic liquids studied had fewer compounds present than liquids of the other classes. With fewer compounds present, differences between experimental and predicted chromatograms were less likely to occur. Conversely, because of the fewer number of compounds present, differences that did occur had a greater effect on correlation. Within the class, correlation increased when using F_{Total} by area, likely due to the detector response factor discussed previously. The aromatic compounds in these liquids were similar to those in gasoline, and the retention index ranges of the liquids fell within that of gasoline. Considering the improvements made to the prediction method when applied to gasoline in previous work, strong correlation for this class was expected.[3, 4]

Table 3.3 Mean PPMC coefficients for comparisons of experimental and predicted chromatograms of aromatic liquids using F_{Total} by mass and area, as well as difference between F_{Total} by mass and area numerical values

Ignitable Liquid	Nominal F_{Total}	Mean PPMC Coefficient		$\lvert F_{Total}$ by area – F_{Total} by mass$\rvert$
		F_{Total} by Mass	F_{Total} by Area	
Adhesive Remover *(Light)*	0.5	0.983 ± 0.007*	0.984 ± 0.007*	0.009 ± 0.006
	0.3	0.973 ± 0.001*	0.972 ± 0.001*	0.022 ± 0.002
	0.1	0.935 ± 0.005*	0.935 ± 0.005*	0.0371 ± 0.0001
Paint Remover *(Light)*	0.5	0.975 ± 0.003*	0.976 ± 0.003*	0.26 ± 0.02
	0.3	0.9678 ± 0.0005*	0.9710 ± 0.0004*	0.33 ± 0.07
	0.1	0.93 ± 0.01*	0.94 ± 0.02*	0.215 ± 0.008
Lacquer Thinner *(Light)*	0.5	0.883 ± 0.006	0.9351 ± 0.0004	0.09 ± 0.01
	0.3	0.741 ± 0.008	0.84 ± 0.01	0.081 ± 0.005
	0.1	0.864 ± 0.004	0.903 ± 0.003	0.049 ± 0.002
Fruit Tree Spray *(Medium)*	0.5	0.989 ± 0.005	0.989 ± 0.005	0.06 ± 0.02
	0.3	0.943 ± 0.008	0.944 ± 0.008	0.07 ± 0.01
	0.1	0.932 ± 0.002*	0.827 ± 0.002*	0.1429 ± 0.0002

*PPMC coefficients reported were calculated after retention time alignment

For the lacquer thinner comparison at F_{Total} = 0.3, moderate correlation was observed using F_{Total} by mass and strong correlation was observed using F_{Total} by area (Table 3.3). However, discrepancies between the experimental and predicted chromatograms were still

present when using F_{Total} by area (Figure 3.7). For 2-butanone and ethyl acetate (I^T = 572 and 601, respectively), the model overpredicted the extent of evaporation. Thus, the remaining area under the experimental ketone peaks not represented in the predicted chromatogram was distributed across the rest of the chromatogram, causing greater predicted abundances for compounds at $I^T > 740$.

The higher abundances for 2-butanone and ethyl acetate in the experimental TIC of the lacquer thinner (Figure 3.7) were due to the higher boiling points and lower vapor pressures of ketones compared to corresponding *n*-alkanes at similar retention indices (Table 3.4). Ketones experience increased hydrogen bonding forces and have greater polarities compared to alkanes, causing evaporation to occur less readily.[10] However, the retention indices of both ketones on the polydimethylsiloxane column do not accurately reflect their corresponding volatilities. The polar compounds likely elute earlier than expected due to decreased interactions with the relatively nonpolar column. To investigate further, the boiling points of *n*-alkanes $C_5 – C_9$ were plotted versus retention index and linear regression was used to predict retention indices for 2-butanone and ethyl acetate, based on their boiling points. The predicted fraction remaining at these individual retention indices (F_{IT}) was then calculated and compared to the experimentally observed values. For 2-butanone, the predicted I^T was 626 and, at a nominal F_{Total} = 0.3, the fraction remaining at this I^T was 0.204. At the same nominal F_{Total} value, the experimentally observed I^T was 572 and the corresponding fraction remaining was 0.063. For ethyl acetate, the predicted I^T was 635 and, at a nominal F_{Total} = 0.3, the fraction remaining at this I^T was 0.236. At the same nominal F_{Total} = 0.3, the experimentally observed I^T was 601 and the corresponding fraction remaining was 0.128. Thus, the misrepresentation of retention index for both ketones led to the overprediction of evaporation.

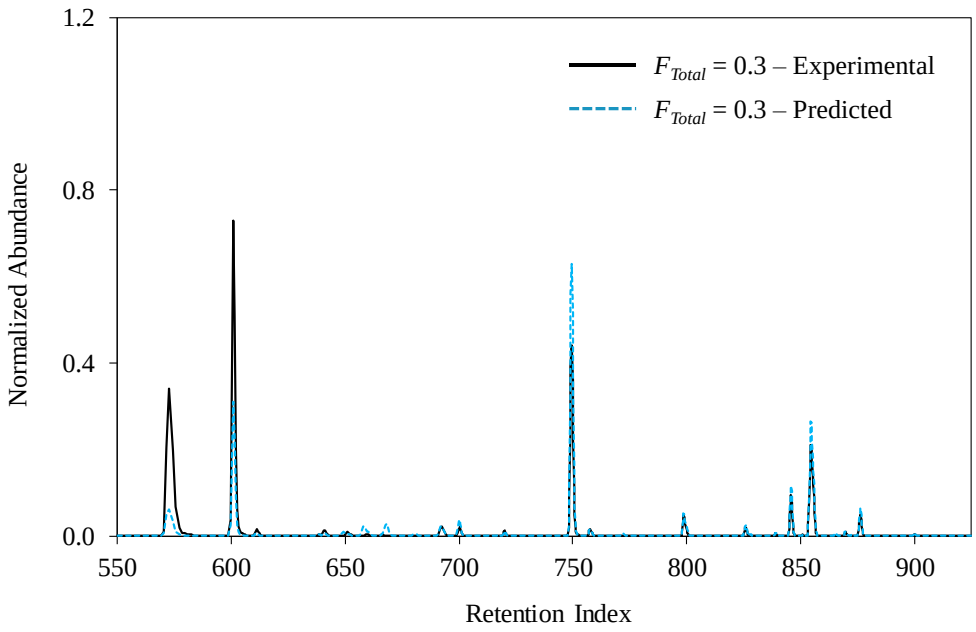

Figure 3.7 Overlay of experimental and predicted chromatograms for lacquer thinner at F_{Total} = 0.3 over the reduced range I^T = 550 – 950. The predicted chromatogram was generated using F_{Total} by area.

Table 3.4 Boiling points and vapor pressures of carbonyl-containing compounds in lacquer thinner and corresponding *n*-alkanes at similar retention indices and carbon numbers[11]

Compound	Retention Index	Boiling Point (°C)	Vapor Pressure at 25 °C (kPa)
n-pentane	500	36.1	68.3
ethyl acetate	572	77.1	12.6
n-hexane	600	68.7	20.2
2-butanone	601	79.6	12.6

The PPMC coefficient for the fruit tree spray at F_{Total} = 0.1 decreased when using F_{Total} by area compared to F_{Total} by mass. The difference in numerical F_{Total} values for this evaporation level was one of the largest across the aromatic liquids (Table 3.3, column 5). As described previously, F_{Total} by area is a better representation of the liquid; however, over- and underprediction of evaporation was present in the predicted chromatogram compared to the experimental chromatogram (Figure 3.8). The larger abundances in the experimental chromatogram between I^T = 940 – 990 were likely due to the increased detector response factor

for alkylbenzenes compared to branched and cycloalkanes.[9] The underprediction above I^T = 990 was a compensation for the overprediction below I^T = 990, similar to the lacquer thinner comparison at F_{Total} = 0.3 (Figure 3.7). Retention-time alignment was also performed for this comparison; however, complete alignment of all peaks was not achieved without causing misalignment of other peaks, which also contributed to the decreased PPMC coefficient.

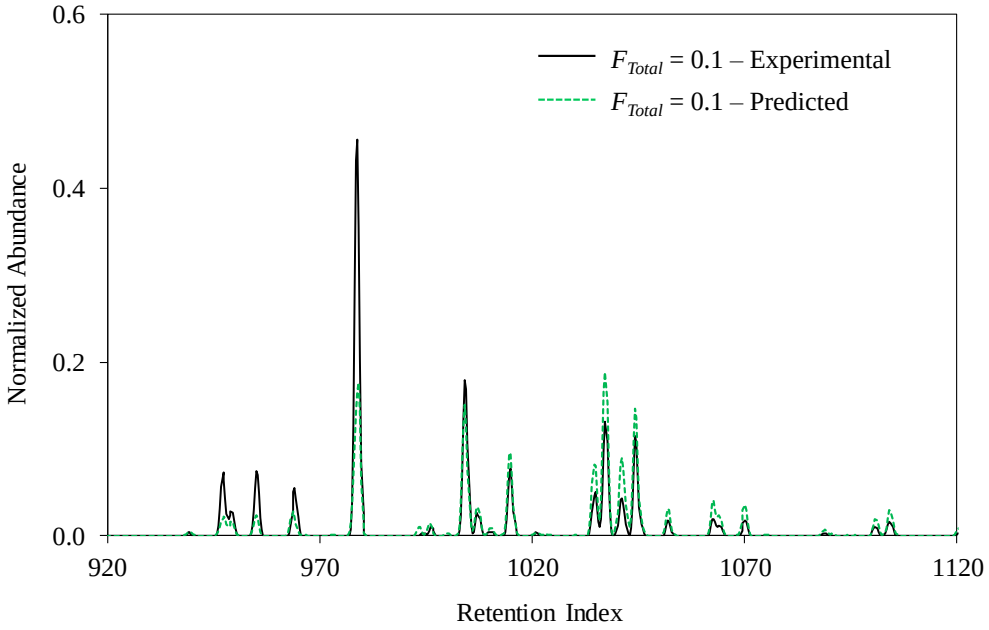

Figure 3.8 Overlay of experimental and predicted chromatograms for fruit tree spray at F_{Total} = 0.1 over the reduced range I^T = 920 – 1120. The predicted chromatogram was generated using F_{Total} by area.

In general, as evaporation level increased, the PPMC coefficients for the four aromatic liquids decreased (Table 3.3). At lower F_{Total} levels, especially F_{Total} = 0.1, peak alignment was necessary for many comparisons to optimize correlation. For example, the mean PPMC coefficient prior to retention time alignment for the adhesive remover at F_{Total} = 0.1 was 0.80; upon alignment, the mean PPMC coefficient increased to 0.935. Misalignments were likely due to the manner in which the compounds interacted with the solvent traveling through the column,

discussed previously for the isoparaffinic paint thinners. The improvement in correlation that was achieved allowed for increased confidence in predictive accuracy for this liquid class.

The largest differences in numerical F_{Total} values were observed for the paint remover at all three evaporation levels (Table 3.3, column 5). With the exception of the fruit tree spray at F_{Total} = 0.1, all other differences were below 0.09. Those associated with the paint remover were similar to F_{Total} differences observed for gasoline in previous work due to the increased detector response factor.[3] The similarities were reasonable given that the paint remover contained the same C_2-alkylbenzenes present in gasoline (see Appendix 3A for unevaporated paint remover TIC). However, the PPMC coefficients increased only slightly when F_{Total} by area was used, whereas larger increases in PPMC coefficients were observed for gasoline. The paint remover only contained the C_2-alkylbenzenes across a narrow retention index range (I^T = 800 – 900) unlike gasoline, which contains many compounds of different chemical classes across a wider retention index range (I^T = 500 – 1350). Therefore, the response factor affects many more compounds in gasoline, especially those at higher retention indices (I^T > 900), resulting in a greater difference in correlation between F_{Total} calculation methods.

3.1.4 Petroleum Distillate Liquids

Petroleum distillates typically consist of *n*-alkanes, branched alkanes, and sometimes branched and cycloalkanes at lower abundances.[5] Five liquids other than those used previously for model development were investigated: charcoal lighter fluid (C_8 – C_{12}), paint thinner (MI KleanStrip®; C_8 – C_{12}), paint thinner (NH KleanStrip®; C_{11} – C_{15}), torch fuel (C_{10} – C_{15}), and lamp oil (C_9 – C_{19}). The two paint thinners were manufactured by the same brand (KleanStrip®) but were purchased in two different states (Michigan (MI)) and New Hampshire (NH)). While the packaging was identical, the chromatographic profiles were different (Figure 3.9), and thus

both liquids were used for model application. Chromatograms of the other unevaporated petroleum distillate liquids are included in Appendix 3A.

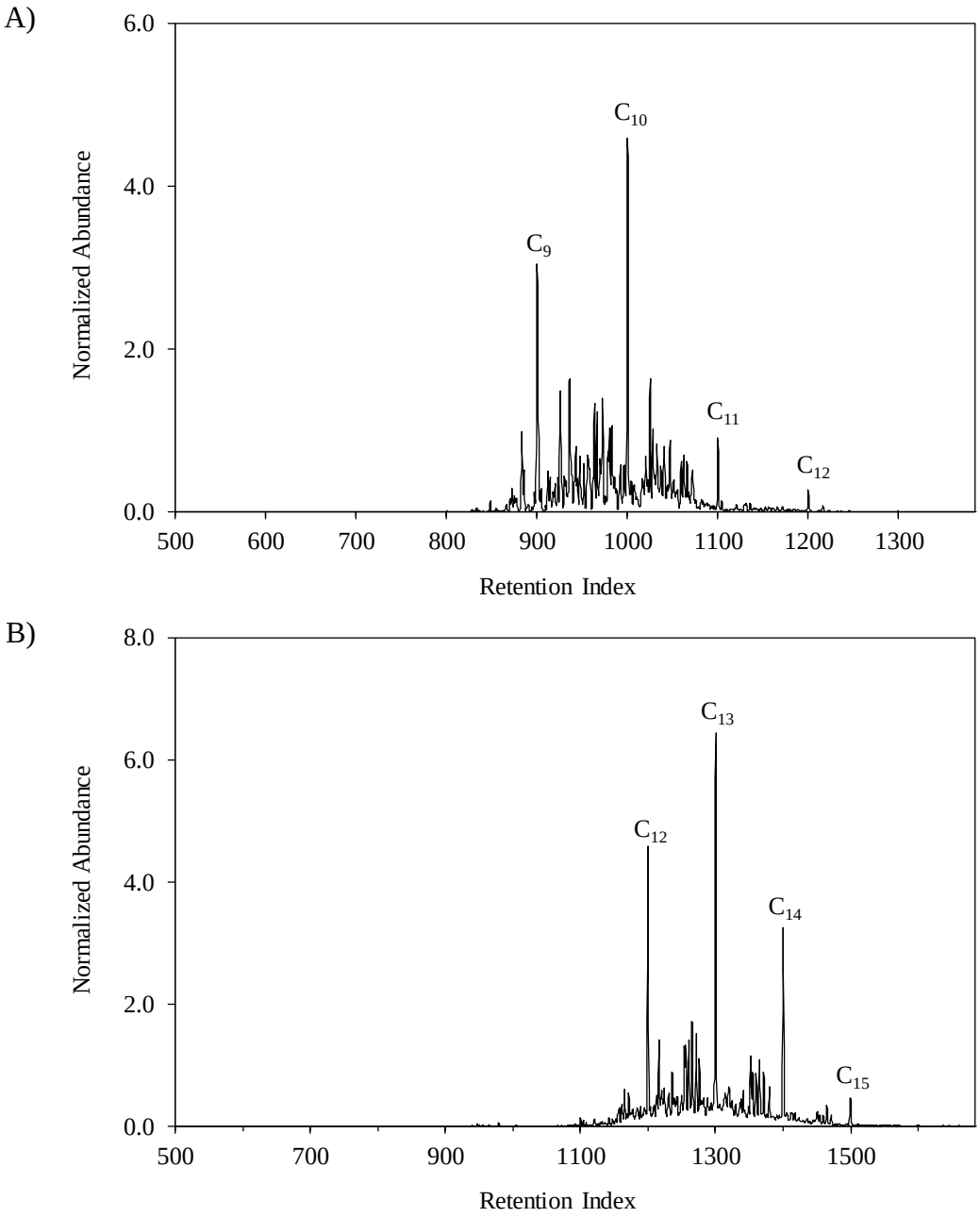

Figure 3.9 TICs of KleanStrip® paint thinner purchased in (A) Michigan and (B) New Hampshire

The NH KleanStrip® paint thinner was a heavy liquid containing compounds C_{11} – C_{15}, and *n*-alkanes were the most abundant compounds (Figure 3.9B). Evaporation had the greatest

effect on the early eluting compounds (I^T < 1300). At F_{Total} = 0.1, the compounds below I^T = 1300 fully evaporated (Figure 3.10). The compounds above I^T = 1300 were present, albeit at lower abundances compared to the chromatogram of the unevaporated liquid (Figure 3.10 compared to Figure 3.9B).

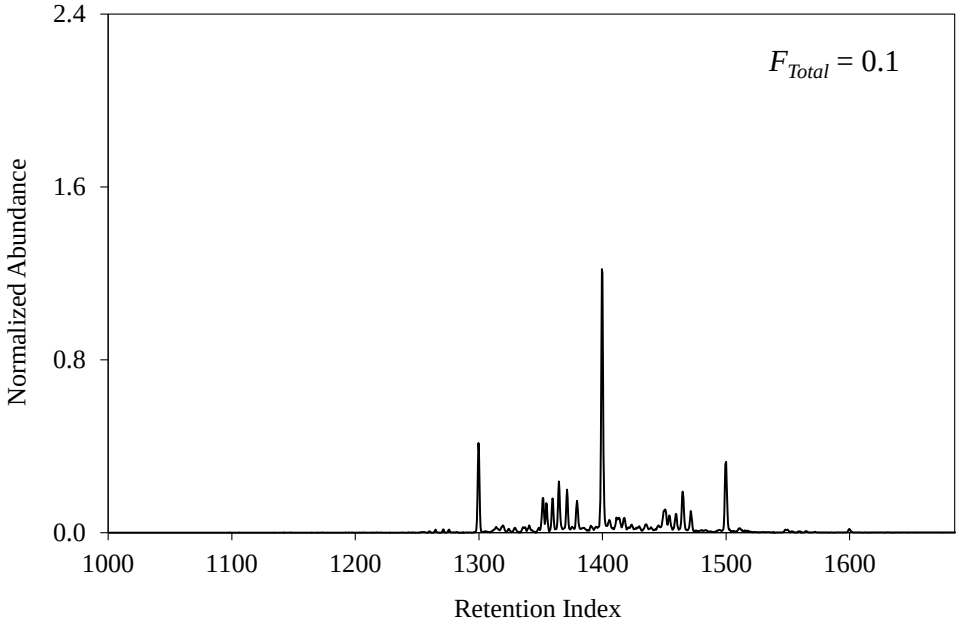

Figure 3.10 TIC of NH KleanStrip® paint thinner experimentally evaporated to F_{Total} = 0.1 across the reduced range I^T 1000 – 1685

For the five petroleum distillate liquids, strong correlation was observed for comparisons at all evaporation levels and both methods of F_{Total} calculation (Table 3.5). Aside from the MI KleanStrip® paint thinner at F_{Total} = 0.1, PPMC coefficients greater than 0.94 were observed. Strong correlation was expected given the use of petroleum distillates for model development. For each comparison, the PPMC coefficients were consistent between F_{Total} by mass and area, which was reasonable given the small differences in experimental F_{Total} values (Table 3.5, column 5). The majority of compounds in the liquids investigated were present between approximately I^T = 900 – 1400 and were less volatile than compounds at lower retention indices

(I^T < 800). Therefore, the detector response factor had less impact at higher F_{Total} levels for these liquids compared to more volatile liquids like gasoline.

Table 3.5 Mean PPMC coefficients for comparisons of experimental and predicted chromatograms of petroleum distillate liquids using F_{Total} by mass and area, as well as difference between F_{Total} by mass and area numerical values

Ignitable Liquid	Nominal F_{Total}	Mean PPMC Coefficient		$\lvert F_{Total}$ by area – F_{Total} by mass$\rvert$
		F_{Total} by Mass	F_{Total} by Area	
Charcoal Lighter Fluid *(Medium)*	0.5	0.991 ± 0.005	0.991 ± 0.005	0.001 ± 0.013
	0.3	0.984 ± 0.002	0.978 ± 0.003	0.024 ± 0.004
	0.1	0.963 ± 0.003	0.95 ± 0.01	0.0264 ± 0.0003
Paint Thinner (MI KleanStrip®) *(Medium)*	0.5	0.980 ± 0.005	0.979 ± 0.005	0.02 ± 0.01
	0.3	0.9790 ± 0.0005	0.978 ± 0.002	0.02 ± 0.01
	0.1	0.880 ± 0.001	0.811 ± 0.006	0.0358 ± 0.0007
Paint Thinner (NH KleanStrip®) *(Heavy)*	0.5	0.975 ± 0.006	0.985 ± 0.003	0.01 ± 0.01
	0.3	0.967 ± 0.004	0.966 ± 0.004	0.0172 ± 0.0001
	0.1	0.965 ± 0.002	0.964 ± 0.001	0.025 ± 0.001
Torch Fuel *(Heavy)*	0.5	0.950 ± 0.001	0.9480 ± 0.0006	0.01 ± 0.01
	0.3	0.981 ± 0.001	0.981 ± 0.001	0.005 ± 0.006
	0.1	0.945 ± 0.002	0.943 ± 0.006	0.002 ± 0.004
Lamp Oil *(Heavy)*	0.5	0.978 ± 0.003	0.977 ± 0.003	0.011 ± 0.009
	0.3	0.980 ± 0.002	0.979 ± 0.001	0.010 ± 0.007
	0.1	0.994 ± 0.006	0.993 ± 0.007	0.027 ± 0.007

Lower correlation was observed when F_{Total} by area was used for the MI KleanStrip® paint thinner at F_{Total} = 0.1 (Table 3.5). While the PPMC coefficient still indicated strong correlation (r = 0.811), it was much lower than the PPMC coefficients for the other liquids and evaporation levels in this class. Overprediction of evaporation at low retention indices (I^T < 1030), especially for C_{10} (I^T = 1000), was the cause of the lower correlation (Figure 3.11). The mean PPMC coefficient across retention indices I^T = 1012 – 1385 (omitting C_{10}) was 0.932, which is approximately 0.12 greater than the PPMC coefficient across the full retention index range (I^T = 500 – 1385). The overprediction was likely due to the higher response factor for this alkane. Based on the PPMC coefficient from I^T = 1012 – 1385, F_{Total} by area was still a more

representative method of F_{Total} calculation compared to F_{Total} by mass and indicated that the model performed with acceptable predictive accuracy for the remaining compounds.

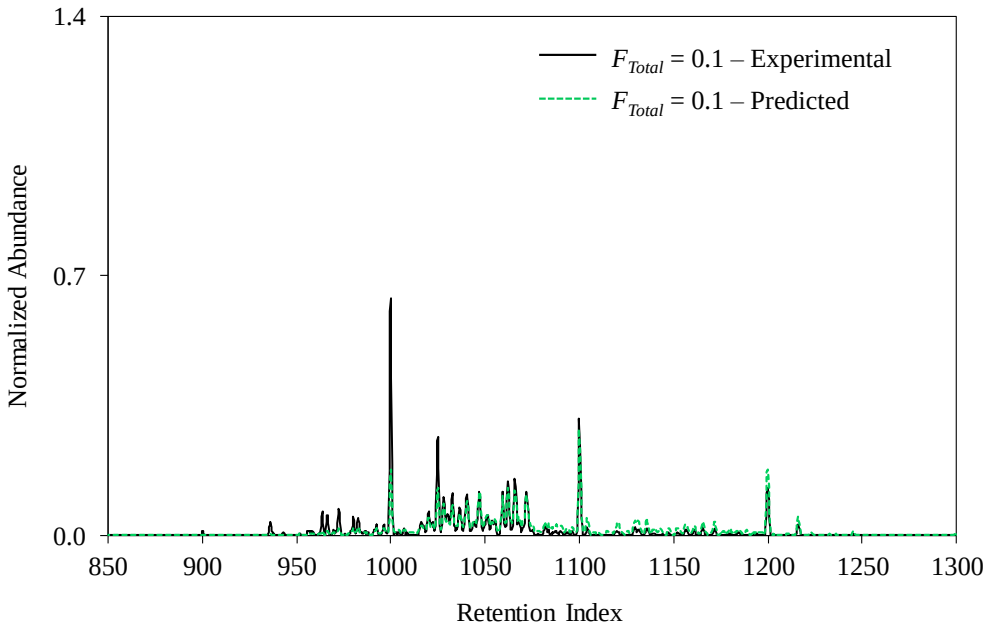

Figure 3.11 Overlay of experimental and predicted chromatogram for MI KleanStrip® paint thinner at F_{Total} = 0.1 over the reduced range I^T = 850 – 1300. The predicted chromatogram was generated using F_{Total} by area.

3.1.5 Gasoline

Gasoline contains compounds of several different chemical classes that span a wide retention index range (I^T = 500 – 1300). These include *n*-alkanes, branched alkanes, cyclic compounds, substituted benzenes and polynuclear aromatics.[5] Fresh gasoline was investigated in this work, and the major compound groups commonly found in gasoline were present in the chromatogram of the unevaporated liquid (Figure 3.12A). The volatile compounds at low retention indices (I^T < 800) were most affect by evaporation, whereas compounds with lower volatilities were affected to a lesser extent. At F_{Total} = 0.1, compounds below I^T = 800 completely

evaporated (Figure 3.12B), and those above I^T = 800 were still present at lower abundances compared to those in the chromatogram of the unevaporated liquid.

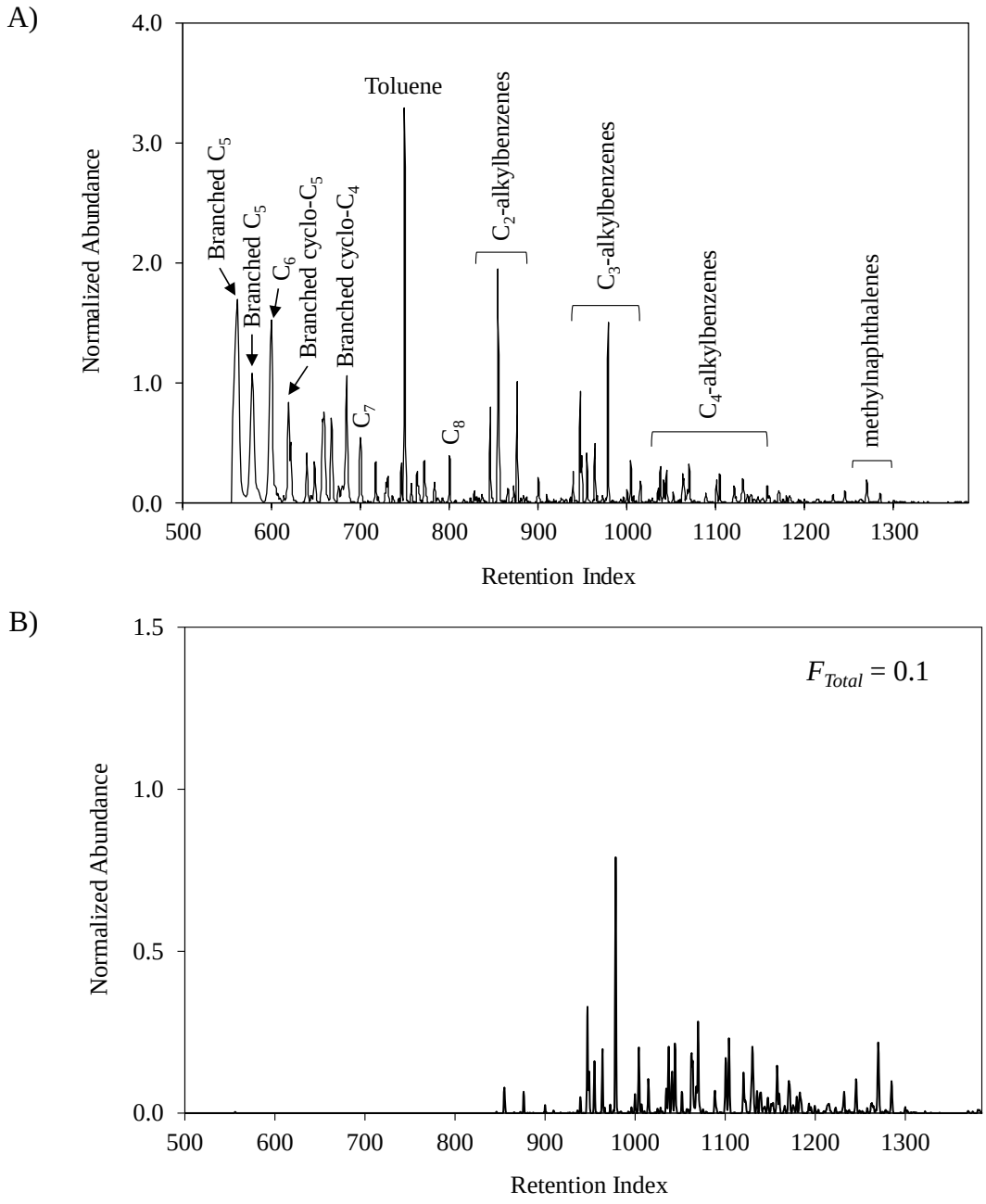

Figure 3.12 TICs of (A) unevaporated gasoline and (B) gasoline experimentally evaporated to F_{Total} = 0.1

For the comparisons at all three evaporation levels and both F_{Total} calculation methods, strong correlation was observed, with PPMC coefficients as high as 0.993 (Table 3.6). The abundances in the predicted chromatograms agreed well with those in the experimental chromatograms, especially for the comparison at F_{Total} = 0.3, for which only small deviations were observed (Figure 3.13). Despite the strong correlation across all evaporation levels, greater differences in numerical F_{Total} levels were observed compared to those in other liquid classes. The greatest difference occurred for the comparison at F_{Total} = 0.3, followed by the comparison at F_{Total} = 0.5 (Table 3.6, column 5). These evaporation levels were associated with the greatest increases in correlation when F_{Total} by area was used. Consistent with previous findings,[3, 4] the higher PPMC coefficients were due to the detector response factor at higher F_{Total} levels. The increase in correlation at F_{Total} = 0.1 was also attributed to the response factor, but the effect had less impact than at higher F_{Total} levels because the compounds at low retention indices (I^T < 800) were completely evaporated.

Table 3.6 Mean PPMC coefficients for comparisons of experimental and predicted chromatograms of gasoline using F_{Total} by mass and area, as well as difference between F_{Total} by mass and area numerical values

Ignitable Liquid	Nominal F_{Total}	Mean PPMC Coefficient		$\lvert F_{Total}$ by area – F_{Total} by mass$\rvert$
		F_{Total} by Mass	F_{Total} by Area	
Gasoline ($C_4 – C_{13}$)	0.5	0.883 ± 0.002	0.976 ± 0.002	0.212 ± 0.006
	0.3	0.857 ± 0.003	0.993 ± 0.003	0.31 ± 0.02
	0.1	0.917 ± 0.002	0.992 ± 0.001	0.078 ± 0.004

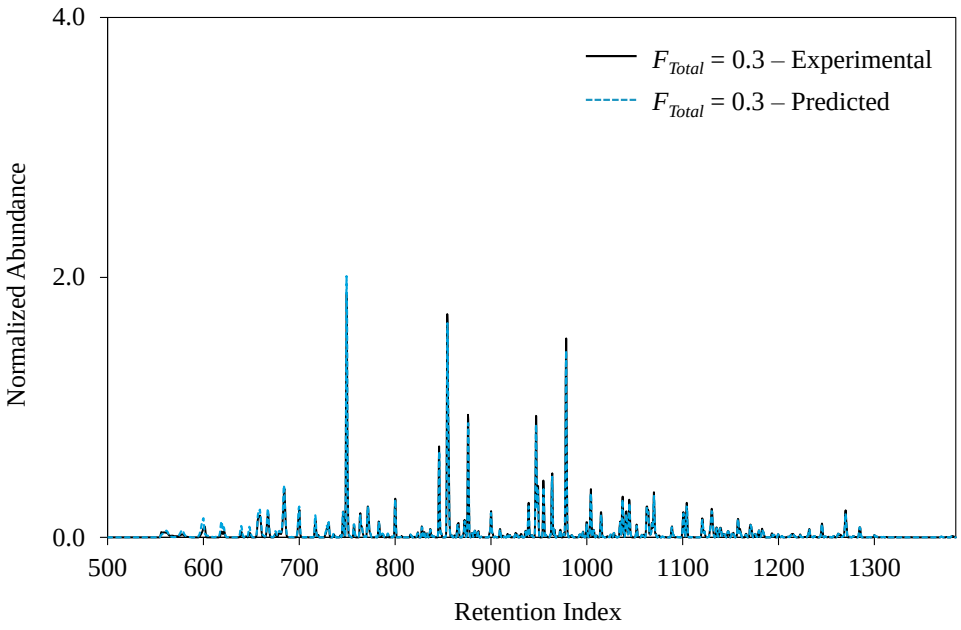

Figure 3.13 Overlay of experimental and predicted chromatograms for gasoline at F_{Total} = 0.3. The predicted chromatogram was generated using F_{Total} by area.

While the PPMC coefficient for the comparison at F_{Total} = 0.5 by area was still greater than 0.97, it was the lowest coefficient across the three evaporation levels using F_{Total} by area. Many of the highly volatile compounds in gasoline (I^T < 800) were still present at F_{Total} = 0.5, whereas these compounds were present at lower abundances or were completely evaporated at F_{Total} = 0.3 and 0.1, respectively. The PPMC coefficient for the comparison at F_{Total} = 0.5 was not as high as those at F_{Total} = 0.3 and 0.1 likely because of slight overprediction of evaporation for compounds between I^T = 500 – 800 (Figure 3.14). The kinetic model was developed for compounds with retention indices across the range I^T = 800 – 2200; therefore, the model may not predict evaporation rate constants as accurately for compounds with I^T < 800. Future work and refinement of the model involves extending the retention index range used for model development to incorporate compounds with I^T < 800. This refinement will allow for more accurate prediction of evaporation rate constants for these highly volatile compounds in ignitable liquids.

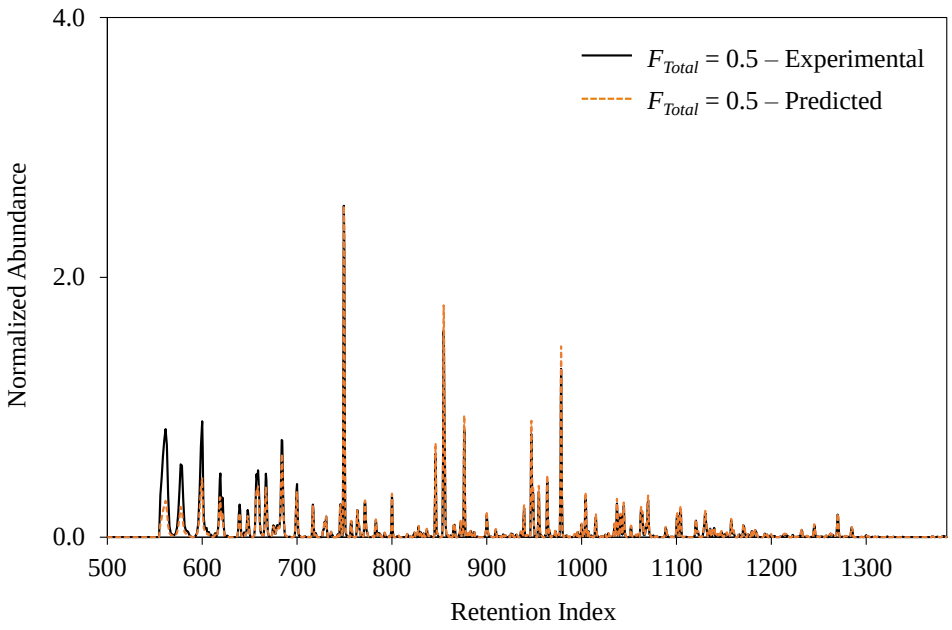

Figure 3.14 Overlay of experimental and predicted chromatograms for gasoline at F_{Total} = 0.5. The predicted chromatogram was generated using F_{Total} by area.

3.2 Identification of Evaporated Liquids Based on Comparison to TIC Reference Collection

To demonstrate model application, a predicted reference collection was generated based on the TICs of the liquids discussed in Section 3.1. Two additional petroleum distillates (kerosene and diesel fuel) were added to increase the number of liquids included in the reference collection. Experimental evaporations were not conducted for kerosene or diesel fuel, as the predictive accuracy of the model was previously demonstrated for these liquids.[1, 2] Using the TIC of each unevaporated liquid, the kinetic model was applied to predict chromatograms corresponding to F_{Total} = 0.9 – 0.1 in increments of 0.1, following the procedure described in Chapter 2, Section 2.4.1. Thus, the final TIC reference collection contained 162 total predicted chromatograms (nine evaporation levels for 18 liquids).

The chromatogram of an experimentally evaporated liquid was compared to all of the predicted TICs for the corresponding liquid, and a PPMC coefficient was calculated for each comparison (Figure 3.15). The resulting coefficients were then plotted as a function of F_{Total}

level to generate a nine-point curve for each liquid (Figure 3.15, right). Similar curves for all liquids in the reference collection were plotted concurrently. The maximum PPMC coefficient and corresponding F_{Total} level across all curves were identified to determine to which liquid the experimental sample was most strongly correlated. For example, the sample chromatogram in Figure 3.15 was most strongly correlated to the Crown® paint thinner at F_{Total} = 0.6, with a maximum PPMC coefficient of 0.9903.

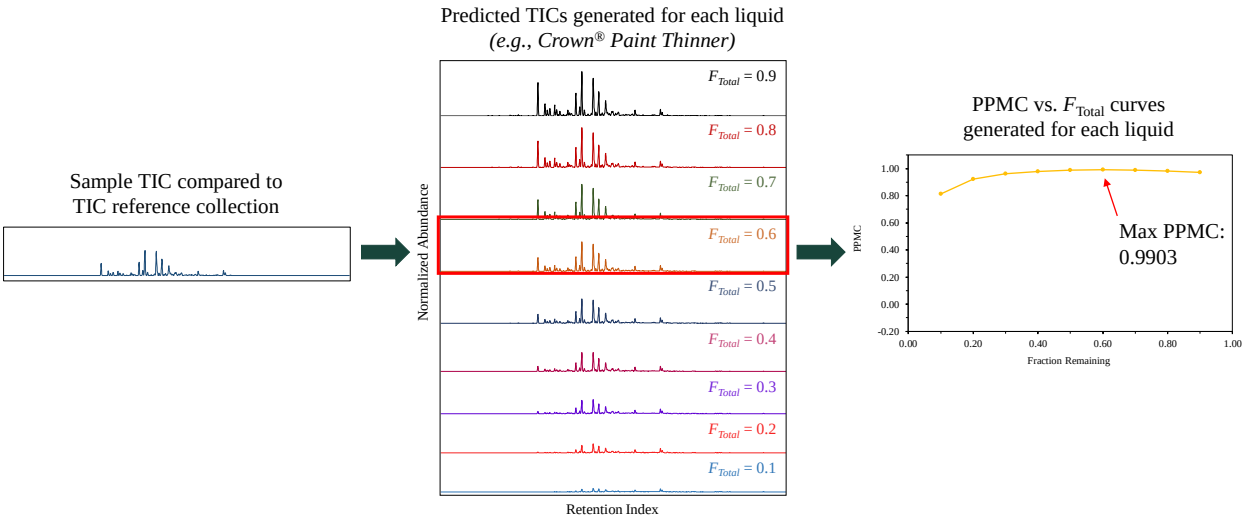

Figure 3.15 Schematic of ignitable liquid identification process using the TIC reference collection

Table 3.7 includes the maximum PPMC coefficients and corresponding liquids for comparisons of five experimentally evaporated liquids, one from each ASTM class. Comparisons for all other liquids are summarized in Appendix 3B. For each experimentally evaporated liquid in Table 3.7, the maximum PPMC coefficient correlated to the same-source liquid and, for all cases, coefficients ranged from 0.9089 to 0.9981 (Table 3.7). Strong correlation was observed across all evaporation levels for each liquid and the majority of PPMC coefficients were greater than 0.97. Comparisons associated with three liquids at F_{Total} = 0.1

resulted in lower coefficients compared to those at F_{Total} = 0.5 and 0.3: marine fuel stabilizer, adhesive remover, and charcoal lighter fluid. However, similar results occurred for the same liquids in Section 3.1 for comparisons of the experimental and predicted chromatograms at F_{Total} = 0.1 by area. For example, comparison of the experimental and predicted chromatograms for adhesive remover at F_{Total} = 0.1 resulted in a mean PPMC coefficient of 0.935 for F_{Total} by area (Table 3.3) and was lower than the PPMC coefficients for the other F_{Total} levels due to slight peak misalignment. The same phenomenon occurred for the comparison of the experimental adhesive remover chromatogram at F_{Total} = 0.1 to the predicted chromatograms in the reference collection. Therefore, these lower PPMC coefficients were reasonable given the comparisons discussed in the previous sections.

Table 3.7 Maximum PPMC coefficients, corresponding ignitable liquids, F_{Total} values, and experimental (Exp.) F_{Total} by area values for comparisons of TICs of experimentally evaporated liquids to TIC reference collection

Ignitable Liquid	Nominal F_{Total}	Liquid at Max PPMC	Max PPMC	F_{Total} at Max PPMC	Exp. F_{Total}
Lighter Fluid *(Isoparaffinic)*	0.5	Lighter Fluid	0.9966	0.6	0.5846
	0.3	Lighter Fluid	0.9871	0.3	0.3598
	0.1	Lighter Fluid	0.9923	0.1	0.0935
Marine Fuel Stabilizer (MFS) *(Naphthenic-Paraffinic)*	0.5	MFS	0.9936	0.4	0.4576
	0.3	MFS	0.9796	0.3	0.2308
	0.1	MFS	0.9089	0.1	0.0402
Adhesive Remover *(Aromatic)*	0.5	Adhesive Remover	0.9767	0.6	0.4916
	0.3	Adhesive Remover	0.9743	0.6	0.2670
	0.1	Adhesive Remover	0.9367	0.1	0.0502
Charcoal Lighter Fluid *(Petroleum Distillate)*	0.5	Charcoal Lighter Fluid	0.9930	0.5	0.4999
	0.3	Charcoal Lighter Fluid	0.9912	0.4	0.2638
	0.1	Charcoal Lighter Fluid	0.9421	0.1	0.0682
Gasoline	0.5	Gasoline	0.9985	0.9	0.7410
	0.3	Gasoline	0.9981	0.6	0.6271
	0.1	Gasoline	0.9863	0.2	0.1891

In general, the F_{Total} levels to which the maximum PPMC coefficients corresponded were close to the nominal F_{Total} values (Table 3.7). However, there were three exceptions for which differences in the nominal F_{Total} and F_{Total} value at maximum PPMC were greater than 0.2: adhesive remover at F_{Total} = 0.3 and gasoline at F_{Total} = 0.5 and 0.3. For the adhesive remover comparison, the PPMC coefficients ranged from 0.9585 to 0.9743 across the nine F_{Total} levels. While the maximum PPMC occurred at F_{Total} = 0.6, the PPMC coefficient for the comparison to the predicted chromatogram at F_{Total} = 0.3 was 0.9724. Even though the PPMC coefficient was higher at F_{Total} = 0.6, the coefficient at F_{Total} = 0.3 was very close to the maximum value and differed by only 0.0019.

The F_{Total} at maximum PPMC for the gasoline comparisons at F_{Total} = 0.5 and 0.3 were reasonable given the respective experimental F_{Total} by area values. At F_{Total} = 0.5, the maximum PPMC coefficient occurred at F_{Total} = 0.9, whereas the experimental F_{Total} value was closest to F_{Total} = 0.7 (Table 3.7). The PPMC coefficients across the nine evaporation levels for this comparison ranged from 0.2531 (F_{Total} = 0.1) to 0.9985 (F_{Total} = 0.9), and the PPMC coefficients at $F_{Total} < 0.6$ were all below 0.90. At F_{Total} = 0.7, the PPMC coefficient was 0.9614, which was close to the maximum PPMC coefficient given the large range in correlation coefficients across all F_{Total} levels. For the comparison at F_{Total} = 0.1, the F_{Total} at maximum PPMC (F_{Total} = 0.6) was closest to the experimental F_{Total} by area (F_{Total} = 0.6271). Therefore, it was reasonable that the maximum correlation appeared at this F_{Total} level. For both gasoline comparisons (F_{Total} = 0.3 and 0.1), the F_{Total} by area values for gasoline were greater than the corresponding nominal values because of the effect of the detector response factor discussed in Section 3.1.5. However, the goal in fire debris analysis focuses on liquid class identification rather than identification of a specific evaporation level. These comparisons demonstrated that liquid identification was

successful and a reasonable estimation of evaporation level was possible using the TIC reference collection.

Another important point to consider is correlation to other liquids in the reference collection. The experimental chromatogram corresponding to $F_{Total} = 0.5$ for a representative liquid from each class was compared to the predicted reference collection (Figure 3.16). Overall, the strongest correlation was observed for comparison of the evaporated liquids to the corresponding predicted chromatograms for the same liquid. For example, in Figure 3.16B, the experimental chromatogram of marine fuel stabilizer at $F_{Total} = 0.5$ was most strongly correlated with the predicted chromatograms of marine fuel stabilizer, with PPMC coefficients ranging from 0.7975 to 0.9936 across the nine evaporation levels. Moderate to no correlation was observed for all other predicted chromatograms in the reference collection. This demonstrated the usefulness of the collection in the determination of the liquid present when the composition was significantly different from the other liquids.

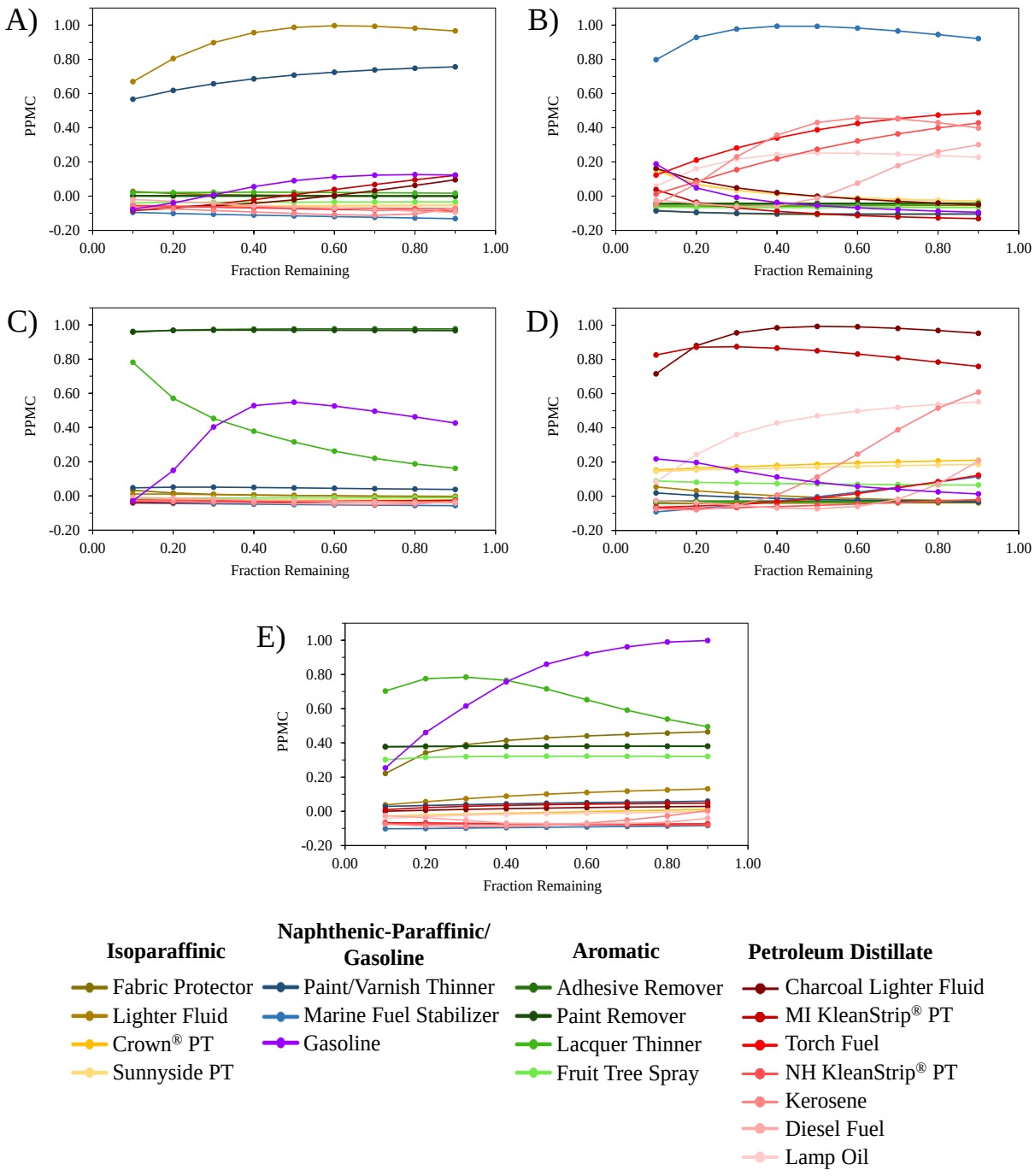

Figure 3.16 PPMC vs. F_{Total} plots for comparisons of experimental chromatograms at F_{Total} = 0.5 to TIC reference collection for (A) lighter fluid (isoparaffinic), (B) marine fuel stabilizer (naphthenic-paraffinic), (C) adhesive remover (aromatic), (D) charcoal lighter fluid (petroleum distillate), and (E) gasoline

For the comparisons of the experimental adhesive remover (Figure 3.16C) and charcoal lighter fluid (Figure 3.16D) TICs at F_{Total} = 0.5 to the reference collection, strong correlation was observed for the same-source liquid as well as predicted chromatograms of a liquid from the same ASTM class. While strongest correlation for the adhesive remover comparison was with the same-source liquid, strong correlation was also observed for predicted chromatograms of paint remover (Figure 3.16C). This occurred because the adhesive remover and paint remover both contained the same three alkylbenzenes (*i.e.*, ethylbenzene, *m,p*-xylene, *o*-xylene). Similarly, for the charcoal lighter fluid comparison, strongest correlation was with the same-source liquid, and strong correlation was also observed for comparisons to the predicted MI KleanStrip® paint thinner chromatograms (Figure 3.16D). The paint thinner and charcoal lighter fluid contained similar compounds, mainly the *n*-alkanes $C_9 - C_{12}$. These liquids were the only petroleum distillates in the collection that both had compounds spanning the retention index range I^T = 800 – 1200 (with no compounds outside this range). In both the adhesive remover and charcoal lighter fluid examples, the liquids that exhibited the second-strongest correlation were of the same ASTM class as the liquid (*i.e.*, aromatic and petroleum distillate, respectively), and moderate to no correlation was observed for all other liquid classes in the reference collection.

Cases also existed for which liquids of ASTM classes other than that of the same-source liquid exhibited stronger correlation than other liquids in the reference collection. For the comparison of isoparaffinic lighter fluid to the reference collection (Figure 3.16A), the strongest correlation was associated with the same-source liquid; however, the second strongest correlation was with the paint and varnish thinner, which is a naphthenic-paraffinic liquid. Predicted chromatograms for all other liquids exhibited little to no correlation. The predicted chromatograms for the paint and varnish thinner had strong correlation because the liquid

contained similar compounds as the lighter fluid (*e.g.*, methylheptane, dimethylcyclohexane, octane, nonane). Additionally, the chromatographic profiles for both liquids spanned the same retention index ranges (I^T = 600 – 1000). Despite the compositional similarities, identification of the correct ASTM liquid class was still possible.

For the comparison of gasoline to the reference collection (Figure 3.16E), strongest correlation was observed for gasoline, and weak to no correlation was observed for the majority of other liquids. However, moderate correlation was observed for comparison of gasoline to the predicted chromatograms of the aromatic liquids, and the highest coefficients for this group were associated with the lacquer thinner. This was due to the presence of many similar aromatic compounds in gasoline and the aromatic liquids. Additionally, gasoline contained many of the same compounds found in the lacquer thinner, specifically toluene and the C_2-alkylbenzenes. The combination of these compounds together caused the lacquer thinner to exhibit stronger correlation than the other liquids in the aromatic class. However, correlation for the lacquer thinner decreased as the maximum PPMC coefficient was approached. The PPMC coefficients for gasoline increased towards the maximum coefficient, which indicated that correlation for the lacquer thinner became weaker upon approaching the correct sample F_{Total}. Therefore, the identification of gasoline was still possible.

3.3 Summary

Broader application of the kinetic model was demonstrated to include liquids from different ASTM classes (isoparaffinic, naphthenic-paraffinic, and aromatic classes), as well as additional liquids from the petroleum distillate and gasoline classes. Following experimental evaporations and comparisons to corresponding predicted chromatograms, the model was determined to perform with good predictive accuracy. Across all liquids and evaporation levels,

PPMC coefficients as high as 0.995 were observed. For liquids other than gasoline, the method of F_{Total} calculation did not seem to have a significant impact on the correlations. Regardless, applying the model to a wider range of liquids proved successful.

A reference collection based on predicted total ion chromatograms was generated and used for model validation. Comparisons of the TICs of the experimentally evaporated liquids to the reference collection resulted in correct identification of the same-source liquid. Additionally, in cases for which correlation of other class liquids was close to that of the same-source liquids, the correct ASTM classes were still identified, which supports the overall goal of fire debris analysis. In all cases, liquid and liquid class identifications demonstrated the success of the reference collection comparisons. The utility of the kinetic model to generate reference collections that can be used for identification purposes in a time- and resource-efficient manner was thus exemplified.

APPENDICES

APPENDIX 3A:

TICs of Unevaporated Ignitable Liquids

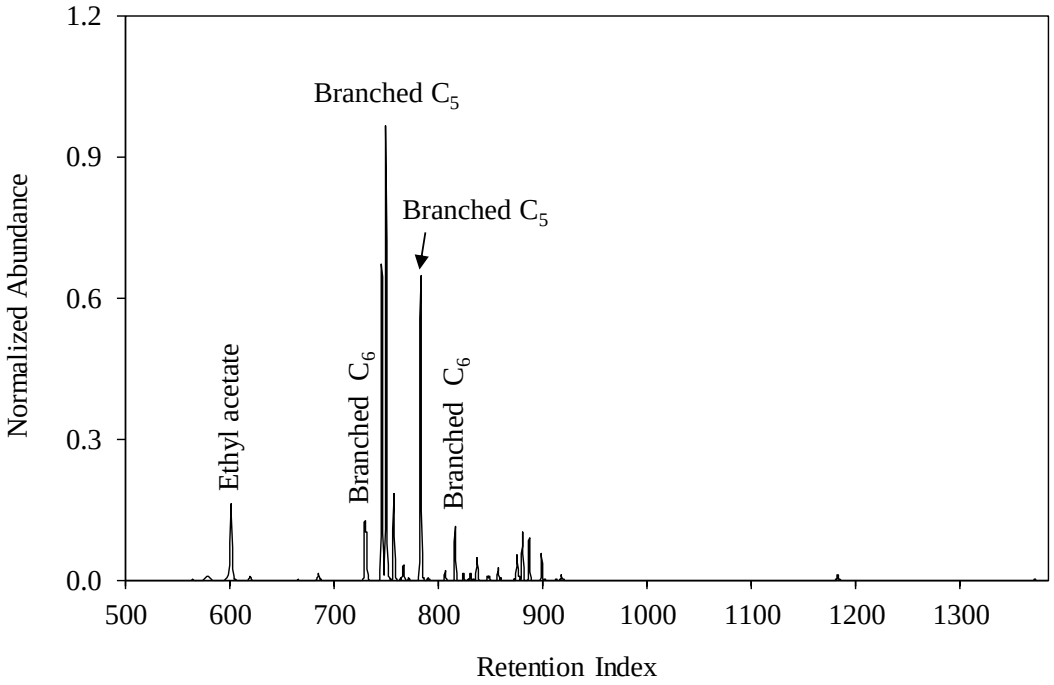

Figure A.5 TIC of unevaporated fabric and upholstery protector (isoparaffinic)

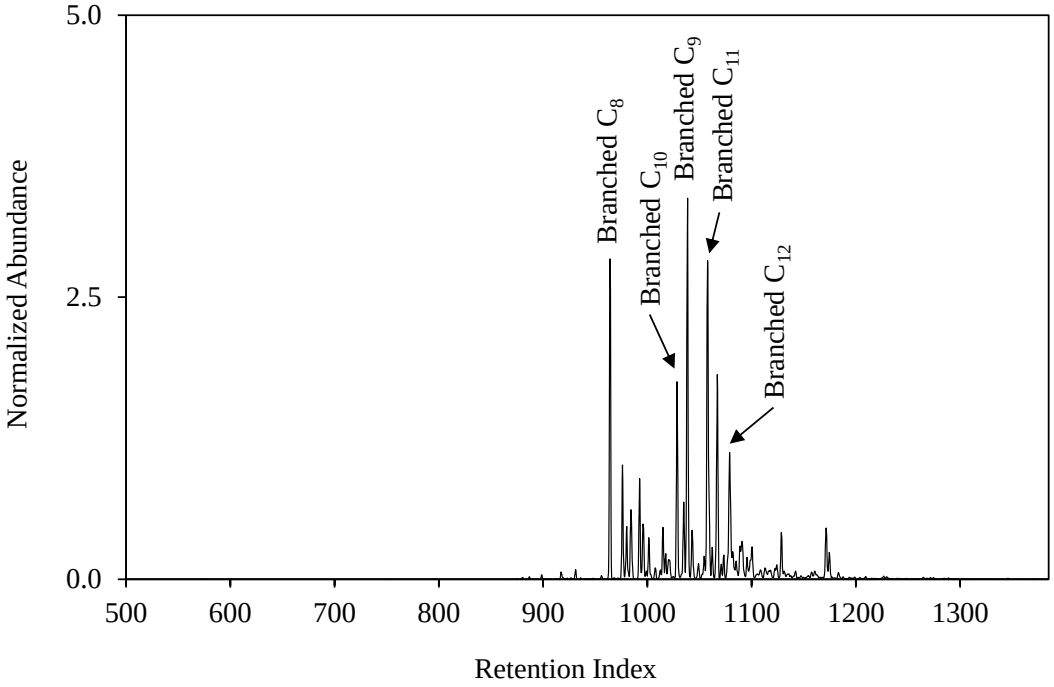

Figure A.6 TIC of unevaporated paint thinner (Crown®; isoparaffinic)

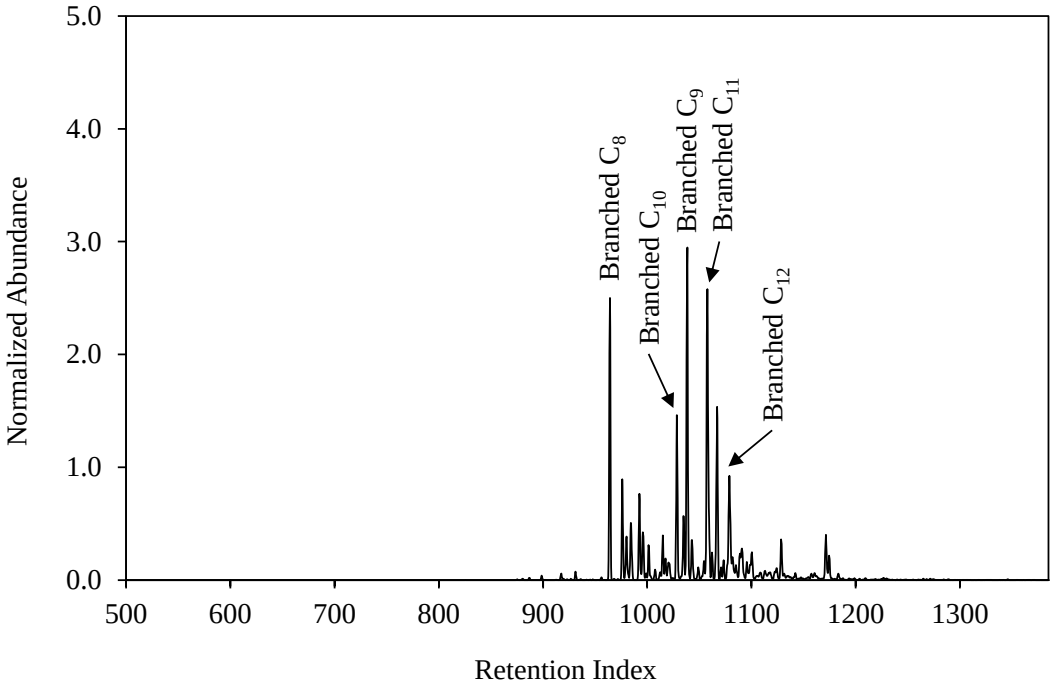

Figure A.7 TIC of unevaporated paint thinner (Sunnyside; isoparaffinic)

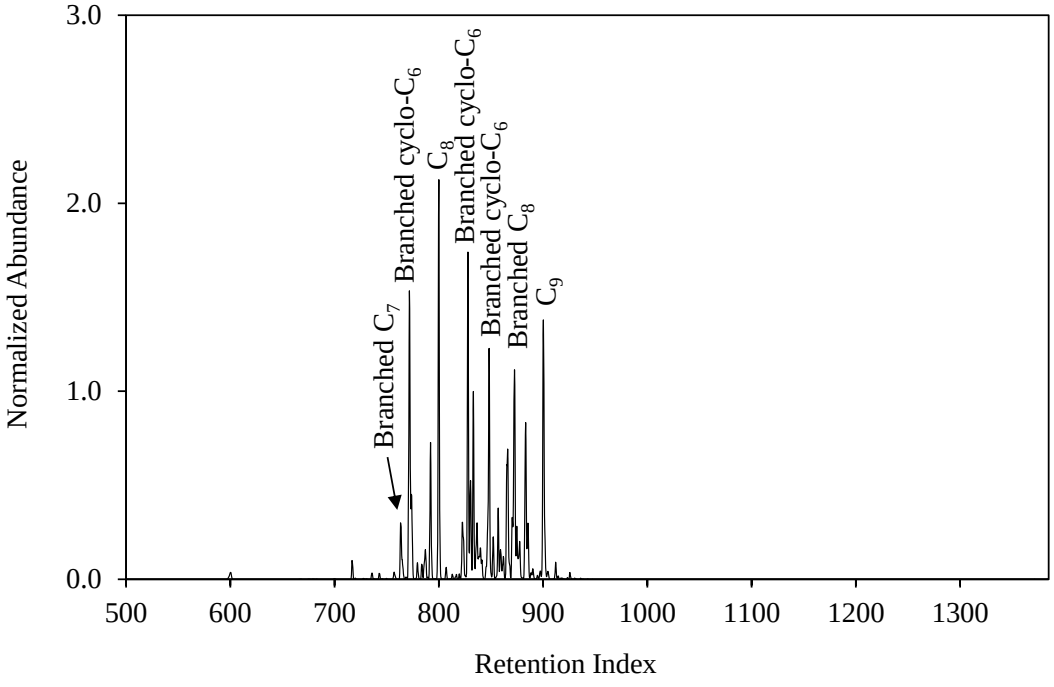

Figure A.8 TIC of unevaporated paint and varnish thinner (naphthenic-paraffinic)

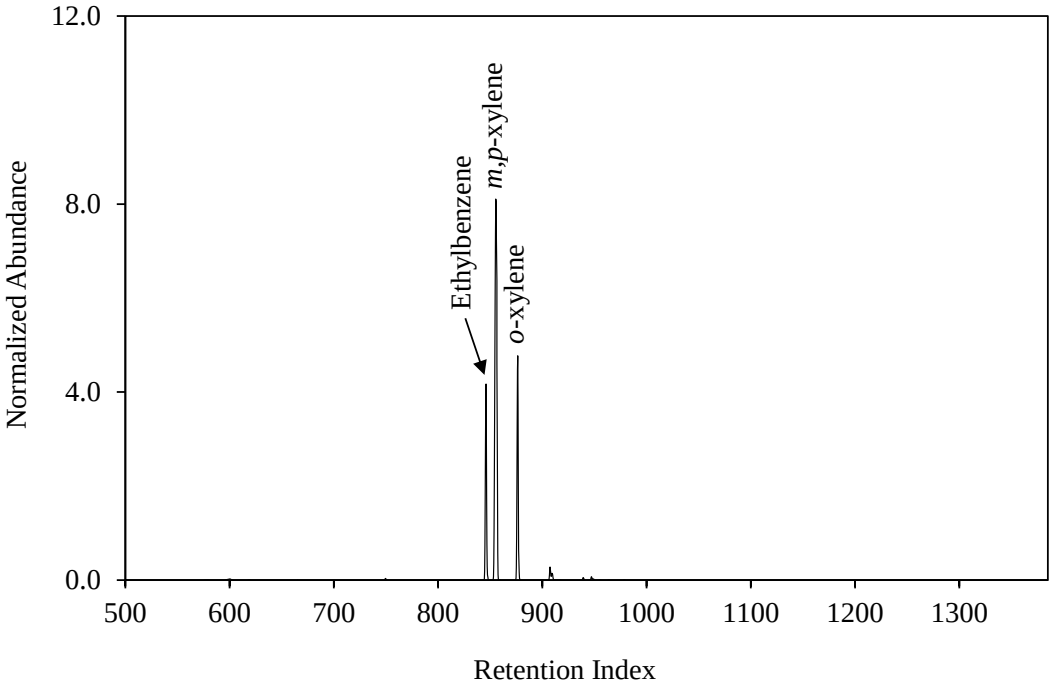

Figure A.9 TIC of unevaporated adhesive remover (aromatic)

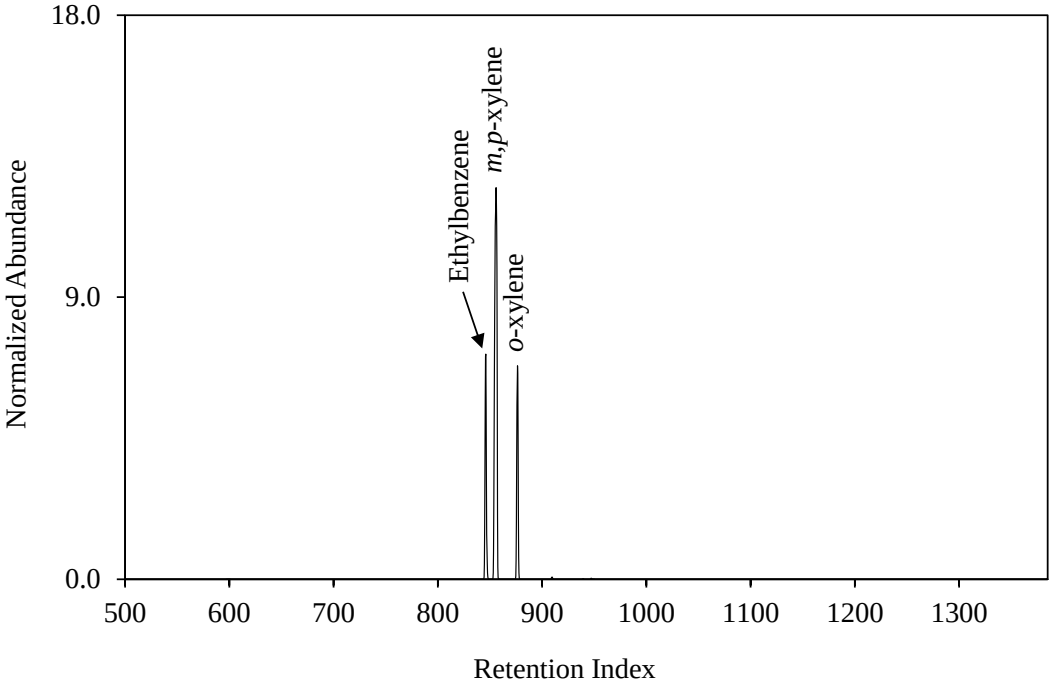

Figure A.10 TIC of unevaporated paint remover (aromatic)

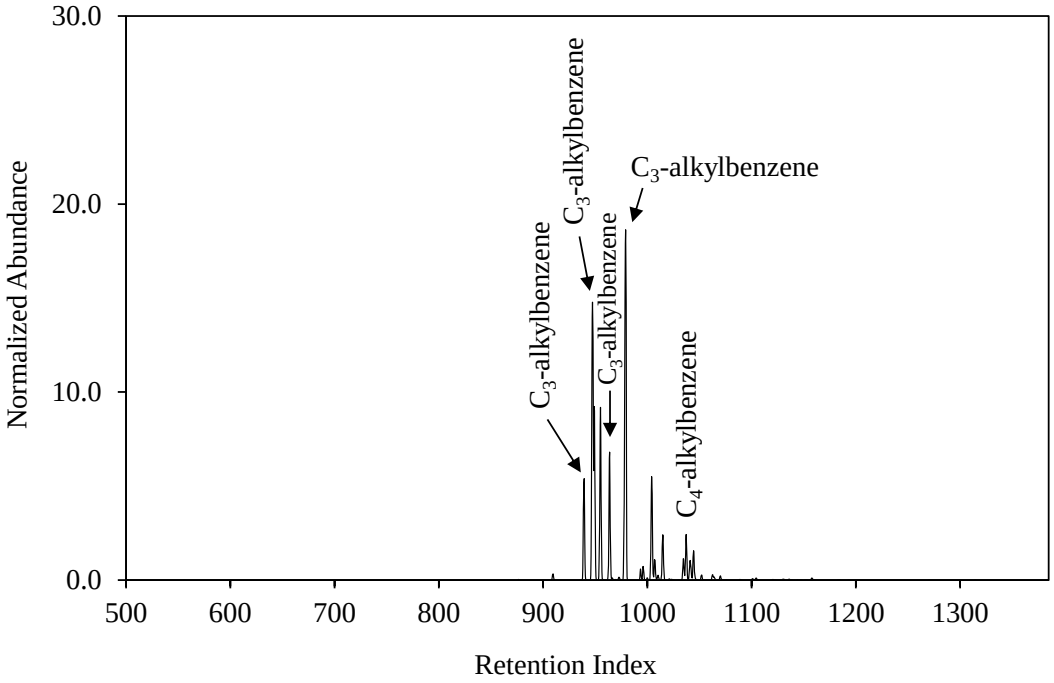

Figure A.11 TIC of unevaporated fruit tree spray (aromatic)

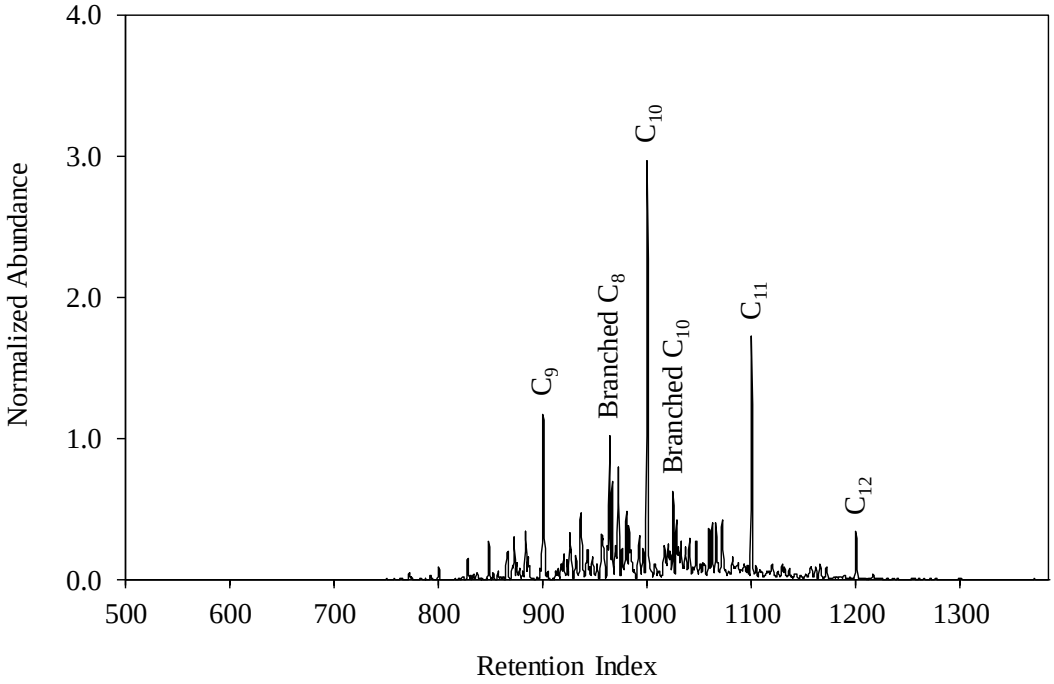

Figure A.12 TIC of unevaporated charcoal lighter fluid (petroleum distillate)

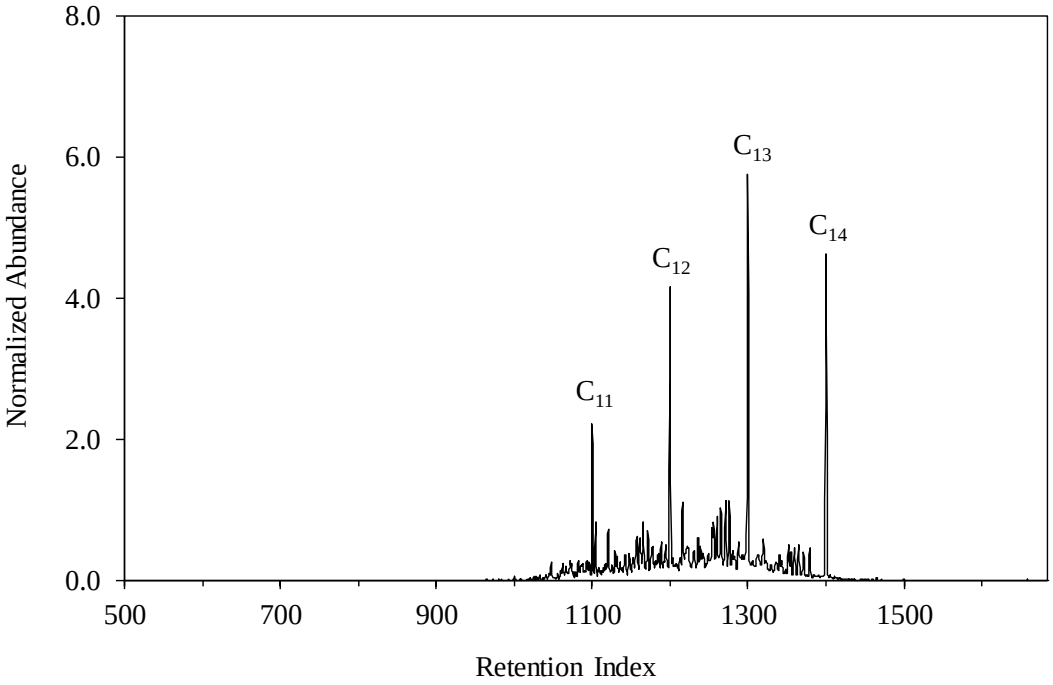

Figure A.13 TIC of unevaporated torch fuel (petroleum distillate)

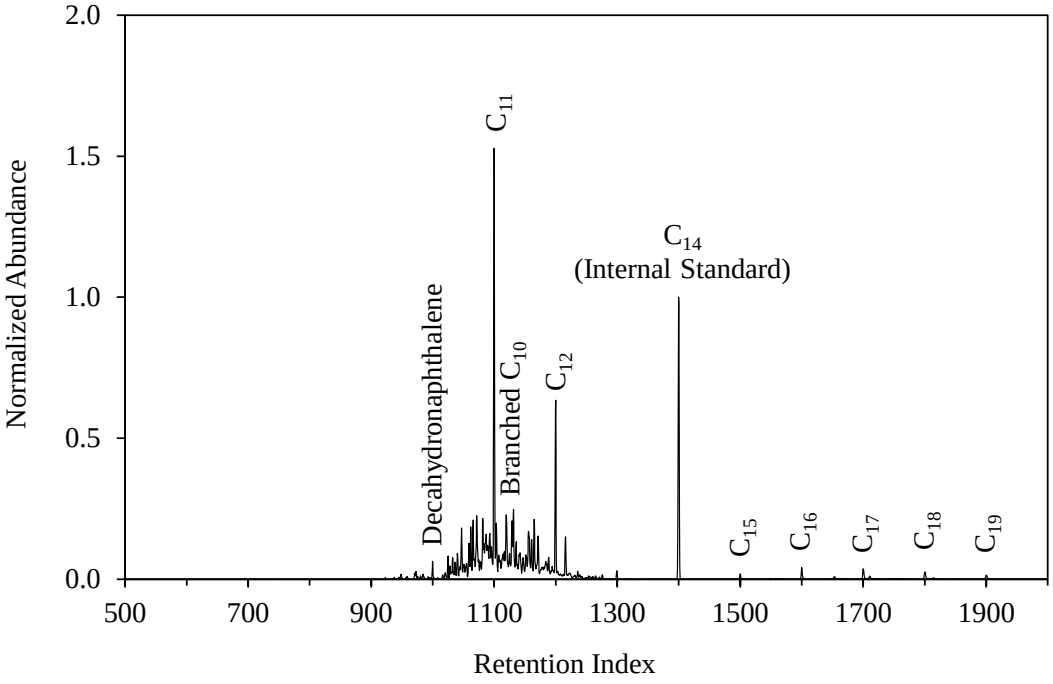

Figure A.14 TIC of unevaporated lamp oil (petroleum distillate)

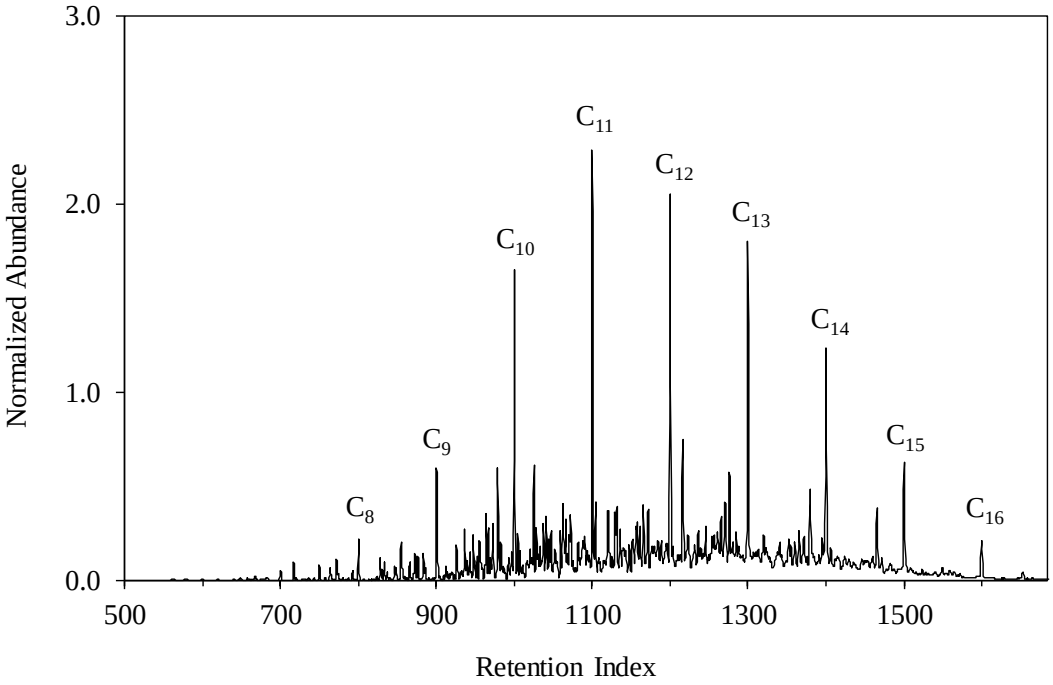

Figure A.15 TIC of unevaporated kerosene (petroleum distillate)

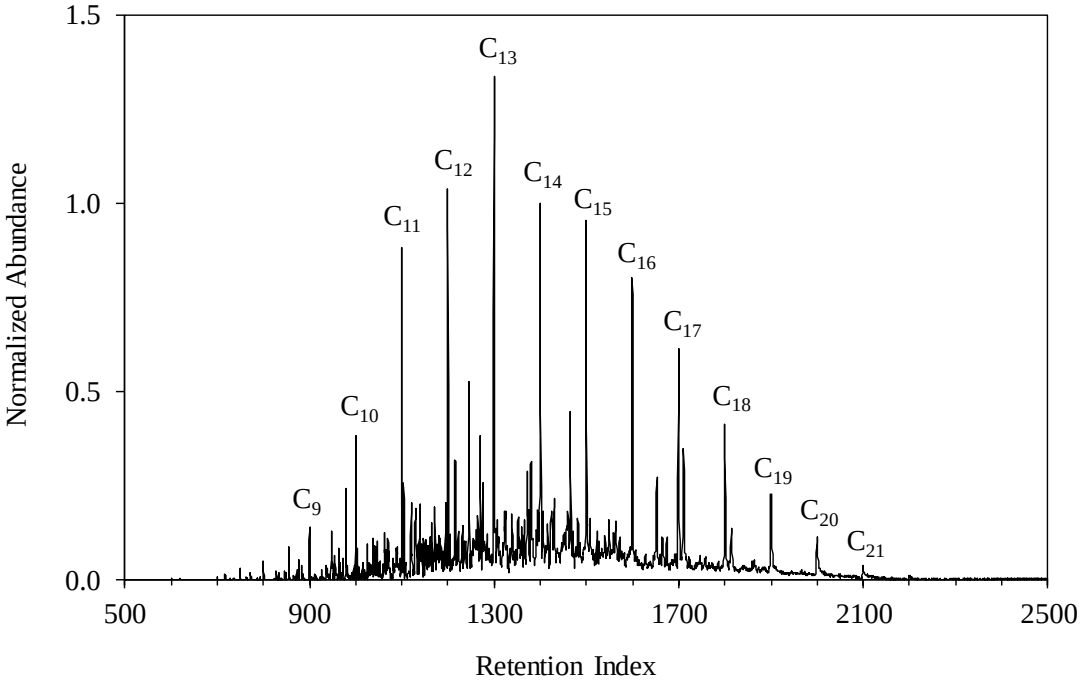

Figure A.16 TIC of unevaporated diesel fuel (petroleum distillate)

APPENDIX 3B:

Maximum PPMC coefficients, corresponding liquids and F_{Total} values for comparisons of experimental TICs to TIC reference collection

Table A.1 Maximum PPMC coefficients, corresponding ignitable liquids, F_{Total} values, and experimental (Exp.) F_{Total} by area values for comparisons of TICs of experimentally evaporated isoparaffinic liquids to TIC reference collection

Ignitable Liquid	Nominal F_{Total}	Liquid at Max PPMC	Max PPMC	F_{Total} at Max PPMC	Exp. F_{Total}
Fabric and Upholstery Protectory *(Light)*	0.5	Fabric and Upholstery Protector	0.9959	0.7	0.5928
	0.3	Fabric and Upholstery Protector	0.9954	0.4	0.3204
	0.1	Fabric and Upholstery Protector	0.6936	0.1	0.0594
Paint Thinner (Crown®) *(Medium)*	0.5	Paint Thinner (Crown®)	0.9903	0.6	0.5077
	0.3	Paint Thinner (Crown®)	0.9931	0.4	0.2863
	0.1	Paint Thinner (Crown®)	0.9814	0.1	0.0728
Paint Thinner (Sunnyside) *(Medium)*	0.5	Paint Thinner (Crown®)	0.9800	0.6	0.5288
	0.3	Paint Thinner (Sunnyside)	0.9899	0.3	0.2746
	0.1	Paint Thinner (Sunnyside)	0.9820	0.1	0.0650

Table A.2 Maximum PPMC coefficients, corresponding ignitable liquids, F_{Total} values, and experimental (Exp.) F_{Total} by area values for comparisons of TICs of experimentally evaporated naphthenic-paraffinic liquids to TIC reference collection

Ignitable Liquid	Nominal F_{Total}	Liquid at Max PPMC	Max PPMC	F_{Total} at Max PPMC	Exp. F_{Total}
Paint and Varnish Thinner *(Light)*	0.5	Paint and Varnish Thinner	0.9669	0.4	0.4438
	0.3	Paint and Varnish Thinner	0.9584	0.2	0.2500
	0.1	Paint and Varnish Thinner	0.9536	0.1	0.0646

Table A.3 Maximum PPMC coefficients, corresponding ignitable liquids, F_{Total} values, and experimental (Exp.) F_{Total} by area values for comparisons of TICs of experimentally evaporated aromatic liquids to TIC reference collection

Ignitable Liquid	Nominal F_{Total}	Liquid at Max PPMC	Max PPMC	F_{Total} at Max PPMC	Exp. F_{Total}
Paint Remover *(Light)*	0.5	Adhesive Remover	0.9840	0.9	0.7679
	0.3	Adhesive Remover	0.9730	0.9	0.5882
	0.1	Adhesive Remover	0.9574	0.9	0.3051
Lacquer Thinner *(Light)*	0.5	Lacquer Thinner	0.9662	0.9	0.6109
	0.3	Lacquer Thinner	0.9895	0.7	0.3888
	0.1	Lacquer Thinner	0.9169	0.4	0.1365
Fruit Tree Spray *(Medium)*	0.5	Fruit Tree Spray	0.9911	0.5	0.4841
	0.3	Fruit Tree Spray	0.9409	0.3	0.2760
	0.1	Fruit Tree Spray	0.9472	0.1	0.0162

Table A.4 Maximum PPMC coefficients, corresponding ignitable liquids, F_{Total} values, and experimental (Exp.) F_{Total} by area values for comparisons of TICs of experimentally evaporated petroleum distillate liquids to TIC reference collection

Ignitable Liquid	Nominal F_{Total}	Liquid at Max PPMC	Max PPMC	F_{Total} at Max PPMC	Exp. F_{Total}
Paint Thinner (MI KleanStrip®) *(Medium)*	0.5	Paint Thinner (MI KleanStrip®)	0.9851	0.6	0.4724
	0.3	Paint Thinner (MI KleanStrip®)	0.9686	0.3	0.3015
	0.1	Paint Thinner (MI KleanStrip®)	0.9320	0.1	0.0618
Paint Thinner (NH KleanStrip®) *(Heavy)*	0.5	Paint Thinner (NH KleanStrip®)	0.9815	0.5	0.4691
	0.3	Paint Thinner (NH KleanStrip®)	0.9604	0.3	0.3130
	0.1	Paint Thinner (NH KleanStrip®)	0.9759	0.1	0.0712
Torch Fuel *(Heavy)*	0.5	Paint Thinner (NH KleanStrip®)	0.9537	0.8	0.4787
	0.3	Torch Fuel	0.9837	0.3	0.2989
	0.1	Torch Fuel	0.9554	0.1	0.0897
Lamp Oil *(Heavy)*	0.5	Lamp Oil	0.9909	0.5	0.4350
	0.3	Lamp Oil	0.9777	0.4	0.1972
	0.1	Lamp Oil	0.9293	0.1	0.0219

REFERENCES

REFERENCES

1. J.W. McIlroy, A.D. Jones and V.L. McGuffin, Gas Chromatographic Retention Index as a Basis for Predicting Evaporation Rates of Complex Mixtures, Anal. Chim. Acta 852 (2014) 257-266.

2. R. Waddell Smith, R.J. Brehe, J.W. McIlroy and V.L. McGuffin, Mathematically Modeling Chromatograms of Evaporated Ignitable Liquids for Fire Debris Applications, Forensic Chem. 2 (2016) 37-45.

3. N.K. Eklund, Further Investigation of a Kinetic Model to Accurately Predict Evaporation of Gasoline. Michigan State University, 2019.

4. N.K. Eklund, B.A. Capistran, V.L. McGuffin and R. Waddell Smith, Improvements in a Kinetic-Based Model to Predict Evaporation of Gasoline, Forensic Chemistry 17 (2020) 100194.

5. ASTM E1618-14 Standard Test Method for Ignitable Liquid Residues in Extracts from Fire Debris Samples by Gas Chromatography-Mass Spectrometry. ASTM. International, West Conshohocken, PA, 2014.

6. J. K. Grob, Peak Broadening or Splitting Caused by Solvent Flooding after Splitless or Cold on-Column Injection in Capillary Gas Chromatography, J. Chromatogr. 213 (1981) 3-14.

7. J. K. Grob, Solvent Effects in Capillar Gas Chromatography, J. Chromatogr. 279 (1983) 225-232.

8. J. K. Grob, Band Broadening in Space in Splitless Injection, J. Chromatogr. 324 (1985) 251-259.

9. N. Gorocs, B. Bek, J. Bozsik, J. Mtyasi and J. Balla, The Determination of Gcms Relative Molar Responses of Benzene and Biphenyl Derivatives, J. Anal. Chem. 69 (2014) 1112-1121.

10. R.L. Smith, Predicting Evaporation Rates and Times for Spills of Chemical Mixtures, Ann. Ocup. Hyg. 45 (2001) 437-445.

11. CRC Handbook of Chemistry and Physics. Cleveland, OH: CRC Press, 1977.

IV. Validation of a Kinetic Model to Predict Extracted Ion Profile (EIP) Reference Collections for Ignitable Liquids from Different ASTM Classes

Identification of ignitable liquids in fire debris samples becomes challenging when the resulting chromatograms contain additional compounds associated with substrate components and pyrolysis products. Extracted ion profiles (EIPs) are therefore used to isolate the compounds attributed to the ignitable liquid(s) present. The work described in this chapter focused on generating a reference collection of predicted EIPs to further demonstrate the applicability of the kinetic model. However, verification of the ability of the model to generate predicted EIPs with acceptable predictive accuracy was necessary, as until this point, the model had only been applied to predict total ion chromatograms (TICs). The TICs from the experimentally evaporated ignitable liquids discussed in Chapter 3 were used for this purpose. Experimental profiles from five EIP compound classes were generated: alkane, cycloalkane, aromatic, indane, and polynuclear aromatic (PNA) classes (see Section 2.4 for *m/z* values used for each profile class). First, comparisons were made between experimental and predicted EIPs to assess the predictive accuracy of the model. Second, the model was used to predict EIPs at different evaporation levels to generate the EIP reference collection. Profiles of experimentally evaporated liquids were then compared to the predicted EIP reference collection to assess the accuracy in identifying the liquid and level of evaporation based on the EIPs.

4.1 Comparison of EIPs of Experimentally Evaporated Liquids to Predicted EIPs

The predictive accuracy of the model when applied to EIPs was assessed for the liquids of the five ASTM classes studied in Chapter 3 (isoparaffinic, naphthenic-paraffinic, aromatic, petroleum distillate, and gasoline classes). Using the TICs of the unevaporated and experimentally evaporated liquids, EIPs were generated for compound classes representative of

the corresponding liquid. For example, the isoparaffinic lighter fluid contained alkanes, cycloalkanes, and PNAs (Figure 3.1A). As such, the corresponding EIPs for these compound classes were generated. However, given that the lighter fluid was an isoparaffinic liquid, the alkane EIP was the most informative and contained the peaks of highest abundances across the three profiles.

The alkane profile generated from the TIC of the unevaporated lighter fluid contained a mixture of branched and normal alkanes across the retention index range I^T = 500 – 950 (Figure 4.1A). The effect of evaporation was greatest for the early eluting compounds (I^T < 800) with the highest volatilities. At F_{Total} = 0.1 (Figure 4.1B), almost all compounds below I^T = 800 evaporated and the abundances of those above I^T = 800 greatly decreased when compared to the EIP of the unevaporated liquid.

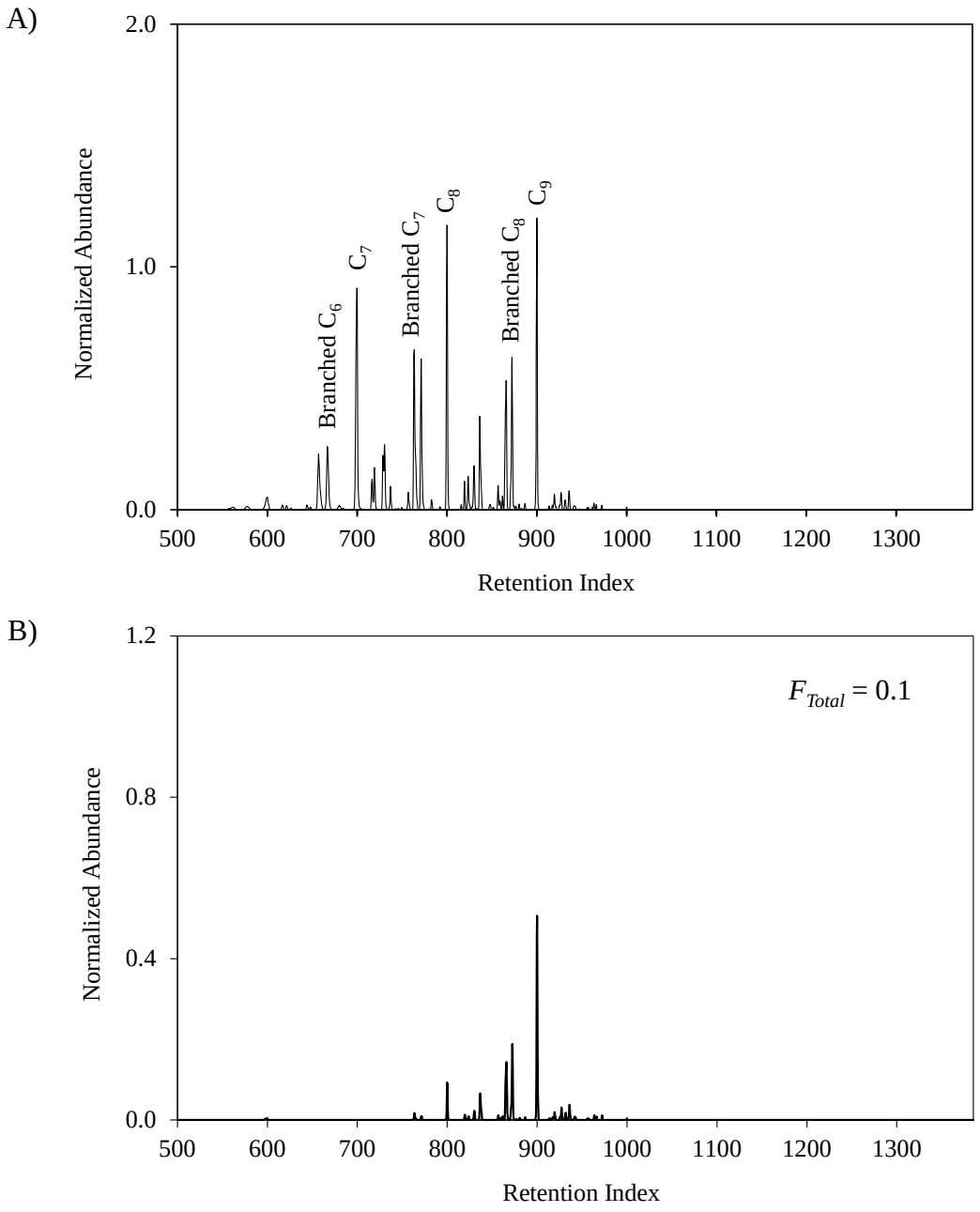

Figure 4.1 Alkane EIPs of (A) unevaporated lighter fluid and (B) lighter fluid evaporated to F_{Total} = 0.1

Comparisons between the experimental and predicted EIPs for the experimentally evaporated liquids resulted in strong correlation across all EIP classes and evaporation levels. Table 4.1 includes the corresponding PPMC coefficients for the comparisons performed for five

liquids, one from each ASTM class. The PPMC coefficients for comparison of experimental and predicted EIPs of the remaining liquids across three evaporation levels are shown in Appendix 4A. While EIPs were generated for representative compound classes for each liquid, some profiles at F_{Total} = 0.1 were not informative because of low abundances (< 0.005). Thus, in cases for which the EIP was not informative due to low abundances at F_{Total} = 0.1, comparisons to predicted profiles were not performed. Of the comparisons that were performed, the majority of PPMC coefficients were greater than 0.9, and more than half were greater than 0.99 (Table 4.1), indicating good predictive accuracy of the model when applied to EIPs.

Table 4.1 PPMC coefficients for comparisons between experimental and predicted EIPs for major compounds classes present in representative liquids from the five ASTM classes. Predicted EIPs were generated using F_{Total} by area.

Ignitable Liquid	Nominal F_{Total}	EIP Class & PPMC Coefficient				
		Alkane	Cycloalkane	Aromatic	Indane	PNA
Lighter Fluid *(Isoparaffinic – Light)*	0.5	0.9977	0.9980	*	*	0.9970
	0.3	0.9983	0.9898	*	*	0.9978
	0.1	0.9921	0.9624	*	*	0.9916
Gasoline	0.5	0.9845	0.9711	0.9914	0.9967	0.9972
	0.3	0.9936	0.9690	0.9991	0.9961	0.9963
	0.1	0.9717	**	0.9944	0.9945	0.9971
Marine Fuel Stabilizer *(Naphthenic-paraffinic – Medium)*	0.5	0.9876	0.9949	*	*	*
	0.3	0.9814	0.9916	*	*	*
	0.1	0.8592	0.9235	*	*	*
Lacquer Thinner *(Aromatic – Light)*	0.5	*	*	0.9958	*	*
	0.3	*	*	0.9969	*	*
	0.1	*	*	0.9762	*	*
MI KleanStrip® Paint Thinner *(Petroleum Distillate – Medium)*	0.5	0.9863	0.9914	0.9730	*	0.9830
	0.3	0.9903	0.9867	0.9785	*	0.9833
	0.1	0.8543	0.8612	**	*	0.8563

*Profile class not representative of liquid (EIPs not generated)
**Comparison not performed due to low abundances in experimental EIP

Gasoline contained compounds of many chemical classes (Figure 3.12A), and thus EIPs were generated for all five profile classes. For all three evaporation levels, the PPMC coefficients

for the comparisons for each class were greater than 0.96 (Table 4.1). The highest PPMC coefficient (r = 0.9991) was associated with the comparison of the experimental and predicted aromatic EIP for gasoline at F_{Total} = 0.3 (Table 4.1). In the aromatic EIP, toluene and the C_2 – C_4-alkylbenzenes were all present, which are important compounds for gasoline identification. The abundances in the predicted EIP compared extremely well with those in the experimental EIP (Figure 4.2). The lowest coefficients were associated with the cycloalkane EIP comparisons; this was likely because cycloalkane compounds are not the most dominant compounds in gasoline and are present at lower abundances compared to alkane, aromatic, indane, and polynuclear aromatic compounds. Nevertheless, strong correlation was observed for the corresponding comparisons.

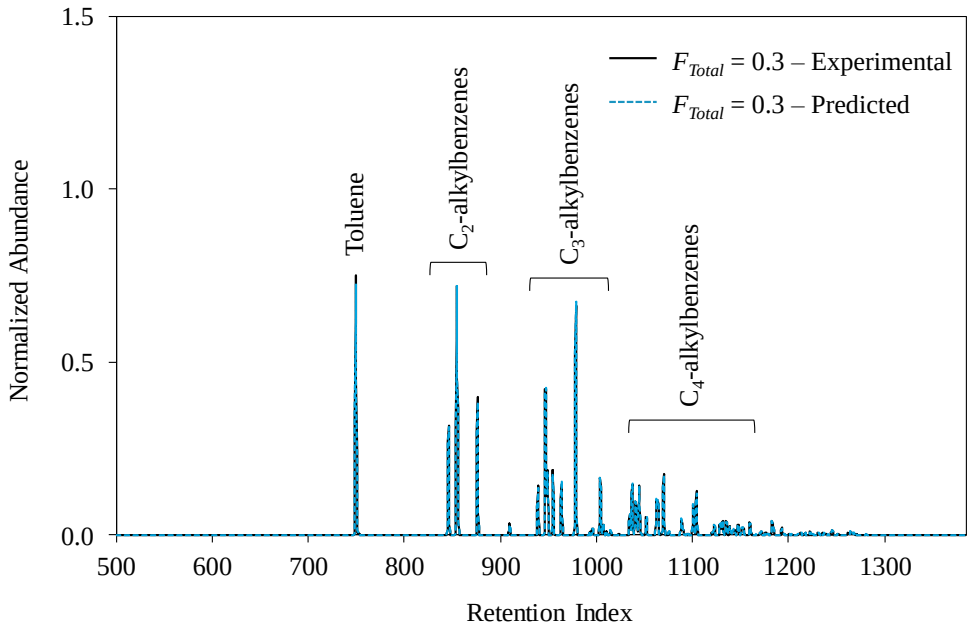

Figure 4.2 Overlay of experimental and predicted aromatic EIPs for gasoline at F_{Total} = 0.3. The predicted EIP was generated using F_{Total} by area.

For the marine fuel stabilizer, PPMC coefficients greater than 0.92 were observed for all EIP comparisons, except for the alkane EIP comparison at F_{Total} = 0.1 (Table 4.1). Because this

is a naphthenic-paraffinic liquid consisting mostly of cycloalkanes with some alkane compounds (Figure 3.4A), EIPs of both compound classes were generated. Comparatively, the PPMC coefficients for the cycloalkane EIP comparisons were greater than the PPMC coefficients for the alkane EIP comparisons at corresponding evaporation levels. Higher PPMC coefficients for the cycloalkane EIP comparisons were reasonable given that the cycloalkane profile was the most representative for this liquid. The lowest PPMC coefficient (r = 0.8592) was associated with the alkane EIP comparison at F_{Total} = 0.1. While the predicted abundances for compounds above I^T = 1300 agreed well with those in the experimental EIP, evaporation was overpredicted for those below I^T = 1300 (Figure 4.3). Overprediction for compounds at similar retention indices was observed for the marine fuel stabilizer at F_{Total} = 0.1 for the TIC comparison (Figure 3.5) and was likely due to the higher response factor for alkanes of higher carbon numbers. The PPMC coefficient for the cycloalkane EIP comparison at F_{Total} = 0.1 (r = 0.9235) was greater than that for the alkane comparison; thus, using both the alkane and cycloalkane profiles together increased confidence in identification.

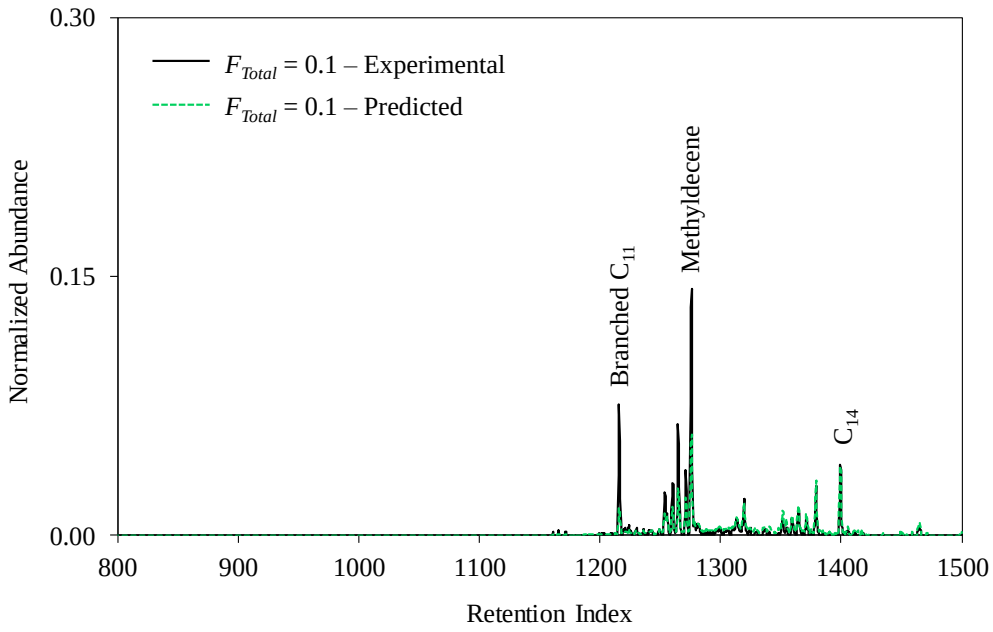

Figure 4.3 Overlay of experimental and predicted alkane EIPs for marine fuel stabilizer at F_{Total} = 0.1 across the reduced range I^T = 800 – 1500. The predicted EIP was generated using F_{Total} by area.

Strong correlation was observed for the lacquer thinner comparisons, with PPMC coefficients greater than 0.97 observed at all evaporation levels (Table 4.1). The lacquer thinner mainly consisted of aromatic compounds (Figure 3.6A), thus the aromatic EIP was the only profile generated for this liquid. The highest PPMC coefficient was associated with the comparison at F_{Total} = 0.3, and the abundances in the predicted EIP agreed well with those in the experimental profile (Figure 4.4). The TIC comparison at F_{Total} = 0.3 (Table 3.3) was associated with one of the lowest mean PPMC coefficients for the aromatic class when F_{Total} by area was used (r = 0.84) because of the overprediction of evaporation for the non-aromatic compounds present in the lacquer thinner. Those compounds were not present in the aromatic EIP; therefore, the PPMC coefficient for the aromatic EIP comparisons (*e.g.*, r = 0.9969 at F_{Total} = 0.3) were higher than those for the TIC comparisons.

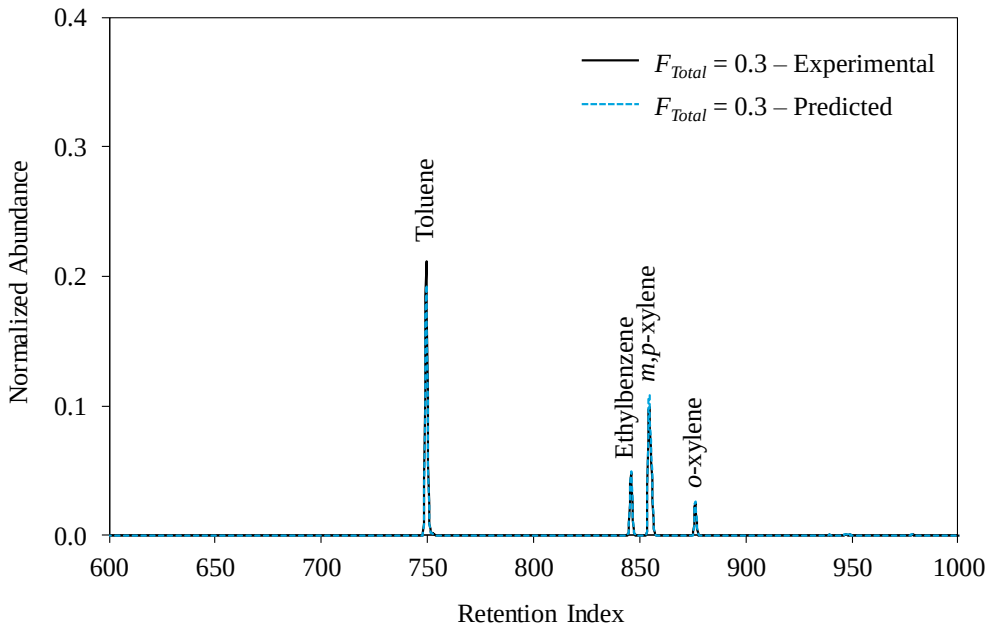

Figure 4.4 Overlay of experimental and predicted aromatic EIPs for lacquer thinner at F_{Total} = 0.3 across the reduced range I^T = 600 – 1000. The predicted EIP was generated using F_{Total} by area.

For the MI KleanStrip® paint thinner, PPMC coefficients above 0.97 were observed for the comparisons of all predicted and experimental EIPs at F_{Total} = 0.5 and 0.3; however, coefficients below 0.9 were observed for the comparisons at F_{Total} = 0.1 (Table 4.1). A similar trend was observed for the TIC comparison for the paint thinner (Table 3.5), for which the PPMC coefficient at F_{Total} = 0.1 by area (r = 0.81) was lower than those at higher F_{Total} levels. Therefore, it was reasonable that the same phenomenon occurred for the EIP comparisons for this liquid. Similar to the TIC comparison, the lower correlation at F_{Total} = 0.1 was due to overprediction of evaporation for compounds around I^T = 1000. For example, for the alkane EIP comparison at F_{Total} = 0.1, the predicted abundance of C_{10} (I^T = 1000) was lower than the abundance in the experimental EIP (Figure 4.5). The PPMC coefficient from I^T = 1030 – 1385 (omitting C_{10}) was 0.9593, whereas the PPMC coefficient across the entire retention index range (I^T = 500 – 1385) was 0.8543. Similar overprediction occurred in the profiles of the other EIP

classes at F_{Total} = 0.1. Given that the compounds around I^T = 1000 are relatively non-volatile, the model was expected to predict the respective abundances with greater accuracy. The paint thinner was experimentally evaporated to F_{Total} = 0.1 a second time and similar results were observed between the experimental and predicted EIPs, rendering the comparisons at this evaporation level anomalies in the data set. However, given the high PPMC coefficients at F_{Total} = 0.5 and 0.3, good predictive accuracy of the model was still demonstrated.

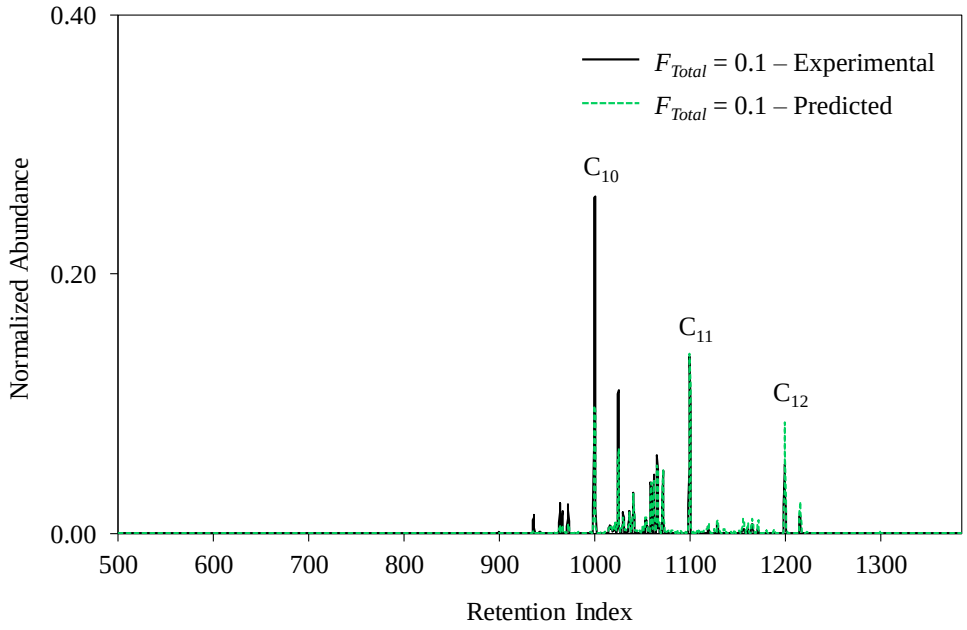

Figure 4.5 Overlay of experimental and predicted alkane EIPs for MI KleanStrip® paint thinner at F_{Total} = 0.1. The predicted EIP was generated using F_{Total} by area.

4.2 Identification of Evaporated Liquids Based on Comparison to EIP Reference Collection

A reference collection of predicted EIPs was generated with the same liquids used for the TIC reference collection in Chapter 3. Profiles were first generated from the TICs of the unevaporated liquids. For a given liquid, only EIPs that contained relevant compounds were included in the reference collection: EIPs that contained no compounds or that contained only noise were not included. The model was then applied to the profiles in the unevaporated states to

generate predicted EIPs from F_{Total} = 0.9 – 0.1 in increments of 0.1. Overall, for the 18 liquids, the EIP reference collection contained a total of 513 predicted EIPs.

Extracted ion profiles of the experimentally evaporated liquids were first compared to the predicted EIP reference collection. As an example, consider the alkane, cycloalkane, and PNA EIPs for Crown® paint thinner experimentally evaporated to F_{Total} = 0.5. The experimentally generated EIPs were compared to the corresponding predicted EIPs for this liquid (Figure 4.6). For each EIP comparison, a plot of PPMC vs. F_{Total} was generated to determine the maximum PPMC coefficient and corresponding F_{Total} value. For the experimental alkane EIP, the maximum PPMC coefficient for comparison to the predicted alkane EIPs was 0.9898, which occurred for comparison to the predicted EIP corresponding to F_{Total} = 0.6. Similarly, for the experimental cycloalkane EIP, the maximum coefficient was 0.9904, associated with the comparison to the predicted cycloalkane EIP at F_{Total} = 0.6. The maximum PPMC coefficient for the comparison of the experimental PNA EIP was 0.9515 for the comparison to the predicted PNA EIP at F_{Total} = 0.5 (Figure 4.6).

Thus, for the Crown® paint thinner, maximum PPMC coefficients of 0.9898, 0.9904, and 0.9515, were observed for the alkane, cycloalkane, and PNA EIPs, respectively. For the Crown® paint thinner example used for comparison to the TIC reference collection (Chapter 3, Figure 3.14), the maximum PPMC coefficient was 0.9903 at F_{Total} = 0.6. The PPMC coefficient for the cycloalkane EIP comparison was extremely similar to the coefficient observed for the TIC comparison. While the maximum PPMC coefficients observed for the alkane and PNA EIP comparisons were less than 0.99, they still indicated strong correlation. When the three EIP comparisons were used together, the high maximum PPMC coefficients for each one increased

support in identification of the liquid as the Crown® paint thinner. Additionally, the EIPs are likely more applicable in a practical setting given substrate interferences in fire debris samples.

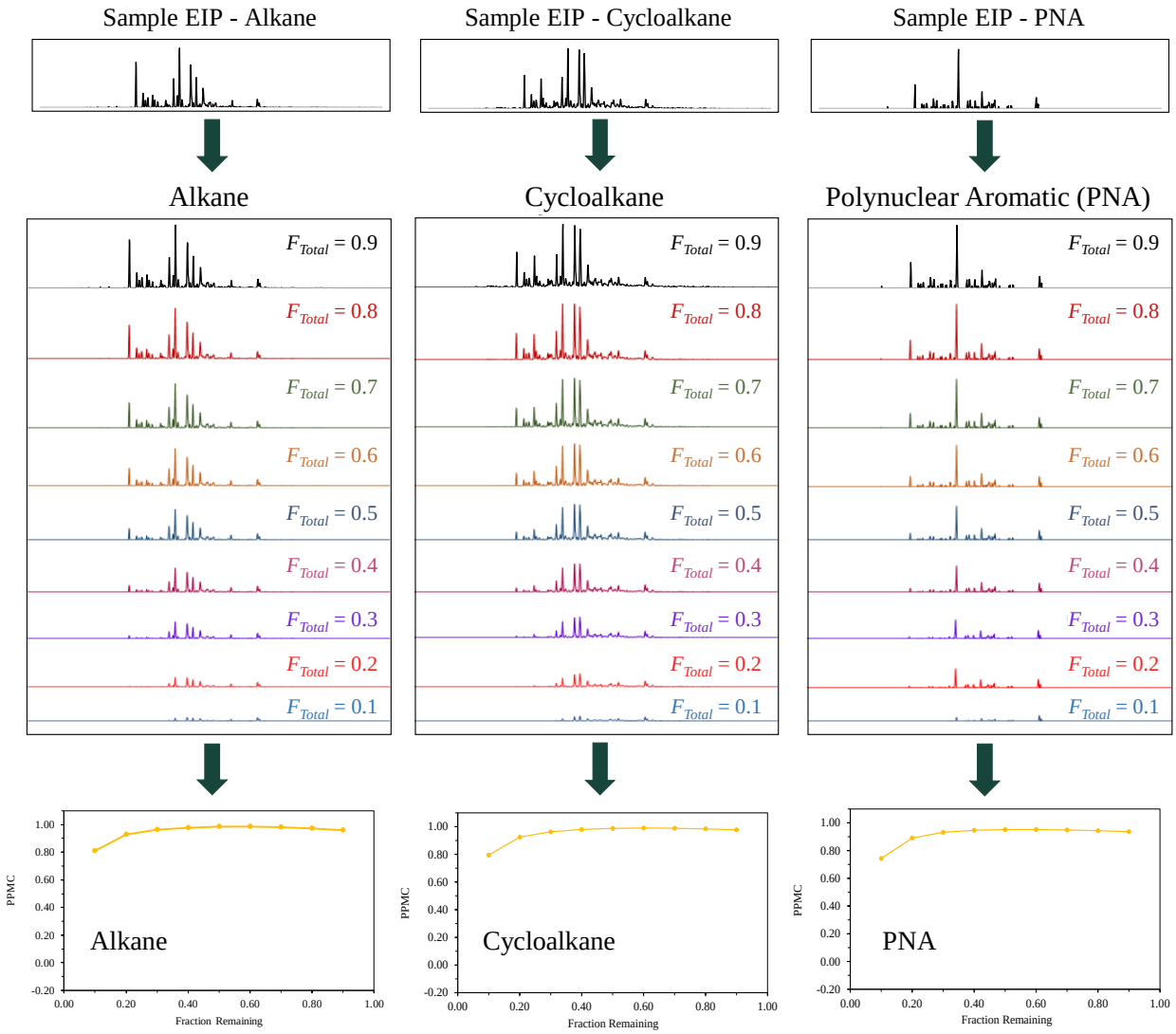

Figure 4.6 Schematic of ignitable liquid identification process using the EIP reference collection

The EIPs generated for the experimentally evaporated liquids discussed in Section 4.1 were compared to the corresponding predicted EIPs in the EIP reference collection to assess the ability of the collection to be used as a tool for ignitable liquid class identification. In general, the majority of comparisons resulted in greatest correlation with the corresponding liquid. The

PPMC coefficients for the comparisons of experimental EIPs to the reference collection for the isoparaffinic lighter fluid are shown in Table 4.2, and the coefficients for the comparisons for the remaining isoparaffinic liquids are in Appendix 4B.

Table 4.2 Maximum PPMC coefficients and corresponding liquids and F_{Total} levels for comparisons of experimental EIPs of lighter fluid (isoparaffinic class) to EIP reference collection

Ignitable Liquid/ EIP Class	Nominal F_{Total}	Liquid at Max PPMC	Max PPMC	F_{Total} at Max PPMC
Lighter Fluid: **Alkane EIPs** *(Light)*	0.5	Lighter Fluid	0.9986	0.7
	0.3	Lighter Fluid	0.9974	0.4
	0.1	Lighter Fluid	0.9893	0.1
Lighter Fluid: **Cycloalkane EIPs** *(Light)*	0.5	Lighter Fluid	0.9990	0.6
	0.3	Lighter Fluid	0.9894	0.3
	0.1	Lighter Fluid	0.9658	0.1
Lighter Fluid: **PNA EIPs** *(Light)*	0.5	Lighter Fluid	0.9971	0.7
	0.3	Lighter Fluid	0.9978	0.7
	0.1	Lighter Fluid	0.9918	0.2

For comparisons of the experimental alkane, cycloalkane, and PNA EIPs to the corresponding predicted EIPs in the reference collection, strong correlation was observed for the same-source liquid at all evaporation levels (Table 4.2). Maximum PPMC coefficients ranged from 0.9658 to 0.9990 across all comparisons. For the alkane and PNA EIP comparisons, strong correlation was also observed for the naphthenic-paraffinic paint and varnish thinner (Figure 4.7A and 4.7B), which contained some of the same alkane and polynuclear aromatic compounds that were present in the lighter fluid. For the cycloalkane EIP comparison, strong correlation was also observed for gasoline (Figure 4.7C), which was reasonable given that gasoline contained similar cyclic compounds at low retention indices ($I^T < 800$). However, for all three EIP comparisons, the PPMC coefficients for the paint and varnish thinner (alkane and PNA EIP comparison) and gasoline (cycloalkane EIP comparison) were less than 0.89, whereas the maximum PPMC coefficients for the lighter fluid were greater than 0.96 across the three EIP

class comparisons. All other liquids exhibited moderate to no correlation for each comparison, which increased confidence in identification as the lighter fluid.

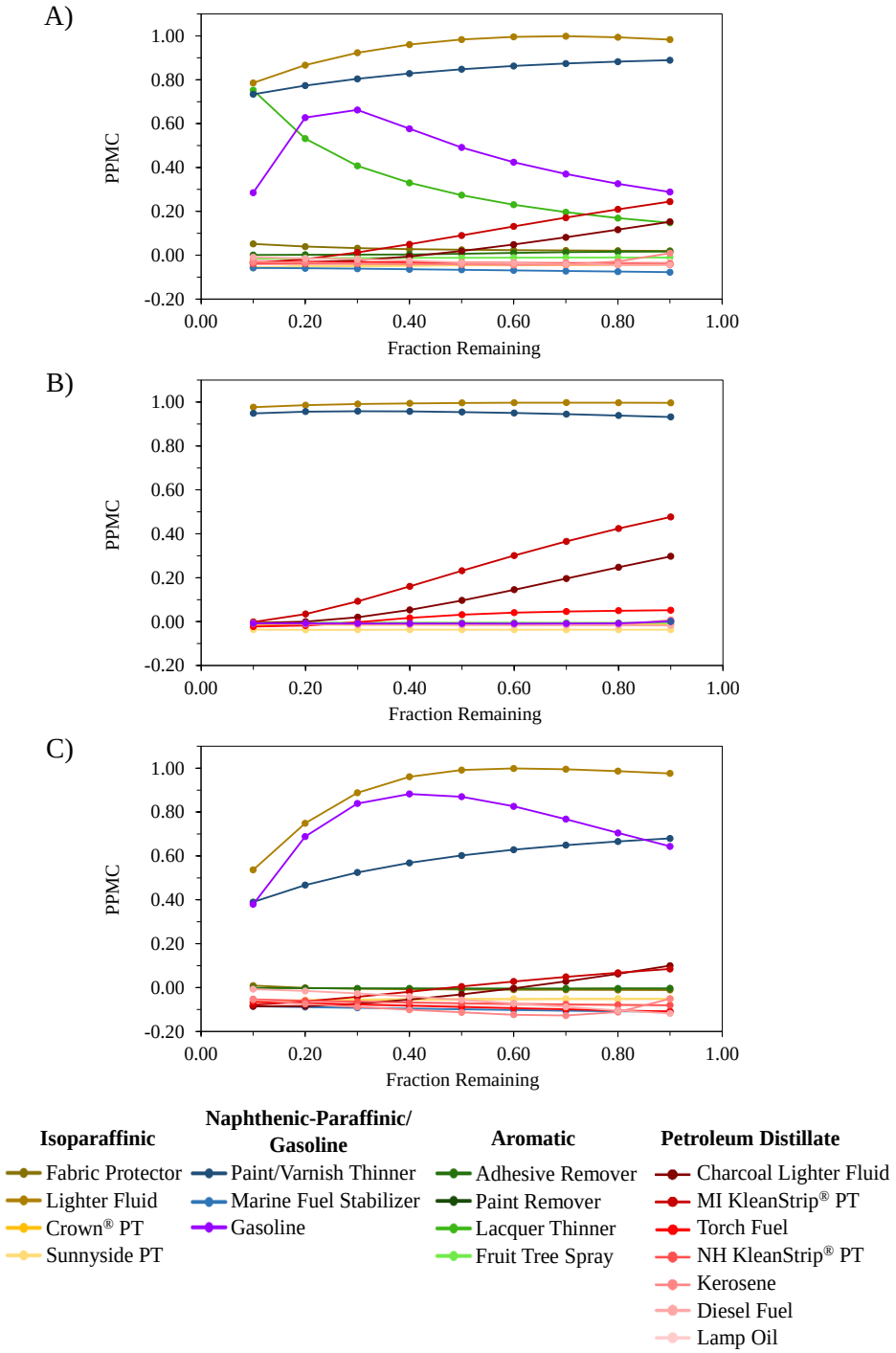

Figure 4.7 PPMC vs. F_{Total} plots for comparisons of lighter fluid (A) alkane EIP, (B) PNA EIP, and (C) cycloalkane EIP at F_{Total} = 0.5 to corresponding predicted EIPs in EIP reference collection

Across all EIP comparisons for the lighter fluid, the F_{Total} levels corresponding to the maximum PPMC coefficient generally agreed with the corresponding nominal F_{Total} values within ± 0.2 (Table 4.2, column 5). The only deviation occurred for the PNA EIP at F_{Total} = 0.3, for which the maximum PPMC coefficient occurred at F_{Total} = 0.7. For this comparison, the PPMC coefficients at all nine F_{Total} levels were very similar and ranged from 0.9792 to 0.9978. The PPMC coefficient at F_{Total} = 0.3 was 0.9927, which was very close to the maximum value. However, identifying liquid class rather than F_{Total} level is the goal in fire debris analysis, and these results show that this is possible.

Representative comparisons for the paint and varnish thinner EIPs to the EIP reference collection are shown in Table 4.3, and all other naphthenic-paraffinic liquid comparisons are shown in Appendix 4B. Each of the paint and varnish thinner EIP comparisons resulted in strongest correlation to the corresponding predicted EIPs of the same-source liquid (Table 4.3), with corresponding F_{Total} levels within ± 0.1 of the nominal F_{Total} levels. Across both profile classes and all three evaporation levels, PPMC coefficients ranged from 0.9682 to 0.9743. For the alkane EIP comparison at F_{Total} = 0.5, strong correlation also was observed for the isoparaffinic lighter fluid (Figure 4.8A). The strong correlation with the isoparaffinic liquid was due to similarities in chromatographic profiles and retention index ranges, which was discussed previously for the comparison of the lighter fluid alkane and PNA EIPs to the reference collection. For the remaining liquids in the reference collection, moderate to weak correlation was observed.

Table 4.3 Maximum PPMC coefficients and corresponding liquids and F_{Total} levels for comparisons of experimental EIPs of paint and varnish thinner (naphthenic-paraffinic class) to EIP reference collection

Ignitable Liquid/ EIP Class	Nominal F_{Total}	Liquid at Max PPMC	Max PPMC	F_{Total} at Max PPMC
Paint and Varnish Thinner: **Alkane EIPs** *(Light)*	0.5	Paint and Varnish Thinner	0.9741	0.5
	0.3	Paint and Varnish Thinner	0.9877	0.3
	0.1	Paint and Varnish Thinner	0.9728	0.1
Paint and Varnish Thinner: **Cycloalkane EIPs** *(Light)*	0.5	Paint and Varnish Thinner	0.9903	0.4
	0.3	Paint and Varnish Thinner	0.9871	0.2
	0.1	Paint and Varnish Thinner	0.9743	0.1

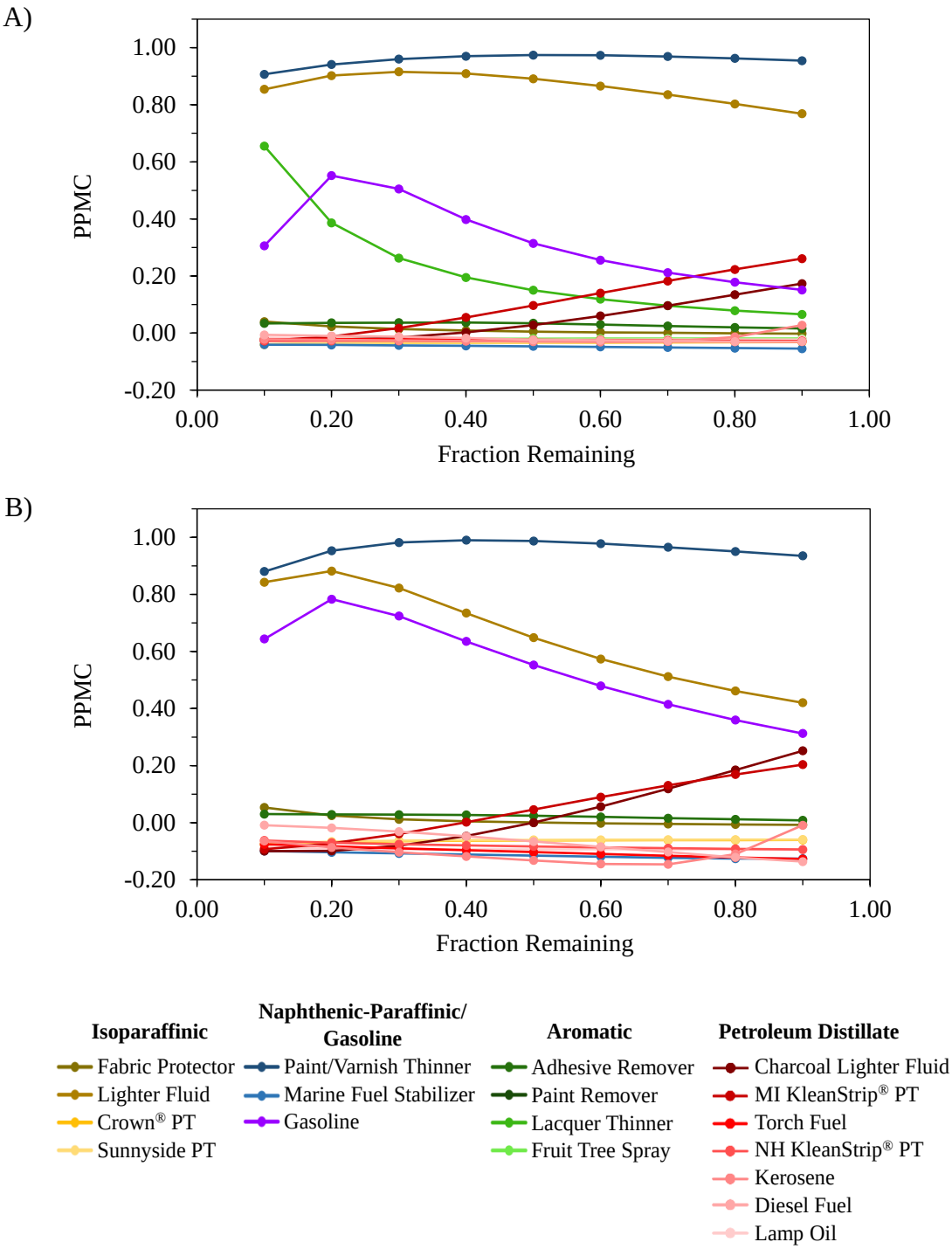

Figure 4.8 PPMC vs. F_{Total} plots for comparisons of paint and varnish thinner (A) alkane EIP and (B) cycloalkane EIP at F_{Total} = 0.5 to corresponding predicted EIPs in EIP reference collection

Figure 4.8B shows the PPMC vs. F_{Total} plot for comparison of the experimental cycloalkane EIP for F_{Total} = 0.5 paint and varnish thinner to the EIP reference collection. At low F_{Total} levels (F_{Total} = 0.1 and 0.2), the experimental EIP strongly correlated to predicted EIPs for lighter fluid (isoparaffinic) and paint and varnish thinner. However, as F_{Total} increased, correlation to the lighter fluid decreased, indicating only moderate correlation, whereas correlation to the paint and varnish thinner remained strong, with PPMC coefficients greater than 0.9. This example highlights the importance of using all sample EIPs to determine liquid class identity. While confusion could arise if only the alkane comparison plot were used in this case, the greater correlation with the same-source liquid in the cycloalkane comparison plot increased confidence in identification of the naphthenic-paraffinic liquid.

Representative comparisons for the adhesive remover EIPs to the EIP reference collection are shown in Table 4.4, and all other aromatic liquids are summarized in Appendix 4B. Comparisons for the adhesive remover experimental EIPs to the predicted aromatic EIPs all resulted in strongest correlation to liquids of the same-source ASTM liquid class (Table 4.4). More specifically, for the comparison at F_{Total} = 0.5, the maximum PPMC coefficient (r = 0.9909) indicated strong correlation to the same-source liquid. While the coefficients for the F_{Total} = 0.3 and 0.1 comparisons also indicated strong correlation, association was to the paint remover, another liquid in the aromatic class. This was reasonable considering that the paint remover contained the same three alkylbenzenes as the adhesive remover but at higher abundances.

Table 4.4 Maximum PPMC coefficients and corresponding liquids and F_{Total} levels for comparisons of experimental EIPs of adhesive remover (aromatic class) to EIP reference collection

Ignitable Liquid/ EIP Class	Nominal F_{Total}	Liquid at Max PPMC	Max PPMC	F_{Total} at Max PPMC
Adhesive Remover: **Aromatic EIPs** *(Light)*	0.5	Adhesive Remover	0.9909	0.7
	0.3	Paint Remover	0.9723	0.2
	0.1	Paint Remover	0.9473	0.1

While correlation was strongest to the paint remover at F_{Total} = 0.3 and 0.1, strong correlation to the adhesive remover was also observed (Figure 4.9). The PPMC coefficients for the adhesive remover at both F_{Total} = 0.3 and 0.1 were very close to those for the paint remover, with average differences less than 0.01. For example, for the comparison at F_{Total} = 0.3 (Figure 4.9A), the maximum PPMC coefficient associated with the adhesive remover predicted EIPs was 0.9623 at F_{Total} = 0.5. This PPMC coefficient was very close to the overall maximum value (r = 0.9723). Similarly, for the comparison at F_{Total} = 0.1 (Figure 4.9B), the maximum PPMC coefficient (r = 0.9360 at F_{Total} = 0.1) was only slightly lower than the overall maximum coefficient (r = 0.9473). Based on these results, the liquid class could be identified (aromatic), but not the specific liquid.

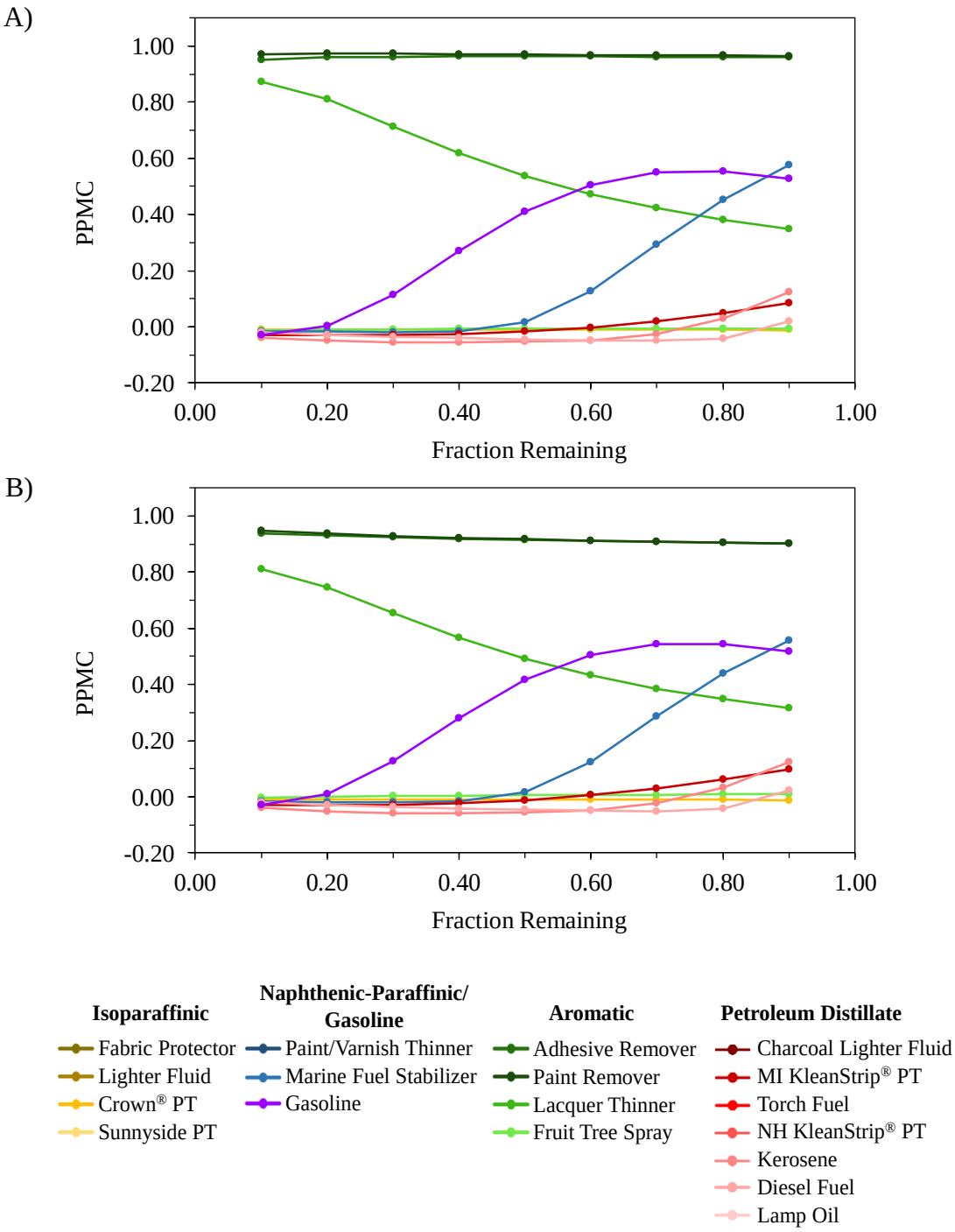

Figure 4.9 PPMC vs. F_{Total} plots for comparisons of adhesive remover experimental aromatic EIPs to predicted EIPs in reference collection at (A) F_{Total} = 0.3 and (B) F_{Total} = 0.1

Comparisons of petroleum distillate liquid EIPs to the EIP reference collection also proved successful in identifying liquid class. When compared to the EIP reference collection, the

experimental EIPs for the charcoal lighter fluid exhibited strongest correlation with the corresponding predicted EIPs for the same-source liquid (Table 4.5). The PPMC coefficients for comparison of experimental and predicted EIPs for the other petroleum distillates are shown in Appendix 4B. Across the three representative EIP classes for the charcoal lighter fluid and for all evaporation levels, PPMC coefficients ranged from 0.9372 to 0.9925. The F_{Total} levels associated with the maximum PPMC coefficients were all close to the nominal levels; any differences were within ± 0.1. The lowest PPMC coefficient (r = 0.9372) occurred for the cycloalkane EIP comparison at F_{Total} = 0.1. Similarly, in Section 4.1, the PPMC coefficient for comparison of the experimental and predicted cycloalkane EIPs at F_{Total} = 0.1 was comparatively lower than those at F_{Total} = 0.5 and 0.3. The lower correlation was due to overprediction of abundances (see Table A.8 in Appendix 4A), similar to the overprediction discussed for the MI KleanStrip® paint thinner. Similar reasons were the cause for the lower PPMC coefficient for this EIP class comparison. Nevertheless, strong correlation was still observed for the same-source liquid.

Table 4.5 Maximum PPMC coefficients and corresponding liquids and F_{Total} levels for comparisons of experimental EIPs of charcoal lighter fluid (petroleum distillate class) to EIP reference collection

Ignitable Liquid/ EIP Class	Nominal F_{Total}	Liquid at Max PPMC	Max PPMC	F_{Total} at Max PPMC
Charcoal Lighter Fluid: **Alkane EIPs** *(Medium)*	0.5	Charcoal Lighter Fluid	0.9925	0.6
	0.3	Charcoal Lighter Fluid	0.9942	0.4
	0.1	Charcoal Lighter Fluid	0.9690	0.2
Charcoal Lighter Fluid: **Cycloalkane EIPs** *(Medium)*	0.5	Charcoal Lighter Fluid	0.9930	0.5
	0.3	Charcoal Lighter Fluid	0.9877	0.3
	0.1	Charcoal Lighter Fluid	0.9372	0.1
Charcoal Lighter Fluid: **PNA EIPs** *(Medium)*	0.5	Charcoal Lighter Fluid	0.9919	0.5
	0.3	Charcoal Lighter Fluid	0.9787	0.3
	0.1	Charcoal Lighter Fluid	0.9608	0.1

Figure 4.10 illustrates the utility of the EIP reference collection for the identification of liquid class present for the charcoal lighter fluid example. The PPMC vs. F_{Total} plots show the

visual depiction of correlation for the comparison of the experimental F_{Total} = 0.3 charcoal lighter fluid EIPs to the corresponding predicted EIPs in the reference collection. All three plots show that strongest correlation was associated with the charcoal lighter fluid itself, and the highest PPMC values were associated with F_{Total} levels closest to the actual evaporation level (F_{Total} = 0.3). Strong correlation was also exhibited for the MI KleanStrip® paint thinner at low F_{Total} levels. These two liquids, both petroleum distillates, contained similar *n*-alkanes and cycloalkanes along the same retention index range (I^T = 800 – 1200).

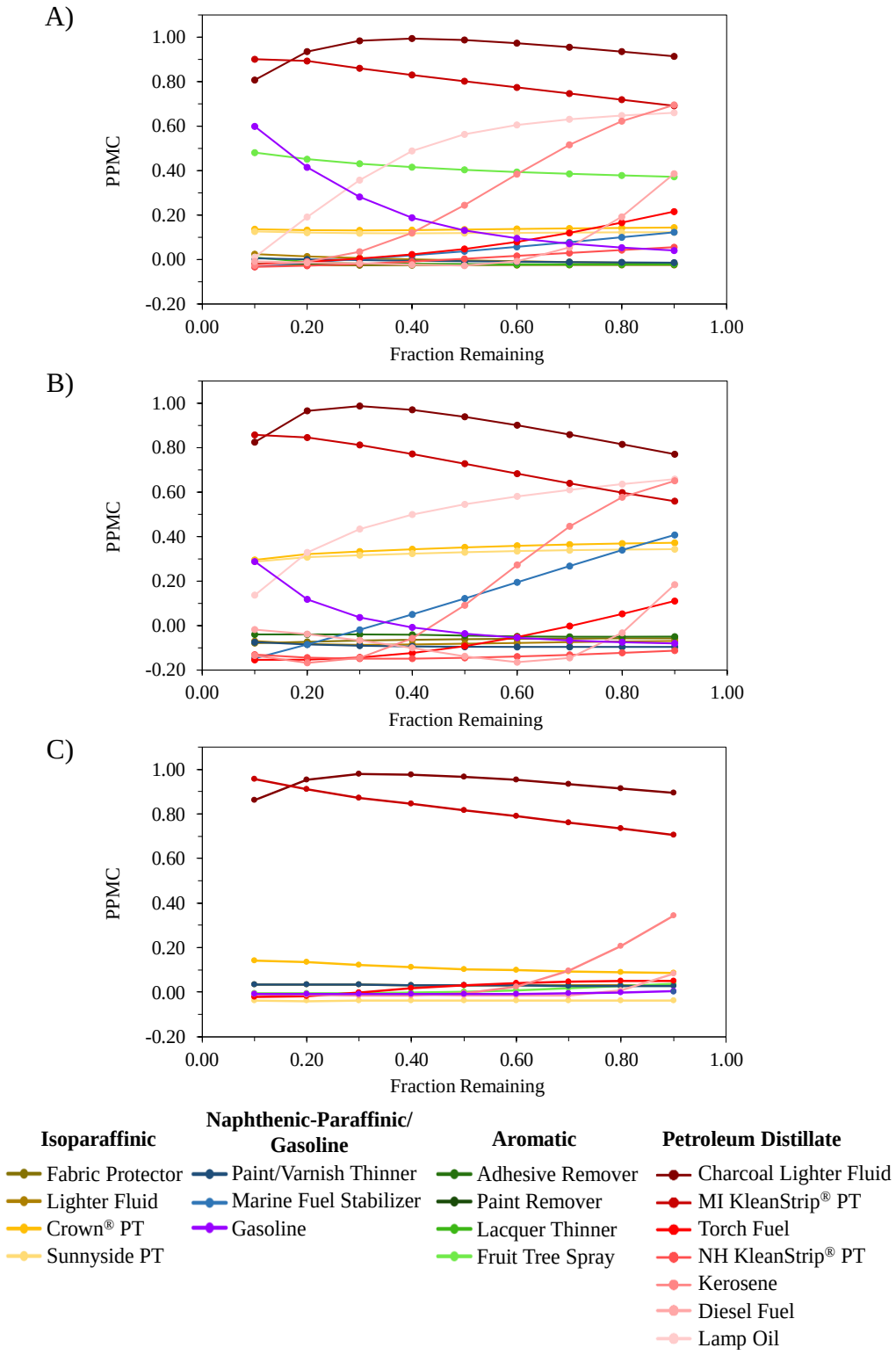

Figure 4.10 PPMC vs. F_{Total} plots for comparisons of charcoal lighter fluid (A) alkane EIP, (B) cycloalkane EIP, and (C) PNA EIP at F_{Total} = 0.3 to corresponding predicted EIPs in EIP reference collection

Lastly, the EIPs for the gasoline sample were compared to the EIP reference collection, and the PPMC coefficients for the comparisons are shown in Table 4.6. The experimental EIPs most strongly correlated to the predicted EIPs for gasoline for each profile class and evaporation level (Figure 4.11). The PPMC coefficients across all comparisons ranged from 0.9332 to 0.9984 (Table 4.6). The F_{Total} levels corresponding to the maximum PPMC coefficients were generally higher than the nominal values, especially for comparisons at F_{Total} = 0.5 and 0.3. This was due to the effect of the detector response factor for gasoline, described previously in Chapter 3. Because the effect leads to greater F_{Total} by area values compared to the nominal F_{Total} values, it was reasonable that the F_{Total} at maximum PPMC was higher than the nominal value, as discussed for the comparison to the TIC reference collection at F_{Total} = 0.5 in Chapter 3, Section 3.2.

Table 4.6 Maximum PPMC coefficients and corresponding liquids and F_{Total} levels for comparisons of experimental EIPs of gasoline to EIP reference collection

Ignitable Liquid/ EIP Class	Nominal F_{Total}	Liquid at Max PPMC	Max PPMC	F_{Total} at Max PPMC
Gasoline: **Alkane EIPs**	0.5	Gasoline	0.9955	0.9
	0.3	Gasoline	0.9934	0.4
	0.1	Gasoline	0.9332	0.1
Gasoline: **Cycloalkane EIPs**	0.5	Gasoline	0.9912	0.9
	0.3	Gasoline	0.9692	0.4
	0.1	*	*	*
Gasoline: **Aromatic EIPs**	0.5	Gasoline	0.9963	0.9
	0.3	Gasoline	0.9984	0.8
	0.1	Gasoline	0.9935	0.3
Gasoline: **Indane EIPs**	0.5	Gasoline	0.9952	0.9
	0.3	Gasoline	0.9934	0.9
	0.1	Gasoline	0.9945	0.8
Gasoline: **PNA EIPs**	0.5	Gasoline	0.9964	0.9
	0.3	Gasoline	0.9957	0.9
	0.1	Gasoline	0.9973	0.9

*Comparison not performed due to low abundances in experimental EIP

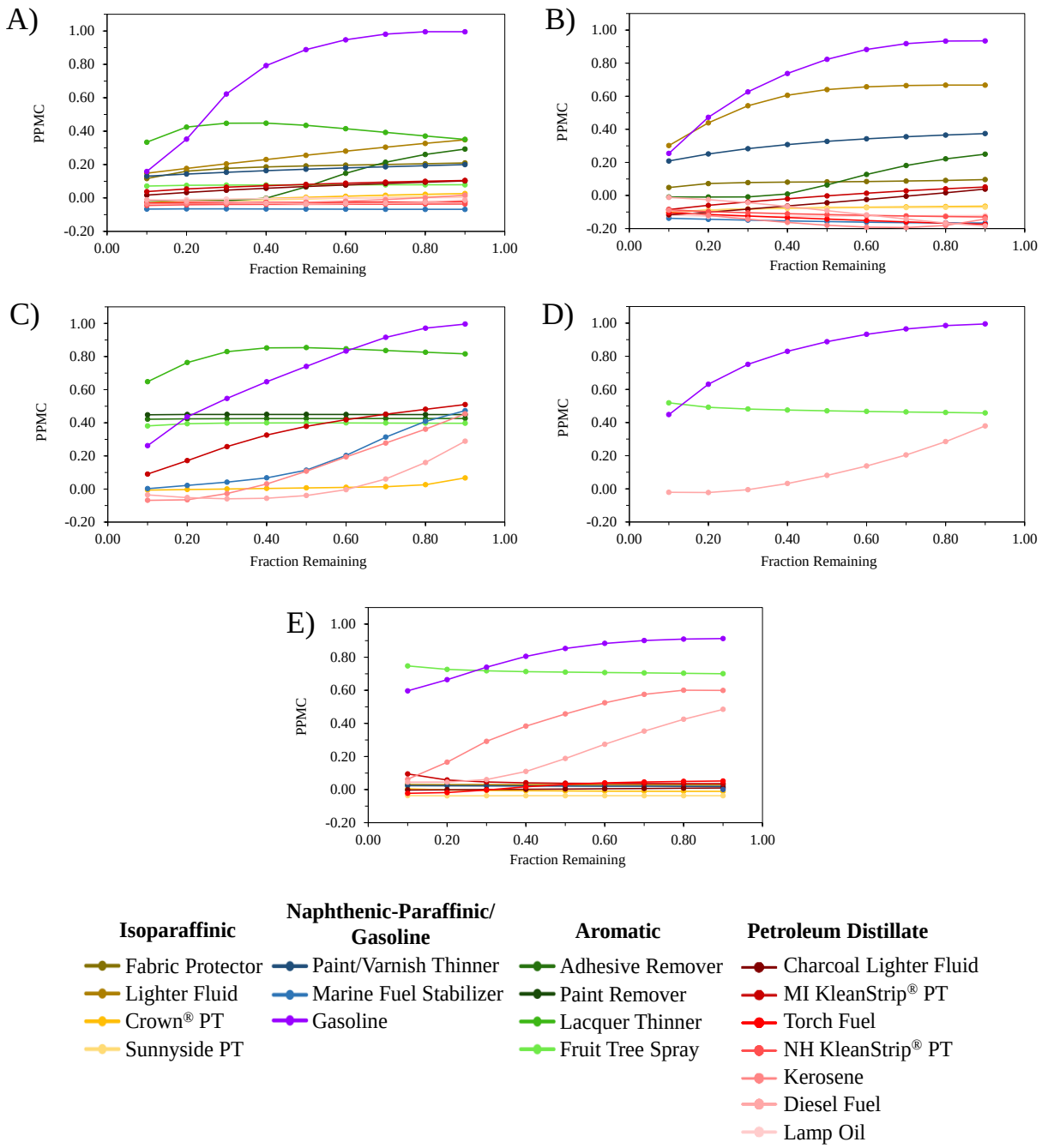

Figure 4.11 PPMC vs. F_{Total} plots for comparisons of gasoline (A) alkane EIP, (B) cycloalkane EIP, (C) aromatic EIP, (D) indane EIP, and (E) PNA EIP at F_{Total} = 0.3 to corresponding predicted EIPs in EIP reference collection

4.3 Summary

Based on comparisons between EIPs of experimentally evaporated liquids and corresponding predicted profiles, the kinetic model accurately predicted profiles of five compound classes. Specifically, across all liquid classes, profile classes, and evaporation levels, PPMC coefficients ranged from 0.8476 to 0.9984, indicating strong correlation. These results demonstrate the ability of the model to predict EIPs at any given evaporation level.

A reference collection containing predicted EIPs was successfully generated. The utility of the collection to aid in the identification of ignitable liquid class was demonstrated through comparisons to liquids experimentally evaporated to known levels. In cases for which the maximum PPMC coefficient corresponded to a liquid other than the same-source liquid or class, the correlation was reasonable given the compounds present in the specific profile. Taking into account all relevant profiles for a given liquid, the correct ASTM class was identified. Generation of the EIP reference collection demonstrated the application of the model for use in the identification of ignitable liquids present in fire debris samples that contain substrate interferences.

APPENDICES

APPENDIX 4A:

PPMC Coefficients for Comparisons of Experimental and Predicted EIPs

Table A.5 PPMC coefficients for comparisons between experimental and predicted EIPs for major compound classes present in isoparaffinic liquids. Predicted EIPs were generated using F_{Total} by area

Ignitable Liquid	Nominal F_{Total}	EIP Class & PPMC Coefficient	
		Alkane	Cycloalkane
Fabric and Upholstery Protector *(Light)*	0.5	0.9948	*
	0.3	0.9826	*
	0.1	**	*
Crown® Paint Thinner *(Medium)*	0.5	0.9876	0.9911
	0.3	0.9913	0.9903
	0.1	0.9598	0.9295
Sunnyside Paint Thinner *(Medium)*	0.5	0.9887	0.9894
	0.3	0.9885	0.9916
	0.1	0.9399	0.8715

*Profile class not representative of liquid (EIPs not generated)
**Comparison not performed due to low abundances in experimental EIP

Table A.6 PPMC coefficients for comparisons between experimental and predicted EIPs for major compound classes present in naphthenic-paraffinic liquids. Predicted EIPs were generated using F_{Total} by area

Ignitable Liquid	Nominal F_{Total}	EIP Class & PPMC Coefficient		
		Aromatic	Cycloalkane	PNA
Paint and Varnish Thinner *(Light)*	0.5	0.9705	0.9895	0.9696
	0.3	0.9858	0.9866	0.9868
	0.1	0.9759	0.9819	0.9824

Table A.7 PPMC coefficients for comparisons between experimental and predicted EIPs for major compound classes present in aromatic liquids. Predicted EIPs were generated using F_{Total} by area

Ignitable Liquid	Nominal F_{Total}	EIP Class & PPMC Coefficient		
		Aromatic	Indane	PNA
Adhesive Remover *(Light)*	0.5	0.9903	*	*
	0.3	0.9614	*	*
	0.1	0.9363	*	*
Paint Remover *(Light)*	0.5	0.9813	*	*
	0.3	0.9596	*	*
	0.1	0.9460	*	*
Fruit Tree Spray *(Medium)*	0.5	0.9906	0.9926	0.9983
	0.3	0.9607	0.9866	0.9976
	0.1	0.8472	0.9572	0.9947

*Profile class not representative of liquid (EIPs not generated)

Table A.8 PPMC coefficients for comparisons between experimental and predicted EIPs for major compound classes present in petroleum distillate liquids. Predicted EIPs were generated using F_{Total} by area

Ignitable Liquid	Nominal F_{Total}	EIP Class & PPMC Coefficient	
		Alkane	Cycloalkane
Charcoal Lighter Fluid *(Medium)*	0.5	0.9934	0.9950
	0.3	0.9857	0.9819
	0.1	0.9181	0.8476
NH KleanStrip® Paint Thinner *(Heavy)*	0.5	0.9882	0.9852
	0.3	0.9739	0.9695
	0.1	0.9763	0.9555
Torch Fuel *(Heavy)*	0.5	0.9790	0.9679
	0.3	0.9923	0.9686
	0.1	0.9745	0.9254
Lamp Oil *(Heavy)*	0.5	0.9806	0.9882
	0.3	0.9834	0.9815
	0.1	0.9954	0.9922

APPENDIX 4B:

Maximum PPMC coefficients, corresponding liquids and F_{Total} values for comparisons of experimental EIPs to EIP reference collection

Table A.9 Maximum PPMC coefficients and corresponding ignitable liquids and F_{Total} values for comparisons of relevant EIPs of experimentally evaporated isoparaffinic liquids to EIP reference collection

Ignitable Liquid/ EIP Class	Nominal F_{Total}	Liquid at Max PPMC	Max PPMC	F_{Total} at Max PPMC
Fabric and Upholstery Protector: **Alkane EIP** *(Light)*	0.5	Fabric and Upholstery Protector	0.9963	0.7
	0.3	Fabric and Upholstery Protector	0.9934	0.4
	0.1	*	*	*
Paint Thinner (Crown®): **Alkane EIP** *(Medium)*	0.5	Paint Thinner (Crown®)	0.9898	0.6
	0.3	Paint Thinner (Crown®)	0.9923	0.4
	0.1	Paint Thinner (Crown®)	0.9796	0.1
Paint Thinner (Crown®): **Cycloalkane EIP** *(Medium)*	0.5	Paint Thinner (Crown®)	0.9929	0.6
	0.3	Paint Thinner (Crown®)	0.9923	0.4
	0.1	Paint Thinner (Crown®)	0.9564	0.2
Paint Thinner (Sunnyside): **Alkane EIP** *(Medium)*	0.5	Paint Thinner (Sunnyside)	0.9894	0.6
	0.3	Paint Thinner (Sunnyside)	0.9898	0.3
	0.1	Paint Thinner (Sunnyside)	0.9790	0.1
Paint Thinner (Sunnyside): **Cycloalkane EIP** *(Medium)*	0.5	Paint Thinner (Sunnyside)	0.9889	0.6
	0.3	Paint Thinner (Sunnyside)	0.9929	0.4
	0.1	Paint Thinner (Sunnyside)	0.9613	0.2

*Comparison not performed due to low abundances in experimental EIP

Table A.10 Maximum PPMC coefficients and corresponding ignitable liquids and F_{Total} values for comparisons of relevant EIPs of experimentally evaporated naphthenic-paraffinic liquids to EIP reference collection

Ignitable Liquid/ EIP Class	Nominal F_{Total}	Liquid at Max PPMC	Max PPMC	F_{Total} at Max PPMC
Marine Fuel Stabilizer: **Alkane EIP** *(Medium)*	0.5	Marine Fuel Stabilizer	0.9877	0.5
	0.3	Marine Fuel Stabilizer	0.9830	0.3
	0.1	Marine Fuel Stabilizer	0.9438	0.1
Marine Fuel Stabilizer: **Cycloalkane EIP** *(Medium)*	0.5	Marine Fuel Stabilizer	0.9944	0.4
	0.3	Marine Fuel Stabilizer	0.9890	0.2
	0.1	Marine Fuel Stabilizer	0.8538	0.1

Table A.11 Maximum PPMC coefficients and corresponding ignitable liquids and F_{Total} values for comparisons of relevant EIPs of experimentally evaporated aromatic liquids to EIP reference collection

Ignitable Liquid/ EIP Class	Nominal F_{Total}	Liquid at Max PPMC	Max PPMC	F_{Total} at Max PPMC
Paint Remover: **Aromatic EIP** *(Light)*	0.5	Paint Remover	0.9815	0.9
	0.3	Paint Remover	0.9598	0.5
	0.1	Paint Remover	0.9473	0.5
Lacquer Thinner: **Aromatic EIP** *(Light)*	0.5	Lacquer Thinner	0.9961	0.8
	0.3	Lacquer Thinner	0.9990	0.6
	0.1	Lacquer Thinner	0.9962	0.4
Fruit Tree Spray: **Aromatic EIP** *(Medium)*	0.5	Fruit Tree Spray	0.9906	0.5
	0.3	Fruit Tree Spray	0.9599	0.3
	0.1	Fruit Tree Spray	0.9407	0.1
Fruit Tree Spray: **Indane EIP** *(Medium)*	0.5	Fruit Tree Spray	0.9951	0.8
	0.3	Fruit Tree Spray	0.9921	0.6
	0.1	Fruit Tree Spray	0.9795	0.1

Table A.12 Maximum PPMC coefficients and corresponding ignitable liquids and F_{Total} values for comparisons of relevant EIPs of experimentally evaporated petroleum distillate liquids to EIP reference collection

Ignitable Liquid/ EIP Class	Nominal F_{Total}	Liquid at Max PPMC	Max PPMC	F_{Total} at Max PPMC
Paint Thinner (MI KleanStrip®): **Alkane EIP** *(Medium)*	0.5	Paint Thinner (MI KleanStrip®)	0.9872	0.6
	0.3	Paint Thinner (MI KleanStrip®)	0.9900	0.4
	0.1	Paint Thinner (MI KleanStrip®)	0.9749	0.2
Paint Thinner (MI KleanStrip®): **Cycloalkane EIP** *(Medium)*	0.5	Paint Thinner (MI KleanStrip®)	0.9946	0.5
	0.3	Paint Thinner (MI KleanStrip®)	0.9851	0.3
	0.1	Paint Thinner (MI KleanStrip®)	0.9351	0.1
Paint Thinner (MI KleanStrip®): **Aromatic EIP** *(Medium)*	0.5	Paint Thinner (MI KleanStrip®)	0.9897	0.6
	0.3	Paint Thinner (MI KleanStrip®)	0.9814	0.4
	0.1	Paint Thinner (MI KleanStrip®)	0.8903	0.2

Table A.12 (cont'd)

Ignitable Liquid/ EIP Class	Nominal F_{Total}	Liquid at Max PPMC	Max PPMC	F_{Total} at Max PPMC
Paint Thinner (MI KleanStrip®): **PNA EIP** *(Medium)*	0.5	Paint Thinner (MI KleanStrip®)	0.9869	0.6
	0.3	Paint Thinner (MI KleanStrip®)	0.9825	0.4
	0.1	Paint Thinner (MI KleanStrip®)	0.9295	0.2
Paint Thinner (NH KleanStrip®): **Alkane EIP** *(Heavy)*	0.5	Paint Thinner (NH KleanStrip®)	0.9898	0.6
	0.3	Torch Fuel	0.9737	0.1
	0.1	Paint Thinner (NH KleanStrip®)	0.9748	0.1
Paint Thinner (NH KleanStrip®): **Cycloalkane EIP** *(Heavy)*	0.5	Paint Thinner (NH KleanStrip®)	0.9842	0.5
	0.3	Paint Thinner (NH KleanStrip®)	0.9663	0.3
	0.1	Paint Thinner (NH KleanStrip®)	0.9539	0.1
Torch Fuel: **Alkane EIP** *(Heavy)*	0.5	Torch Fuel	0.9802	0.5
	0.3	Torch Fuel	0.9922	0.4
	0.1	Torch Fuel	0.9781	0.2
Torch Fuel: **Cycloalkane EIP** *(Heavy)*	0.5	Torch Fuel	0.9736	0.4
	0.3	Torch Fuel	0.9703	0.2
	0.1	Torch Fuel	0.9449	0.1
Lamp Oil: **Alkane EIP** *(Heavy)*	0.5	Lamp Oil	0.9802	0.6
	0.3	Lamp Oil	0.9827	0.4
	0.1	Lamp Oil	0.9970	0.2
Lamp Oil: **Cycloalkane EIP** *(Heavy)*	0.5	Lamp Oil	0.9875	0.4
	0.3	Lamp Oil	0.9789	0.2
	0.1	Lamp Oil	0.9777	0.1

V. Application of a Kinetic Model to Identify Ignitable Liquids in Blind Samples and Large-Scale Burn Samples

Determining the ASTM liquid class of an ignitable liquid present in fire debris samples can be difficult amidst the presence of ignitable liquid evaporation and substrate interferences. The work in this chapter focused on demonstrating practical application of the predicted reference collections to identify ignitable liquids in evaporated blind samples and in large-scale burn samples. In both cases, the utility of the reference collections to aid in the identification of the ASTM liquid class present was assessed. Single-blind samples were prepared by analysts other than the original analyst and consisted of liquids within the total ion chromatogram (TIC) and extracted ion profile (EIP) reference collections. More realistic samples were collected from large-scale burns conducted under conditions resembling those of actual fires, and thus the collected samples were similar to those that would be submitted to a forensic laboratory for analysis. The use of the EIP reference collection was especially relevant for the large-scale burn samples due to the presence of substrate interferences.

5.1 Identification of Ignitable Liquids in Single-Blind Samples

Three liquids (blind samples A – C) were selected from the 18 liquids in the TIC and EIP reference collections. Each blind sample was experimentally evaporated to a different, pre-selected F_{Total} level. The identities of the liquids and respective F_{Total} levels remained unknown to the original analyst. The TIC and representative EIPs of each blind sample were compared to the corresponding reference collections to determine the maximum PPMC coefficient, corresponding liquid, and F_{Total} level.

The TIC of blind sample A indicated the presence of cyclo- and branched alkanes that eluted across the approximate retention index range I^T = 1000 – 1400 (Figure 5.1A). Upon

comparison of the sample TIC to the TIC reference collection, strong correlation was observed for the marine fuel stabilizer (naphthenic-paraffinic). The maximum PPMC coefficient was 0.9743, which was observed for comparison to the predicted TIC of marine fuel stabilizer corresponding to F_{Total} = 0.6. Moderate to no correlation was observed for all other liquids in the collection, with PPMC coefficients less than 0.52 (Figure 5.1B).

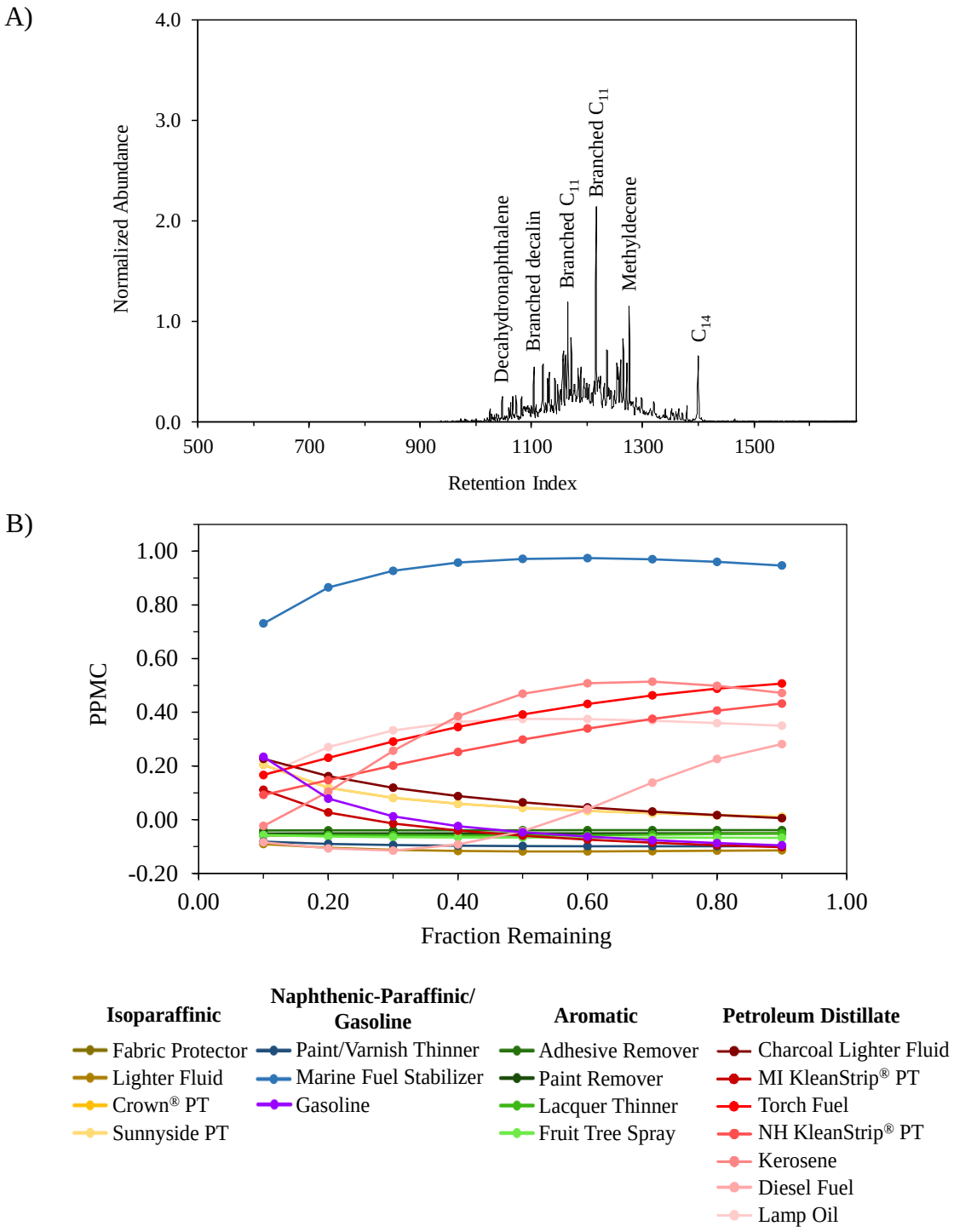

Figure 5.1 (A) TIC of single-blind sample A and (B) PPMC vs. F_{Total} plot for comparison of the TIC of blind sample A to the TIC reference collection

Using the TIC of blind sample A, EIPs were generated for the alkane and cycloalkane classes and were compared to the corresponding predicted profiles in the EIP reference collection. For the comparison of the sample alkane EIP to the predicted alkane EIPs, strongest correlation was observed for the marine fuel stabilizer. The maximum PPMC coefficient was 0.9443 and corresponded to the predicted alkane EIP at F_{Total} = 0.6. Moderate to no correlation was observed for all other liquids, with PPMC coefficients less than 0.5 (Figure 5.2A). Overall, the PPMC coefficients for the remaining liquids in the alkane EIP collection were lower when compared to the corresponding coefficients in the TIC reference collection comparison (Figure 5.1B), which indicated lower correlation with these liquids when the alkane EIP was used.

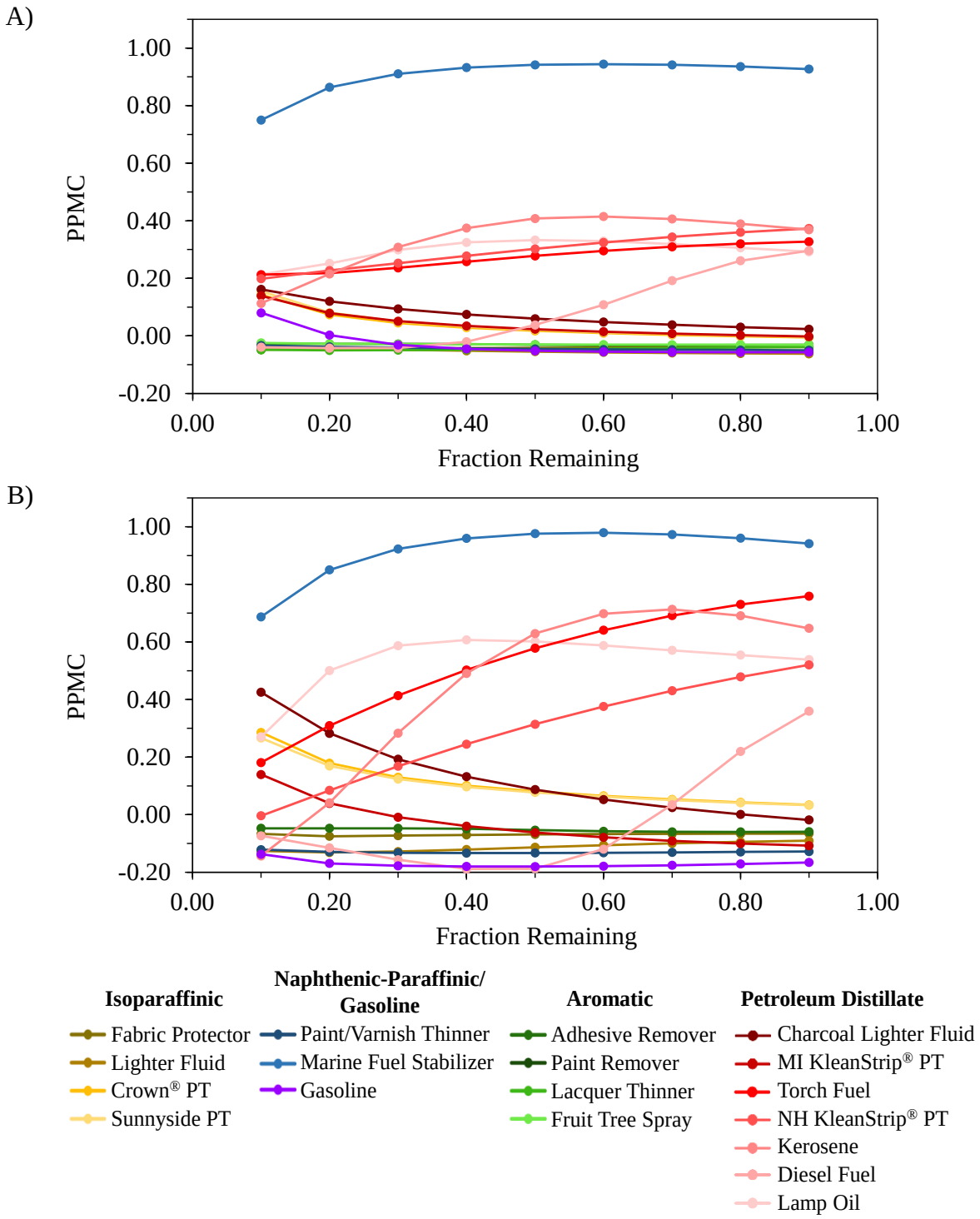

Figure 5.2 PPMC vs. F_{Total} plots for comparisons of EIPs of blind sample A to (A) the predicted alkane EIPs and (B) the predicted cycloalkane EIPs in the reference collection

For the comparison of blind sample A to the predicted cycloalkane EIPs, strongest correlation was also observed for the marine fuel stabilizer (Figure 5.2B). The maximum PPMC coefficient was 0.9793 and corresponded to F_{Total} = 0.6, similar to the alkane EIP comparison. While moderate to no correlation was observed for all other liquids in the collection, the corresponding maximum PPMC coefficients were higher compared to those for the alkane EIP comparison, especially those for torch fuel (r = 0.7590), kerosene (r = 0.7131), and lamp oil (r = 0.6070). The higher coefficients were due to the similarities of cycloalkane compounds at similar retention indices between these liquids and the sample liquid. However, using the correlation plots for the alkane and cycloalkane EIP comparisons together increased confidence in identification of the liquid as the naphthenic-paraffinic marine fuel stabilizer. This identification was correct, and the blind sample had been experimentally evaporated to F_{Total} = 0.6. The maximum PPMC coefficient for the comparison of the cycloalkane EIP (r = 0.9793) was greater than that for the alkane EIP comparison (r = 0.9443) and the TIC reference collection comparison (r = 0.9743), which was reasonable as cycloalkanes are the dominant compounds present in the marine fuel stabilizer. Overall, use of both reference collections was successful for correct ASTM liquid class identification, and use of the EIP reference collection allowed for increased confidence in identification.

Blind samples B and C were also correctly identified (both liquid and F_{Total} level) using the TIC and EIP reference collections. The corresponding TICs, EIPs, and correlation plots for the corresponding comparisons are included in the Appendix. For blind sample B, the maximum PPMC coefficient for the comparison to the TIC reference collection was 0.9979, associated with the predicted TIC for torch fuel at F_{Total} = 0.7. Comparisons of the alkane and cycloalkane EIPs to the corresponding profiles in the EIP reference collection also resulted in maximum

correlation with torch fuel. Maximum PPMC coefficients of 0.9977 at F_{Total} = 0.8 and 0.9973 at F_{Total} = 0.7 were observed for the alkane and cycloalkane EIP comparisons, respectively. The blind sample was, in fact, torch fuel and was evaporated to F_{Total} = 0.72.

For blind sample C, comparison to the TIC reference collection resulted in maximum correlation with the paint and varnish thinner (r = 0.9865) at F_{Total} = 0.6. For the comparisons to the EIP reference collection, maximum correlation was also observed for the paint and varnish thinner for the alkane EIP (r = 0.9827 at F_{Total} = 0.7), cycloalkane EIP (r = 0.9907 at F_{Total} = 0.6), and PNA EIP (r = 0.9821 at F_{Total} = 0.8). The paint and varnish thinner was the correct liquid identity, and the blind sample was evaporated to F_{Total} = 0.6. Through the comparisons to both reference collections, the identities and evaporation levels of blind samples A – C were properly identified.

5.2 Identification of Ignitable Liquids in Large-Scale Burn Samples

5.2.1 Comparison of Burn Sample A to TIC and EIP Reference Collections

The utility of the TIC and EIP reference collections was ultimately assessed by comparing the TICs and EIPs of large-scale burn samples to the corresponding predicted collections. Comparisons were first performed for burn sample A, which was collected from an area of flooring that was covered by furniture. Thus, flames had limited access to this area during the fire and the ignitable liquid used for the burn cell (*i.e.*, NH KleanStrip® paint thinner) did not extensively evaporate. As a result, the sample consisted primarily of unburned carpet. The resulting TIC contained minor substrate interferences, and the abundances of the ignitable liquid compounds were much greater than the substrate compounds (Figure 5.3A). Through mass spectral comparisons, compounds between approximately I^T = 850 – 1100 (*e.g.*, styrene, methylstyrene, and branched C_{11}) were determined to be associated with the substrate, whereas

compounds between approximately I^T = 1100 – 1500 (*e.g.*, C_{11} – C_{15}) were determined to be associated with the paint thinner.

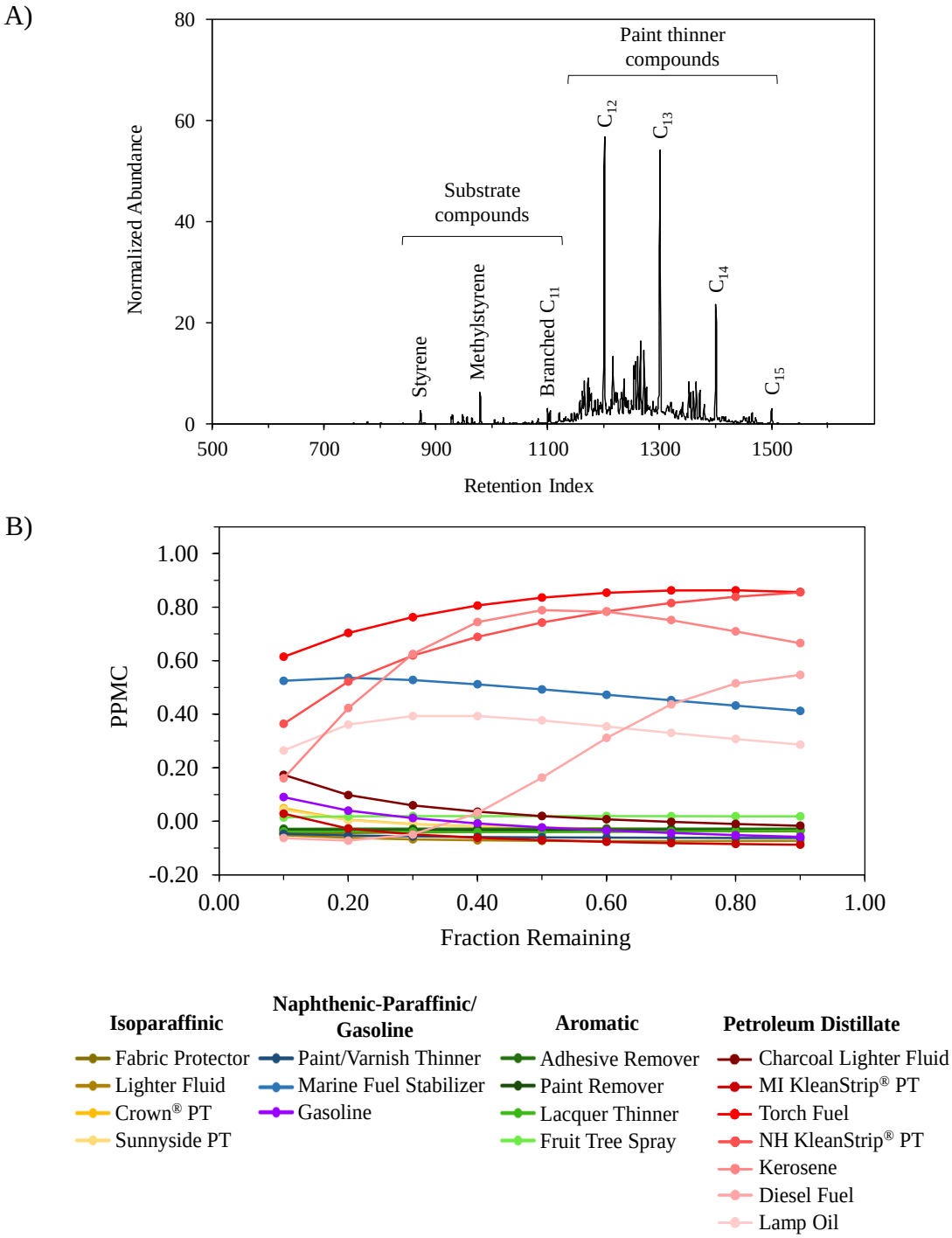

Figure 5.3 (A) TIC of burn sample A and (B) PPMC vs. F_{Total} plot for comparison of the TIC of burn sample A to the TIC reference collection

Comparison of the TIC from burn sample A to the TIC reference collection resulted in greatest correlation with the petroleum distillate liquids (Figure 5.3B). Maximum correlation was observed for comparisons to torch fuel, with a maximum PPMC coefficient of 0.8626 at F_{Total} = 0.8. However, maximum correlation with the NH KleanStrip® paint thinner (r = 0.8550) was only approximately 0.008 lower than the overall maximum PPMC coefficient. Weak to no correlation was observed for the majority of other liquids in the reference collection. Moderate correlation was observed for the marine fuel stabilizer (naphthenic-paraffinic), likely because this liquid contains similar normal alkanes when compared to the sample liquid. However, the associated correlation coefficient decreased as the F_{Total} at maximum PPMC was approached. The PPMC coefficients for the majority of the petroleum distillate liquids increased towards the F_{Total} at maximum PPMC, increasing confidence in identification of the petroleum distillate liquid.

Representative EIPs for burn sample A included the alkane and cycloalkane profiles (Figure 5.4). Compared to the sample TIC (Figure 5.3A), only the compounds associated with the ignitable liquid were present in both profiles. Normal alkanes were the dominant compounds in the alkane EIP (Figure 5.4A), whereas the cycloalkane EIP (Figure 5.4B) contained cyclic compounds as well as alkanes due to the *m/z* values used to generate the profile, discussed previously in Chapter 4.

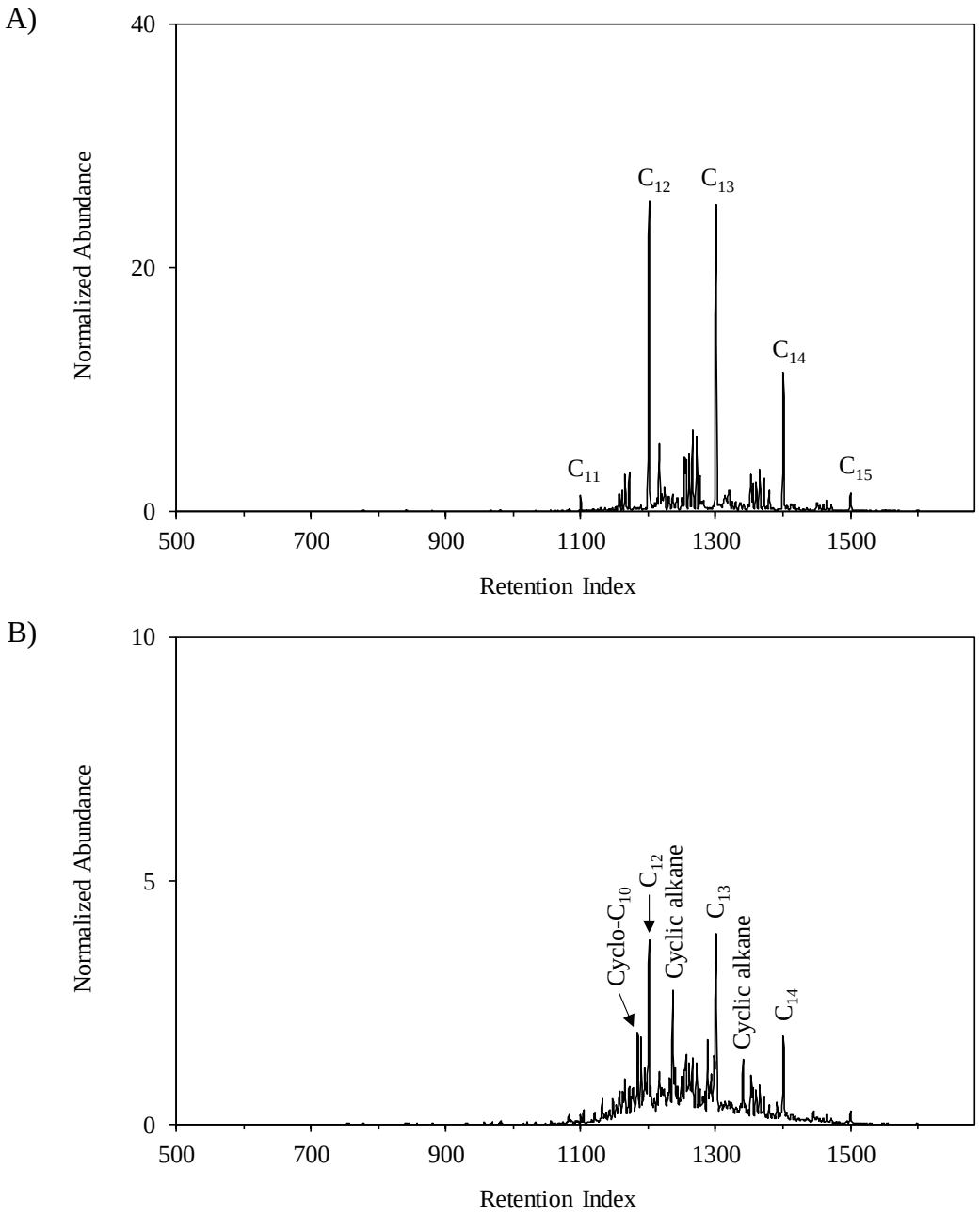

Figure 5.4 Extracted ion profiles for (A) the alkane class and (B) the cycloalkane class for burn sample A

Comparisons of the alkane and cycloalkane EIPs to the EIP reference collection resulted in strong correlation to petroleum distillate liquids (Figure 5.5). For the comparison to the predicted alkane EIPs, maximum correlation (r = 0.8745) was observed for comparison to the

predicted EIP for the same-source liquid (*i.e.*, NH KleanStrip® paint thinner) at F_{Total} = 0.9. The seemingly high F_{Total} level at maximum correlation was due to the area in which the burn sample was collected (*i.e.*, in an area of flooring covered by furniture). Irrespective of evaporation level, the greatest correlation was still observed for the petroleum distillate class, which aligns with the goal of fire debris analysis; that is, to identify the class of ignitable liquid present.

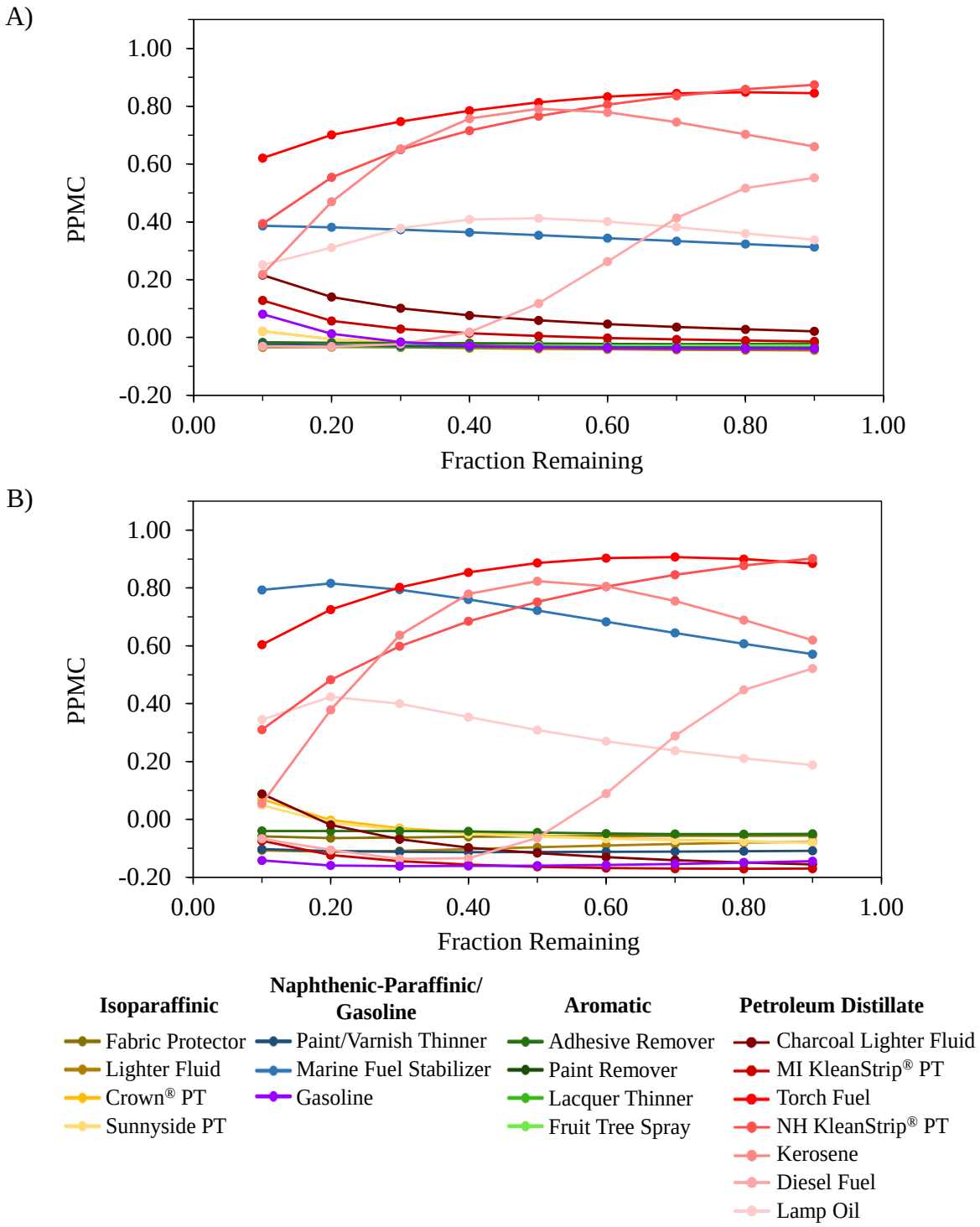

Figure 5.5 PPMC vs. F_{Total} plots for comparisons of the EIPs for burn sample A to (A) the predicted alkane EIPs and (B) the predicted cycloalkane EIPs in the reference collection

Upon comparison of the burn sample cycloalkane EIP to the corresponding predicted profiles, correlation was again strongest for the petroleum distillate liquids (Figure 5.5B). The maximum PPMC coefficient was 0.9069, which was observed for comparison to the predicted EIP for torch fuel at F_{Total} = 0.7. The maximum PPMC coefficient associated with the NH KleanStrip® paint thinner (*i.e.*, the same-source liquid) was 0.9018 at F_{Total} = 0.9, approximately 0.005 less than the overall maximum coefficient. The correlation coefficients for the marine fuel stabilizer were also higher for the cycloalkane comparison than for the alkane comparison, likely because cycloalkanes are the dominant compound class present in the liquid. However, the associated correlation decreased as F_{Total} approached that of maximum correlation.

The maximum PPMC coefficient for the cycloalkane comparison (r = 0.9069) was greater than the maximum coefficient for the alkane comparison (r = 0.8745) and for the TIC reference collection comparison (r = 0.8622). The cyclic compounds present at the corresponding retention indices in the cycloalkane EIP of burn sample A are more common among the liquids in the reference collection, whereas only four liquids contain all *n*-alkanes C_{11} – C_{15}. Regardless, the maximum PPMC coefficients were higher when using the EIP reference collection compared to the TIC reference collection, and using the alkane and cycloalkane EIP comparisons together increased confidence in identification of a heavy petroleum distillate liquid in burn sample A.

5.2.2 Comparison of Burn Sample B to TIC and EIP Reference Collections

A greater contribution of substrate interferences was observed in the TIC of burn sample B compared to burn sample A. Through mass spectral comparisons, compounds present such as styrene and estragole were determined to be associated with the substrate, among others present at low abundances. Despite the higher number of substrate contributions, compounds associated with the ignitable liquid (*i.e.*, gasoline) were still identified (Figure 5.6A). Evaporation of

gasoline was evident based on the absence of volatile compounds at low retention indices (I^T < 800). Compounds characteristic for gasoline identification were present at higher retention indices (I^T > 800).

Upon comparison of the TIC of burn sample B to the TIC reference collection, strong correlation was observed for gasoline, moderate correlation was observed for fruit tree spray, and weak to no correlation was observed for all other liquids (Figure 5.6B). The maximum PPMC coefficient was 0.8389, which was observed for comparison to the predicted TIC for gasoline at F_{Total} = 0.2. Correlation coefficients for gasoline increased as F_{Total} level decreased, which is consistent with evaporation levels observed for gasoline in a fire.[1] Moderate correlation was observed for comparison of burn sample B to fruit tree spray, with PPMC coefficients ranging from 0.6601 at F_{Total} = 0.9 to 0.7142 at F_{Total} = 0.1. This moderate correlation was likely due to the similarities of aromatic compounds present in the fruit tree spray and gasoline, mainly substituted benzenes at higher retention indices (I^T = 900 – 1100).

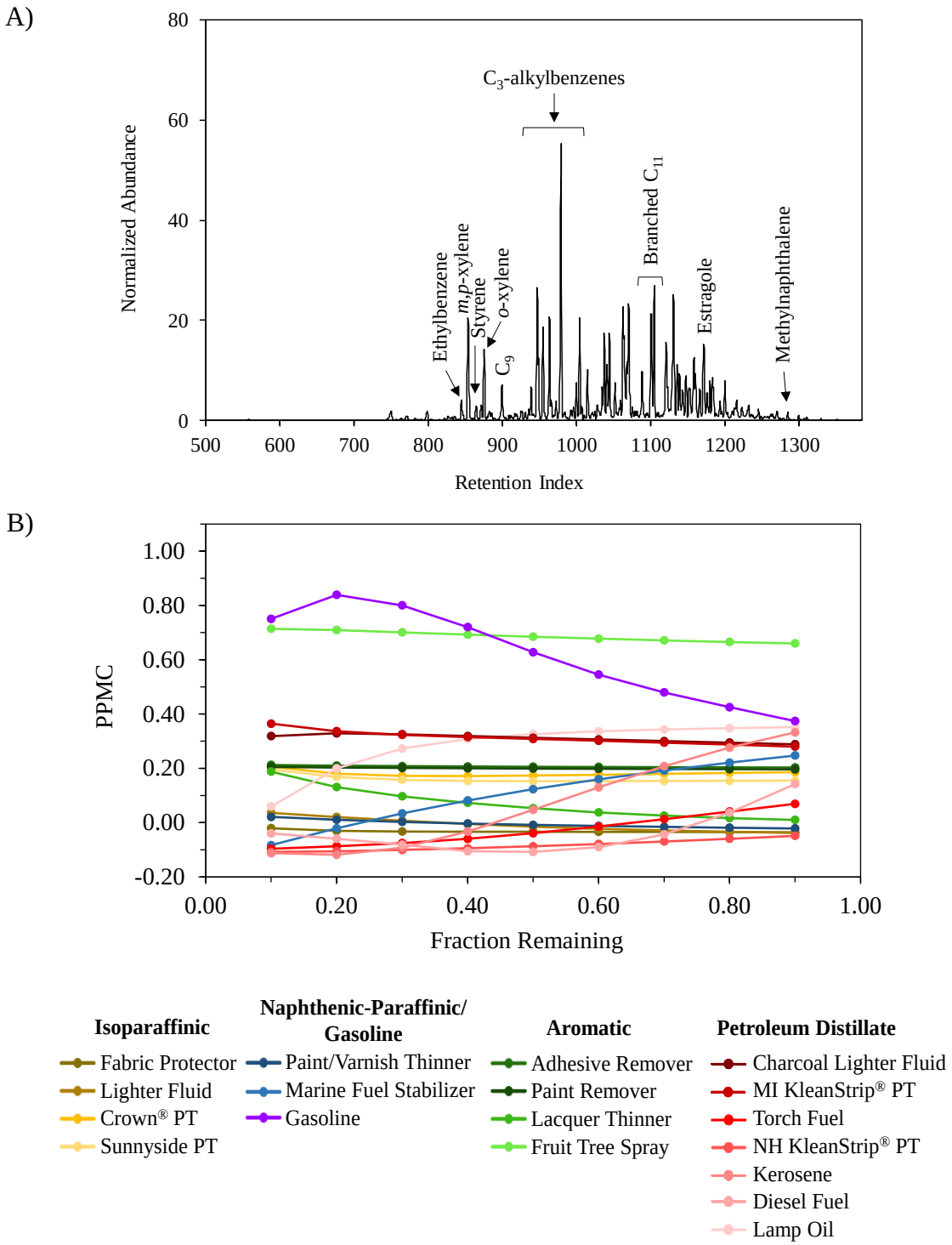

Figure 5.6 (A) TIC of burn sample B and (B) PPMC vs. F_{Total} plot for comparison of the TIC of burn sample B to the TIC reference collection

Extracted ion profiles for burn sample B were generated for the alkane, aromatic, indane, and PNA classes (Figure 5.7), which represent the major compound classes present in gasoline. For all four profiles, most compounds below I^T = 800 were not present, which was indicative of evaporation of the most volatile compounds in gasoline.

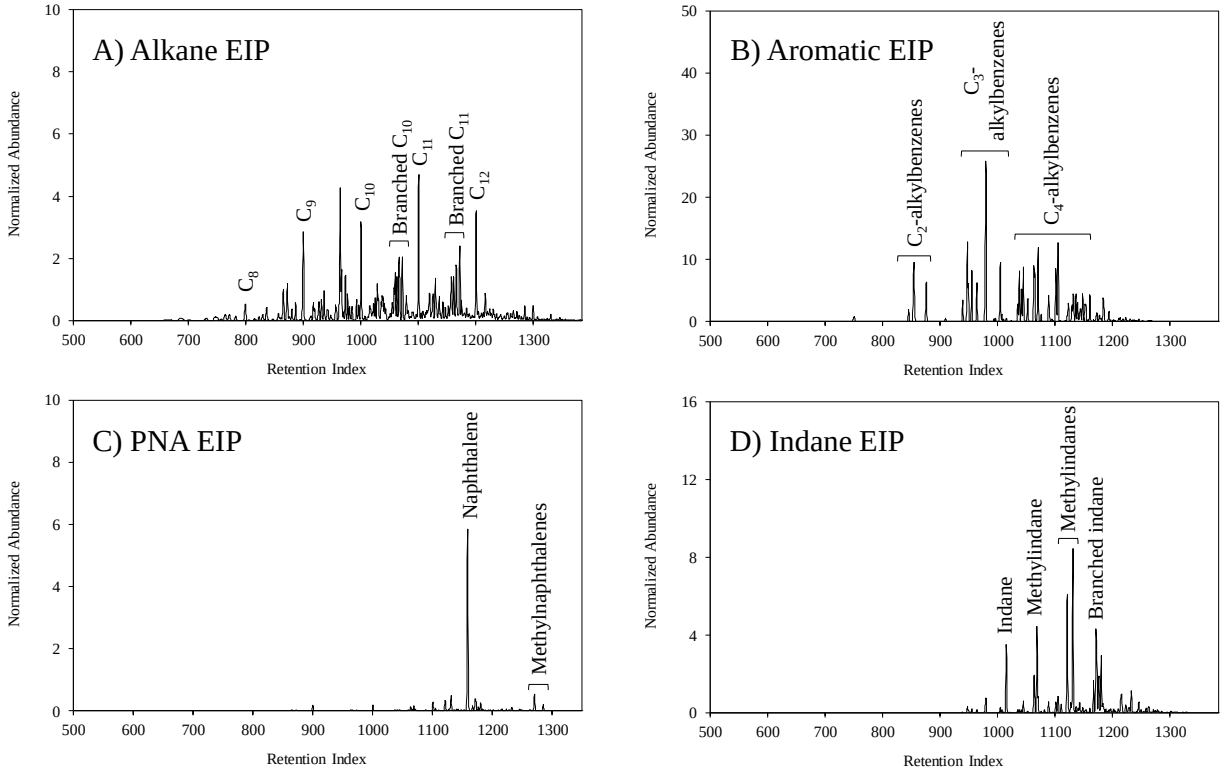

Figure 5.7 Extracted ion profiles for (A) the alkane class, (B) the aromatic class, (C) the polynuclear aromatic class, and (D) the indane class for burn sample B

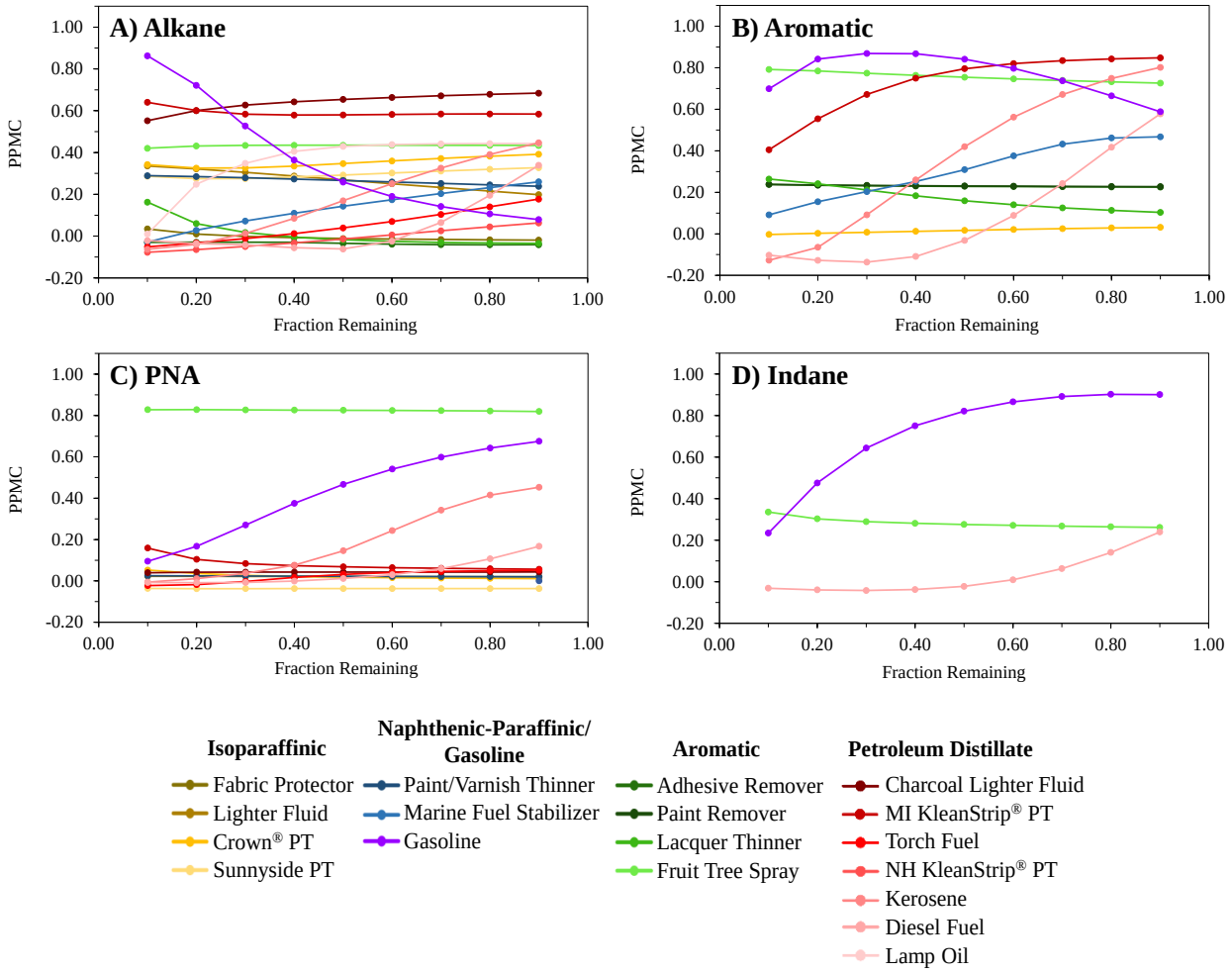

Figure 5.8 PPMC vs. F_{Total} plots for comparisons of the EIPs of burn sample B to (A) the predicted alkane EIPs, (B) the predicted aromatic EIPs, (C) the predicted PNA EIPs, and (D) the predicted indane EIPs in the reference collection

For comparison of the alkane EIPs, strongest correlation was observed for gasoline, and correlation ranged from moderate to none for all remaining liquids in the reference collection (Figure 5.8A). The maximum PPMC coefficient was 0.8629 and was associated with the predicted alkane EIP for gasoline at F_{Total} = 0.1. Correlation for gasoline steadily increased as F_{Total} decreased, which increased confidence in identification given that gasoline was likely present at low evaporation levels in the burn sample. Coefficients for the other liquids generally remained relatively constant across the nine F_{Total} levels.

The aromatic EIP for burn sample B contained compounds corresponding to the aromatic compounds that are characteristic of gasoline (Figure 5.7B), whereas identification of these compounds was difficult in the sample TIC (Figure 5.6A). For comparison to the EIP reference collection, correlation ranged from strong to none for all liquids (Figure 5.8B). The maximum PPMC coefficient (r = 0.8686) was observed for the comparison to the predicted aromatic EIP for gasoline corresponding to F_{Total} = 0.3. Maximum PPMC coefficients for three other liquids of different ASTM classes were close to the overall maximum value, with two indicating strong correlation and one indicating moderate correlation: MI KleanStrip® paint thinner (r = 0.8477 at F_{Total} = 0.9), kerosene (r = 0.8005 at F_{Total} = 0.9), and fruit tree spray (r = 0.7917 at F_{Total} = 0.1). Because the correlation coefficients for these liquids were close to the maximum value for gasoline, a visual comparison was performed to confirm that the predicted aromatic EIP for gasoline was the most similar to the sample aromatic EIP (Figure 5.9).

While the predicted aromatic EIPs for the four closest-correlating liquids all had compounds present at retention indices similar to those in the burn sample aromatic EIP, the gasoline predicted EIP was verified as the profile with the most similarities (Figure 5.9). The retention index range in the burn sample EIP was most similar to that in the gasoline EIP. A similar range was observed in the MI KleanStrip® paint thinner profile, which was reasonable given that the corresponding PPMC coefficient was only approximately 0.02 less than that for the gasoline comparison. The retention index ranges and compounds present in the predicted EIPs for kerosene and fruit tree spray were visually less similar than those in the gasoline EIP, which led to the lower PPMC coefficients for these comparisons. Additionally, the abundance ratios of compounds in the gasoline EIP were more similar to those in the sample EIP, thus

supporting the overall higher corresponding PPMC coefficient and increasing confidence in identification of gasoline for the aromatic class.

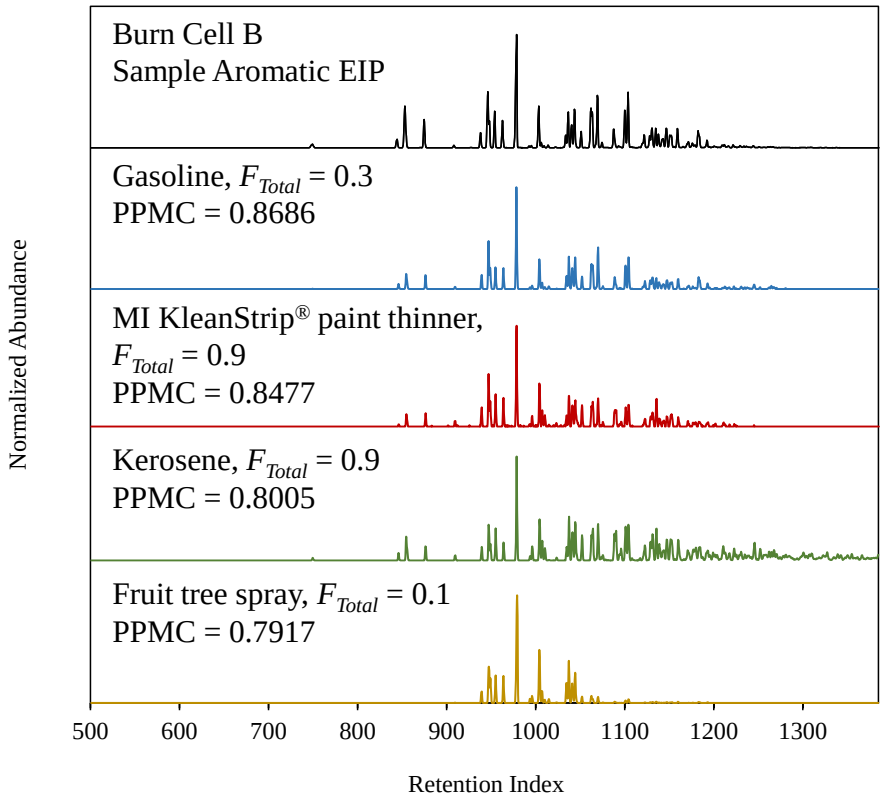

Figure 5.9 Aromatic EIP for burn sample B (black) and predicted aromatic EIPs for gasoline at F_{Total} = 0.3 (blue), MI KleanStrip® paint thinner at F_{Total} = 0.9 (red), kerosene at F_{Total} = 0.9 (green), and fruit tree spray at F_{Total} = 0.1 (yellow)

While the PNA EIP of burn sample B contained the fewest compounds, the associated compounds (naphthalene and the methylnaphthalenes) are important to gasoline identification (Figure 5.7C). Not all liquids in the reference collection contain PNA compounds; hence, the number of liquid comparisons for this EIP class was fewer than those for the alkane or aromatic classes (Figure 5.8C). The maximum PPMC coefficient for the burn sample PNA EIP comparison was 0.8283 and was associated with the predicted PNA EIP for fruit tree spray at

F_{Total} = 0.2. However, gasoline was the liquid with second highest correlation, with an associated maximum PPMC coefficient of 0.6751 at F_{Total} = 0.9. Because gasoline was the liquid of highest correlation in the alkane and aromatic EIP comparisons, a visual comparison was performed between the sample PNA EIP and predicted PNA EIPs for the fruit tree spray and gasoline at F_{Total} levels corresponding to maximum correlation (Figure 5.10).

While the maximum PPMC coefficient associated with the comparison to the PNA EIP for gasoline was lower than the coefficient for fruit tree spray comparison, the predicted profile for gasoline was more similar in terms of compounds present and exhibited higher correlation in the corresponding regions (Figure 5.10). Naphthalene (I^T = 1158) and 2-methylnaphthalene (I^T = 1270) were present in the EIPs for fruit tree spray and gasoline. An additional methylnaphthalene isomer (1-methylnaphthalene; I^T = 1284) was present in the gasoline EIP; both methylnaphthalenes are necessary for gasoline identification. Across retention indices I^T = 1100 – 1300, the PPMC coefficient for the comparison of the PNA EIP for burn sample B to the gasoline EIP (r = 0.8367) was greater than that for comparison to the fruit tree spray EIP (r = 0.8292). Similarly, across retention indices I^T = 1200 – 1300, the corresponding PPMC coefficient for gasoline (r = 0.9641) was even greater than that for fruit tree spray (r = 0.7999). The overall PPMC coefficient for the fruit tree spray comparison was higher than that for gasoline because of slight misalignments of low abundance peaks below I^T = 1280. Complete alignment of such peaks was not possible without causing misalignment of the peaks above I^T = 1280. However, the presence of both methylnaphthalene isomers in the EIP of the burn sample and the higher correlation with gasoline in the corresponding retention index region increased confidence in identification of gasoline.

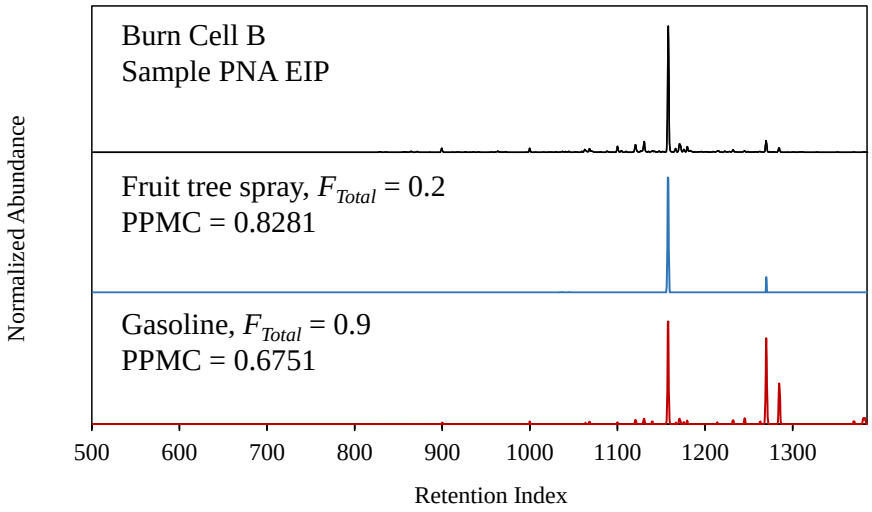

Figure 5.10 PNA EIP for burn sample B (black) and predicted PNA EIPs for fruit tree spray at F_{Total} = 0.2 (blue) and gasoline at F_{Total} = 0.9 (red)

For comparison to the predicted PNA EIPs for gasoline, the maximum PPMC coefficient was observed at a high F_{Total} level (F_{Total} = 0.9) (Figure 5.8C) compared to those expected in fire debris samples. While the methylnaphthalene isomers were present at a ratio commonly present in gasoline (2:1), naphthalene was present at a higher abundance than expected. Upon analysis of burn samples containing no ignitable liquid, it was determined that naphthalene was present as a pyrolysis product of the flooring substrates. In addition to the naphthalene present in the gasoline used as the ignitable liquid, the presence of the substrate interference led to an increased abundance of the compound. Thus, the burn sample EIP appeared to contain gasoline at a lower evaporation level than was actually present, and the abundance ratio of compounds were most similar to that in the gasoline predicted PNA EIP at F_{Total} = 0.9. However, investigation of the substrate interference and performance of the visual comparison led to a better understanding of the substrate interference and allowed for association with gasoline to be confirmed.

For the comparison of the indane EIP for burn sample B to the EIP reference collection, strongest correlation was observed for gasoline (Figure 5.8D). While only three liquids in the

reference collection contained indane compounds, the corresponding EIP for the burn sample was important for liquid identification due to the high abundances of compounds present (Figure 5.7D). The maximum PPMC coefficient was 0.9021, which was observed for comparison to the predicted indane EIP for gasoline corresponding to F_{Total} = 0.8. The maximum coefficient was one of the highest across all EIP class comparisons for burn sample B. Because the correlation coefficients associated with the predicted indane EIPs for fruit tree spray and diesel fuel were all less than 0.4, definitive correlation to gasoline was evident for this profile class (Figure 5.8D).

The F_{Total} at maximum PPMC for the indane EIP comparison was unexpectedly high (F_{Total} = 0.8) for a burn sample in which gasoline was present. For general comparisons to the predicted EIPs in the reference collection, results are expected to follow thermodynamic behavior. For profiles with largely involatile compounds, such as the burn sample indane EIP, the compounds remaining in the profile preconcentrate as other volatile compounds evaporate. Thus, for comparisons to the predicted profiles for the same-source liquid, the associated PPMC coefficients would be expected to be highest at low F_{Total} levels and decrease as F_{Total} increases. The comparison of the burn sample indane EIP to the gasoline predicted indane EIPs resulted in a trend opposite of that expected for thermodynamically-consistent behavior, in which the highest PPMC coefficient was associated with the highest F_{Total} level. Future work to investigate the cause of this opposite trend is necessary; however, the strong correlation to the same-source liquid still demonstrated the benefit of performing EIP comparisons for a complex burn sample.

Using the comparisons from all four EIP classes for burn sample B, identification of gasoline was achieved. Gasoline was associated with maximum correlation in three out of the four class comparisons. While the maximum PPMC coefficient for the PNA EIP comparison was associated with a different liquid, correlation was greater for gasoline for regions in which

relevant peaks were present. When comparing the burn sample profiles to the EIP reference collection, the corresponding maximum coefficients were greater than the maximum PPMC coefficient for the comparison to the TIC reference collection (r = 0.8389). The greater correlation achieved through the use of the EIP reference collection allowed for increased confidence in identification of the ignitable liquid present in a burn sample with moderate substrate interferences.

5.2.3 Comparison of Burn Sample C to TIC and EIP Reference Collections

The TIC for burn sample C contained the greatest contributions from substrate interferences and evaporation (Figure 5.11A) compared to burn samples B and A. The area in the burn cell from which this debris sample was collected suffered significant damage from the fire, and the carpet covering the wood subfloor was completely burned. The dominant compounds identified in the TIC of burn sample C were (1R)-2,6,6-trimethylbicyclo[3.1.1]hept-2-ene and β-pinene, neither of which was characteristic of the ignitable liquid in the sample (*i.e.*, gasoline). Through comparison of the TIC of the burn sample to the TIC of unburned wood subfloor (Figure 5.11B), the majority of peaks in the burn sample were attributed to the substrate. Nonetheless, alkylbenzenes and other aromatics that are characteristic of gasoline were present, albeit at relatively low abundances (Figure 5.11A).

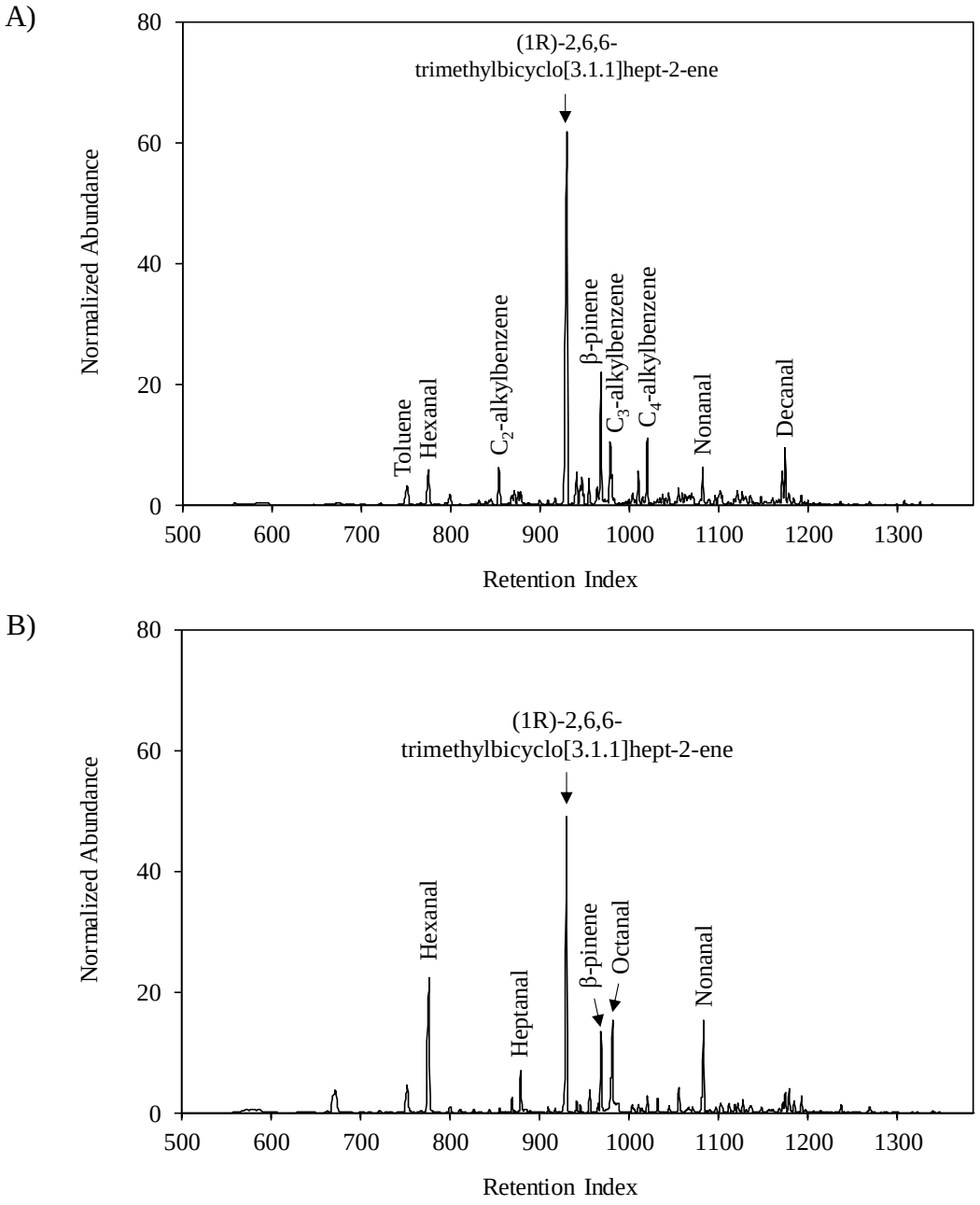

Figure 5.11 TICs of (A) burn sample C and (B) unburned wood subfloor

The TIC of burn sample C was compared to the predicted TICs in the reference collection; however, identification of ASTM ignitable liquid class was not possible because correlation to all liquids was weak, with PPMC coefficients less than 0.2 (Figure 5.12). The maximum PPMC coefficient was 0.1382, which was observed for comparison to the predicted

TIC of the fruit tree spray corresponding to F_{Total} = 0.3. For comparison, the maximum PPMC coefficient observed among the predicted TICs for gasoline was 0.1342 at F_{Total} = 0.3. Because the burn sample TIC contained major substrate interferences, low correlation coefficients were expected.

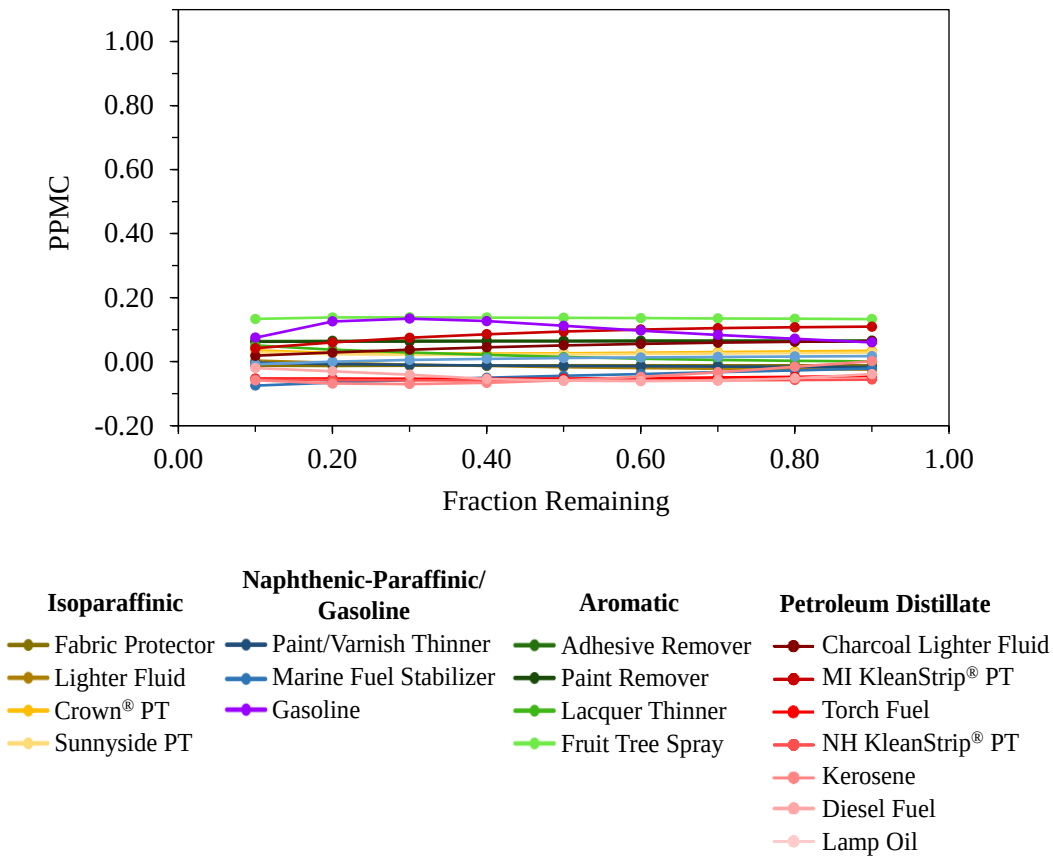

Figure 5.12 PPMC vs. F_{Total} plot for comparison of TIC of burn sample C to the TIC reference collection

Representative EIPs for burn sample C were generated for the alkane, aromatic, and indane classes (Figure 5.13), which are consistent with the majority of representative compound classes in gasoline. Evaporation of gasoline was evident by the absence of compounds below I^T = 800 in most EIPs. Compounds below I^T = 800 in the alkane EIP were associated with the substrate.

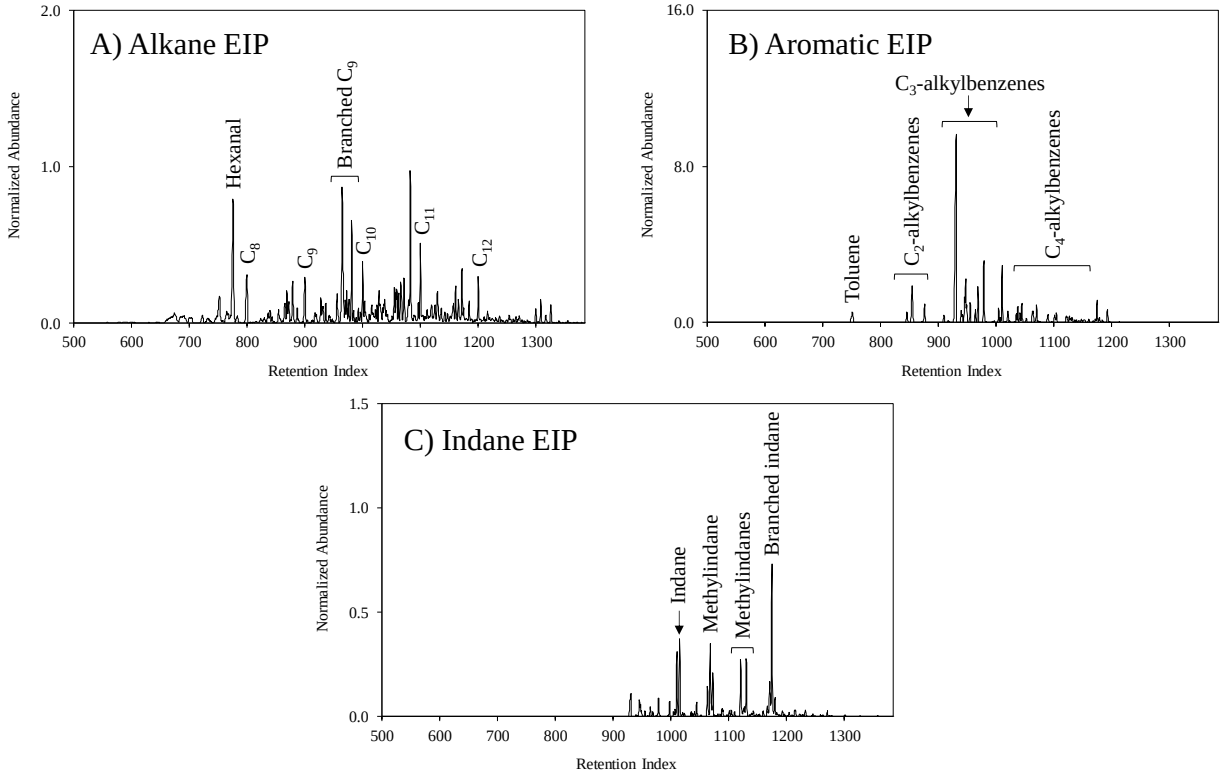

Figure 5.13 Extracted ion profiles for (A) the alkane class, (B) the aromatic class, and (C) the indane class for burn sample C

Upon comparison of the alkane EIP for burn sample C to the predicted alkane EIPs, moderate correlation was observed for gasoline, and weak to no correlation was observed for all other liquids (Figure 5.14A). Low PPMC coefficients were expected given the extent of substrate interferences present in this sample. Nevertheless, the maximum PPMC coefficient of 0.5336 was observed for comparison to the predicted alkane EIP for gasoline corresponding to F_{Total} = 0.1. Weak to no correlation was observed for all other liquids, with PPMC coefficients less than 0.4. Similar to the alkane EIP comparison for burn sample B, correlation with gasoline increased as F_{Total} decreased. The PPMC coefficients associated with the predicted alkane EIPs for gasoline at the two lowest F_{Total} levels (*i.e.*, F_{Total} = 0.1 and 0.2) were greater than the coefficients for all other liquids. No major changes in correlation were observed as a function of evaporation

for the remaining liquids, and the majority of liquids exhibited relatively constant correlation across the F_{Total} range.

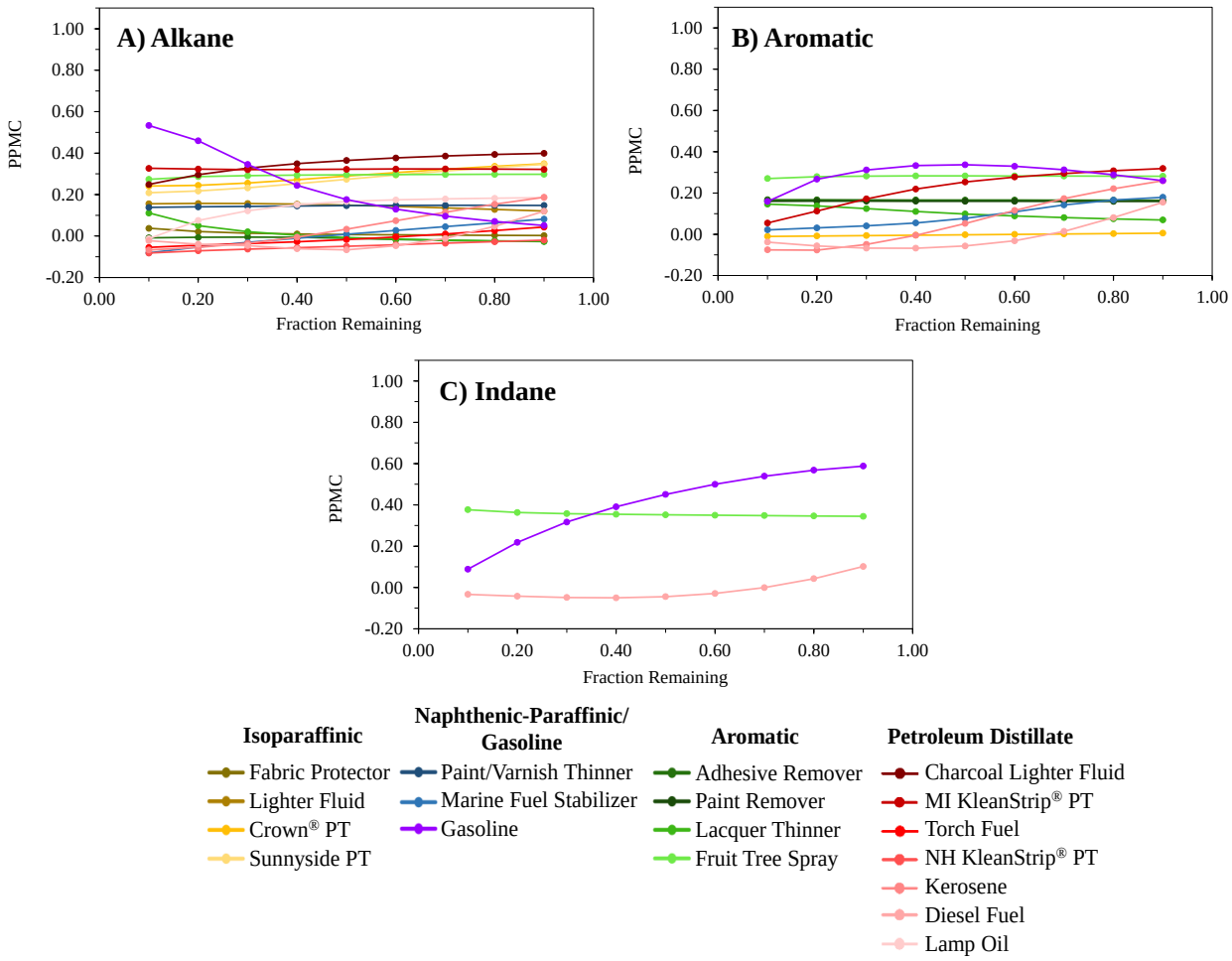

Figure 5.14 PPMC vs. F_{Total} plots for comparisons of EIPs of burn sample C to (A) the alkane EIPs, (B) the aromatic EIPs, and (C) the indane EIPs in the reference collection

Comparison of the aromatic EIP for burn sample C to the predicted aromatic EIPs resulted in weak to no correlation for all liquids in the reference collection (Figure 5.14B). Despite the overall lower correlation, maximum correlation was still observed for the predicted aromatic EIPs for gasoline, with an associated maximum PPMC coefficient of 0.3370 at F_{Total} = 0.5. However, maximum correlation coefficients associated with the MI KleanStrip® paint

thinner (r = 0.3186 at F_{Total} = 0.9) and fruit tree spray (r = 0.2829 at F_{Total} = 0.5) were close to the overall maximum value. Thus, a visual comparison was performed to verify that the liquid of highest correlation was gasoline (Figure 5.15).

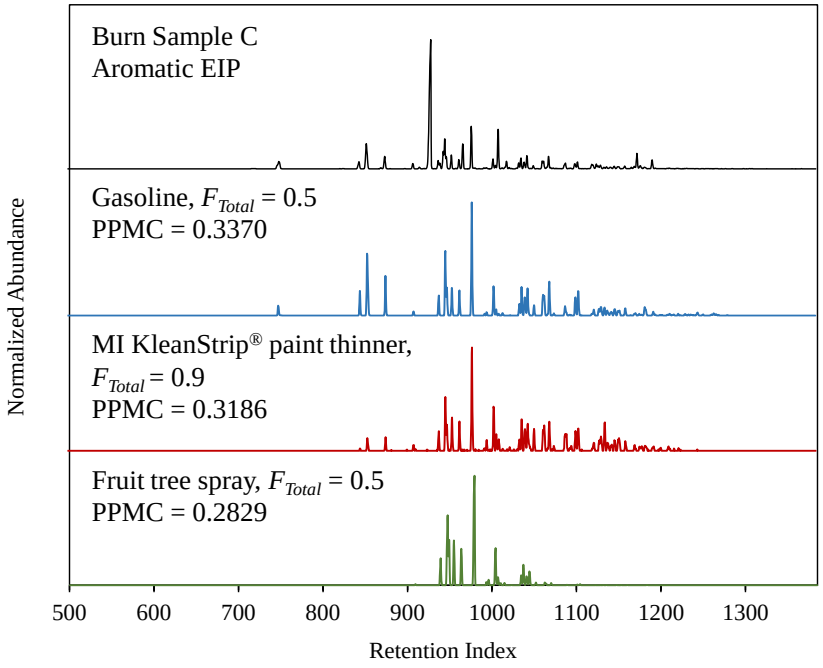

Figure 5.15 Aromatic EIP for burn sample C (black) and predicted aromatic EIPs for gasoline at F_{Total} = 0.5 (blue), MI KleanStrip® paint thinner at F_{Total} = 0.9 (red), and fruit tree spray at F_{Total} = 0.5 (green)

The predicted aromatic EIP for gasoline was confirmed to have the most similarities with the aromatic EIP for burn sample C (Figure 5.15). The retention index ranges were most similar for both profiles, and the C_2-, C_3-, and C_4-alkylbenzenes, as well as toluene, were all present at similar abundance ratios. While some alkylbenzenes were present in the predicted aromatic EIPs for the MI KleanStrip® paint thinner and fruit tree spray, not all were present across the entire retention index range of the sample EIP, which led to decreased correlation. The compounds at I^T = 929 in the burn sample EIP was identified as a substituted cycloalkane through mass spectral comparison. This compound was attributed to the substrate and was the reason for overall lower

correlation for the comparisons of this profile class. For example, across the retention index range I^T = 936 – 1385 (omitting substrate peak), the PPMC coefficients for the three highest-correlating liquids were as follows: 0.7202 (gasoline), 0.7160 (MI KleanStrip® paint thinner), and 0.6569 (fruit tree spray). Regardless, gasoline was the liquid associated with maximum correlation and was confirmed as such through the visual comparison.

For the comparison of the indane EIP of burn sample C to the corresponding predicted EIPs, correlation coefficients were highest for gasoline (Figure 5.14C). The maximum PPMC coefficient was 0.5880, which was observed for comparison to the predicted indane EIP for gasoline corresponding to F_{Total} = 0.9 and which indicated moderate correlation. Weak correlation was observed for the predicted EIPs of fruit tree spray and diesel fuel, increasing confidence in gasoline identification. Similar to the indane EIP comparison for burn sample B, the maximum PPMC coefficient for comparison to the gasoline predicted EIPs was associated with a high F_{Total} level, and the coefficients decreased as F_{Total} decreased. While future work is necessary to determining the cause of this phenomenon for the indane EIP comparisons, association with gasoline was still demonstrated.

The ignitable liquid present in burn sample C was identified as gasoline based on comparisons for all sample EIPs together. Maximum correlation was observed for gasoline for all profile comparisons based on similarities of retention index ranges and compounds present with the corresponding profiles for the burn sample. Substrate interferences were minimized using EIPs, and higher PPMC coefficients were observed for all comparisons to the EIP reference collection relative to the TIC reference collection comparison (r = 0.1382). While the PPMC coefficients associated with the EIP comparisons indicated moderate correlation at best, use of the correlation plots for each comparison provided an objective method for the analysis of

this fire debris sample. Thus, the EIP reference collection was demonstrated to be a useful tool to aid in the identification of an ignitable liquid present in a burn sample with major substrate interferences and liquid evaporation.

5.3 Summary

The identification of ignitable liquids and corresponding ASTM classes in single-blind samples was successful using the TIC and EIP predicted reference collections. The correct liquid and liquid class were identified for each sample as well as the corresponding F_{Total} level. Using the TIC reference collection, maximum coefficients as high as 0.9979 were observed for the same-source liquid. Using the EIP reference collection, corresponding PPMC coefficients as high as 0.9977 were observed. Thus, increased confidence in identification was achieved using both reference collections.

The broader application of the model and reference collections was further demonstrated through the identification of liquid class present in large-scale burn samples with varying degrees of substrate interferences. Associated comparisons to the EIP reference collection resulted in higher correlation coefficients relative to the TIC reference collection comparisons. For almost all comparisons, maximum correlation was with the same-source liquid or liquid class. Of the comparisons to the EIP reference collection, a few cases occurred for which correlation coefficients associated with liquids of other classes were close to the overall maximum coefficient. For such cases, visual comparisons performed as supplements to the statistical comparisons allowed for confirmation of the maximum correlation associated with the same-source liquid. Overall, the success of the reference collections when applied to large-scale burn samples demonstrated the practical application of the kinetic model for samples most similar to those analyzed in forensic laboratories.

APPENDIX

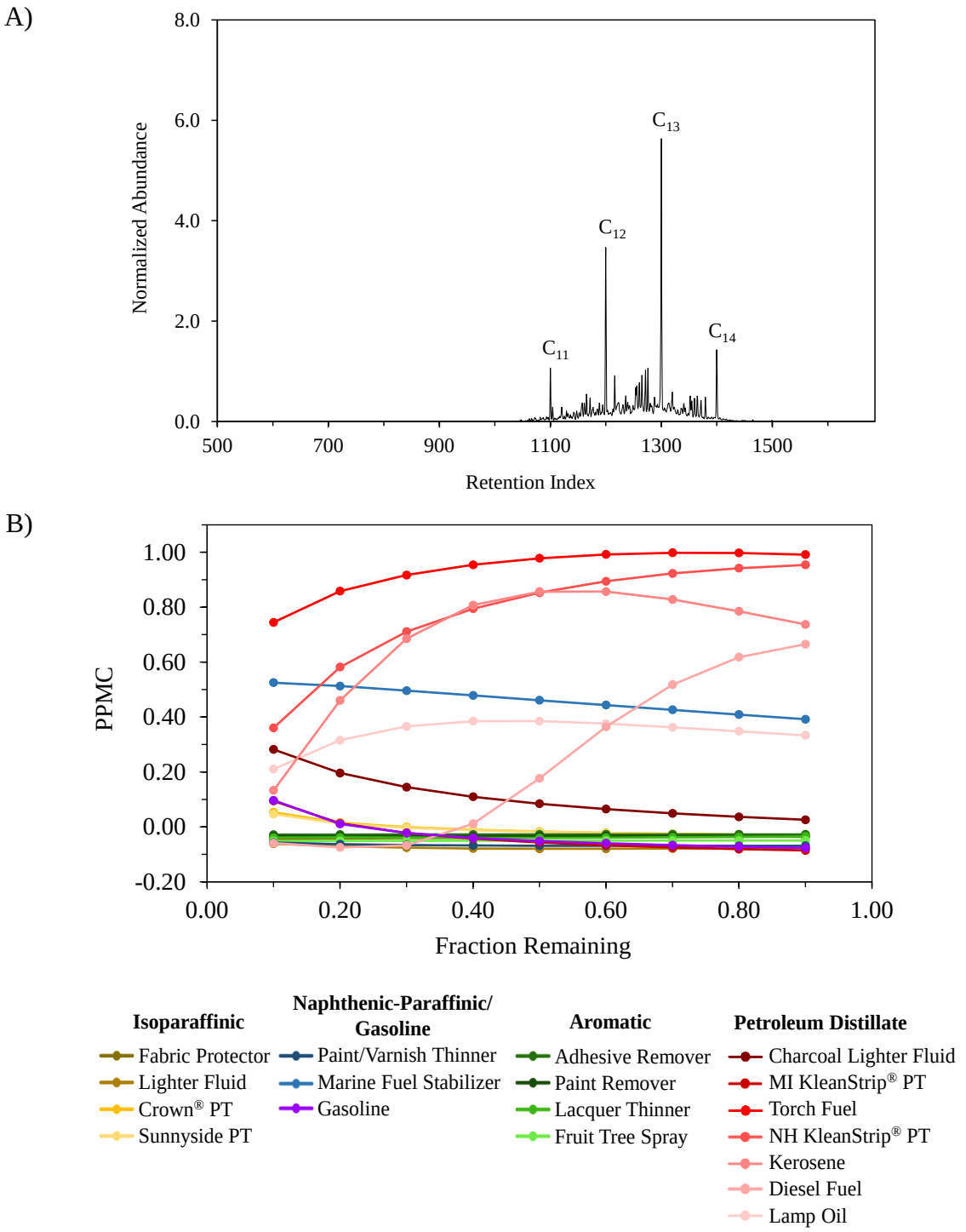

Figure A.17 (A) TIC of single-blind sample B and (B) PPMC vs. F_{Total} plot for comparison of the TIC of blind sample B to the TIC reference collection

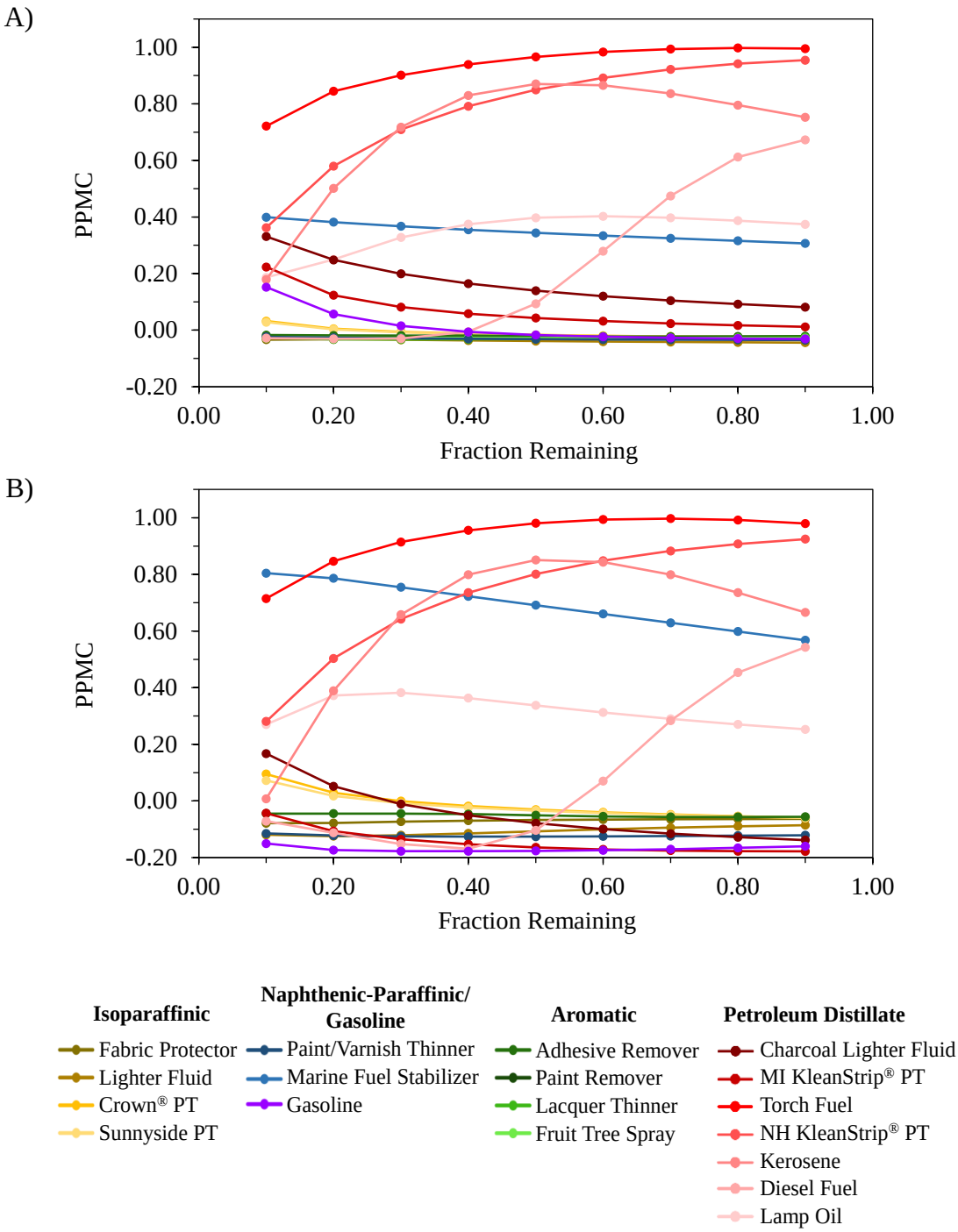

Figure A.18 PPMC vs. F_{Total} plots for comparisons of EIPs of blind sample B to (A) the predicted alkane EIPs and (B) the predicted cycloalkane EIPs in the reference collection

Table A.13 Maximum PPMC coefficients and corresponding liquids, F_{Total} at maximum PPMC, and experimental F_{Total} level for comparisons of the TIC and EIPs for blind sample B to the TIC and EIP reference collections

Blind Sample	Max PPMC	Liquid at Max PPMC	F_{Total} at Max PPMC	Experimental F_{Total}
Blind Sample B: **TIC**	0.9979	Torch fuel	0.7	0.72
Blind Sample B: **Alkane EIP**	0.9977	Torch fuel	0.8	
Blind Sample B: **Cycloalkane EIP**	0.9973	Torch fuel	0.7	

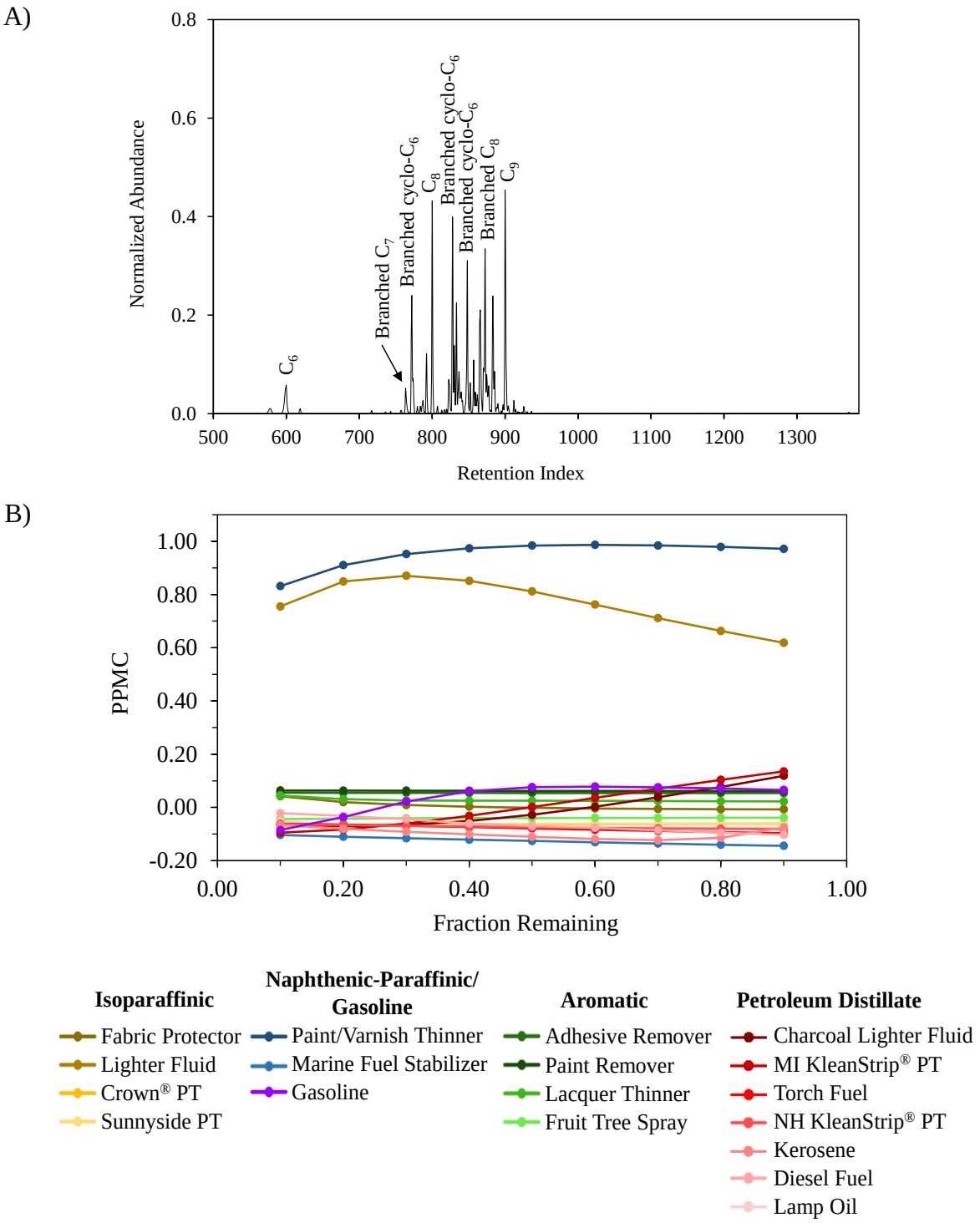

Figure A.19 (A) TIC of single-blind sample C and (B) PPMC vs. F_{Total} plot for comparison of the TIC of blind sample C to the TIC reference collection

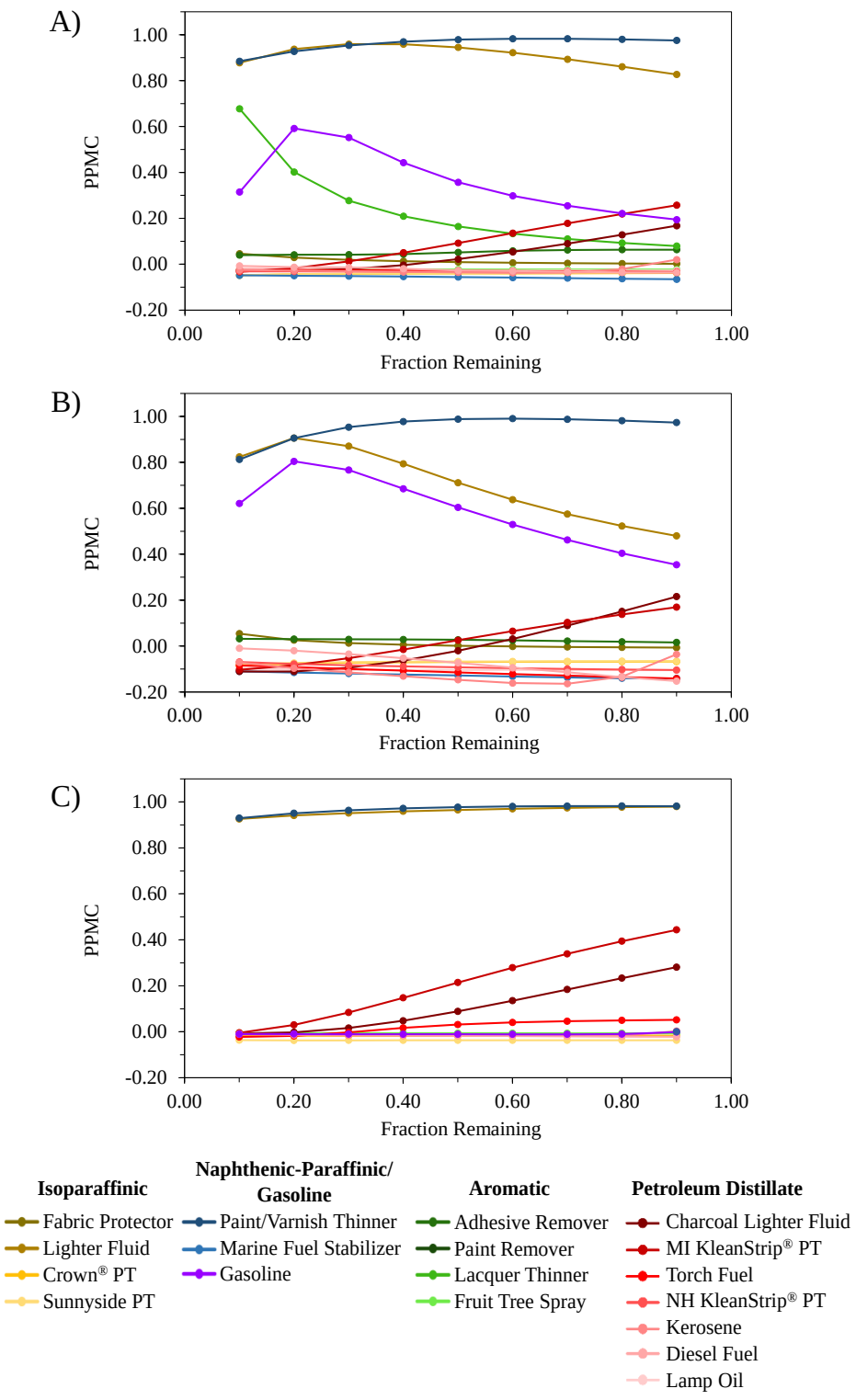

Figure A.20 PPMC vs. F_{Total} plots for comparisons of EIPs of blind sample C to (A) the predicted alkane EIPs, (B) the predicted cycloalkane EIPs, and (C) the predicted PNA EIPs in the reference collection

Table A.14 Maximum PPMC coefficients and corresponding liquids, F_{Total} at maximum PPMC, and experimental F_{Total} level for comparisons of the TIC and EIPs for blind sample C to the TIC and EIP reference collections

Blind Sample	Max PPMC	Liquid at Max PPMC	F_{Total} at Max PPMC	Experimental F_{Total}
Blind Sample C: **TIC**	0.9865	Paint and varnish thinner	0.6	0.6
Blind Sample C: **Alkane EIP**	0.9827	Paint and varnish thinner	0.7	
Blind Sample C: **Cycloalkane EIP**	0.9907	Paint and varnish thinner	0.6	
Blind Sample C: **PNA EIP**	0.9821	Paint and varnish thinner	0.8	

REFERENCES

REFERENCES

1. H.L. Birks, A.R. Cochran, T.J. Williams and G.P. Jackson, The Surprising Effect of Temperature on the Weathering of Gasoline, Forensic Chem. 4 (2017) 32-40.

VI. Conclusions and Future Work

6.1 Conclusions

Identification of ignitable liquids in fire debris samples is currently achieved by comparing the total ion chromatograms (TICs) and extracted ion profiles (EIPs) of samples to reference collections containing TICs and EIPs of evaporated liquids. However, the process of generating such collections has been proved to be time- and resource-intensive. The kinetic model developed by McIlroy *et al.* can be used to generate predicted TICs using only the chromatogram of unevaporated liquids.[1, 2] This alleviates the need to perform experimental evaporations of such liquids and does not require the identities of compounds within each liquid to be known. Good predictive accuracy of the model was demonstrated for petroleum distillates, and subsequent work improved the prediction accuracy of the model for application to gasoline through modifications to instrument parameters and prediction methods.[1-3]

The first part of this work focused on expanding the application of the kinetic model to predict the TICs and EIPs of ignitable liquids of other ASTM classes, specifically those of the isoparaffinic, naphthenic-paraffinic, and aromatic classes. For such liquids, the model accurately predicted the corresponding TICs at three F_{Total} levels (F_{Total} = 0.5, 0.3, and 0.1), with observed PPMC coefficients as high as 0.995. For application to EIPs, good predictive accuracy was demonstrated when predicting profiles of representative compound classes for each of the liquids studied. Correlation coefficients as high as 0.9984 were observed across all profiles and evaporation levels. These results demonstrated that the model could be applied to predict EIPs at any given evaporation level with acceptable predictive accuracy.

Reference collections were successfully generated containing predicted TICs and EIPs of eighteen liquids across five ASTM classes (*i.e.*, isoparaffinic, naphthenic-paraffinic, aromatic, petroleum distillate, and gasoline). For each liquid, the corresponding predicted TICs and EIPs

were generated for nine evaporation levels. Model validation was performed by comparing the experimental TICs and EIPs of the evaporated liquids to the corresponding collections. For all comparisons, the maximum PPMC coefficients were associated with the same-source liquid or a liquid of the same class. Through the use of both collections, the correct ASTM class was identified for each comparison. Using the EIP reference collection, the comparisons for all relevant profiles for a given liquid together increased confidence in identification of the liquid class, with PPMC coefficients generally greater than those for the comparisons to the TIC reference collection. Through the comparisons to the reference collections, validation of the kinetic model to accurately generate predicted TICs and EIPs for use in identifying ignitable liquid class was achieved.

The second part of this work focused on the practical application of the model through comparisons of TICs and EIPs of blind samples to the predicted reference collections for the purpose of ignitable liquid identification. Three blind samples were prepared and analyzed; upon comparing the corresponding TICs and EIPs to the reference collections, the correct ignitable liquid and liquid class were identified, as well as the corresponding F_{Total} level. Across all comparisons to both collections, PPMC coefficients as high as 0.9979 were observed. Additionally, for comparisons to the EIP reference collection, using the results from all relevant profiles for a given sample resulted in increased confidence in identification of the liquid class.

The practical application of the model was ultimately demonstrated through the comparison of TICs and EIPs of large-scale burn samples to the corresponding reference collections to aid in identifying the liquid class present. Given that these samples were collected from large-scale burns, they most closely resembled those submitted to forensic laboratories for analysis. For each of the burns, the ignitable liquids used (*i.e.*, paint thinner and gasoline) are

ignitable liquids commonly found in debris samples from intentional fires. The samples also had varying degrees of substrate interferences. For the samples with minor and moderate substrate interferences, maximum correlation with the same-source liquid class was observed for comparisons to the TIC reference collection; PPMC coefficients as high as 0.8622 were observed. Identification of liquid class was not possible for the TIC comparison of the sample with major substrate interferences, which was reasonable given the extent of interferences present.

For all burn samples, EIPs proved effective in minimizing substrate interferences. Comparisons of the relevant profiles to the EIP reference collection resulted in increased correlation relative to the corresponding comparisons to the TIC reference collection. For the majority of EIP comparisons, maximum correlation was observed for the predicted profiles for the same-source liquid or the same liquid class, with observed PPMC coefficients as high as 0.9069. Visual comparisons were performed for cases in which correlation of other ASTM class liquids was close to that of maximum correlation; in such cases, the predicted profiles for the same source-liquid were confirmed as having the greatest correlation to the sample profiles. For each burn sample, the EIP comparisons for all relevant profiles increased confidence in identification of the correct liquid class present. For samples with major substrate interferences, the EIP reference collection was especially useful for the liquid class identification. While the PPMC coefficients were lower overall for these samples because of the extent of substrate interferences, the correlation plots for each comparison demonstrated an objective analysis method for fire debris samples. Through the analysis of the large-scale burn samples, the practical application of the model was demonstrated for the generation of predicted reference collections to be used as tools in fire debris analysis.

6.2 Future Work

Given that in-house reference collections generated at forensic laboratories are unlikely to contain ignitable liquids of all brands and manufacturers, it is possible that a liquid present in a fire debris sample could be of a different identity and/or ASTM class than those in the collections. Thus, the utility of the predicted reference collections generated in this work to aid in the identification of liquids present in samples of such nature could be assessed in future work. Specifically, blind samples that contain liquids of the same ASTM class but not the same identities as any of those in the reference collections could be prepared and analyzed. Similar preparations could be conducted for blind samples that contain liquids of different identities and ASTM classes than those in the collections. Through comparison of the corresponding TICs and EIPs to the reference collections, the maximum correlation should be associated with the same ASTM liquid class or the liquid class most similar to that of the sample liquid. Upon testing this hypothesis, the broader application of the predicted reference collections would be assessed.

The burn samples used in this work were all from burns conducted under similar conditions; because the samples were collected from the floors of the burn cells, the substrate interferences corresponding to carpet or wood subfloor were similar in each sample TIC. Thus, different burn samples could be collected that are prepared on substrates other than those used in this work. For example, ignitable liquids could be spiked onto substrates such as laminate or cardboard, which produce different substrate interferences. Additionally, because only two ignitable liquids were used for the large-scale burns in this work, ignitable liquids, or combination of liquids, of other identities or ASTM classes could be used to increase the complexity of such samples.

Refinements to the kinetic model are also necessary to incorporate additional aspects of fires and predict TICs and EIPs with even greater accuracy than demonstrated in this work. First,

the retention index range used initially for model development needs to be expanded to incorporate compounds with retention indices below I^T = 800. This refinement would allow for more accurate predictions of evaporation for liquids in which these volatile compounds are present. Secondly, the temperatures of a fire can exceed 1000 °C, and as demonstrated by Birks *et al.*, temperature has a direct effect on evaporation and the distribution of compounds present in ignitable liquids at different temperatures.[4, 5] To incorporate temperature in the kinetic model developed by McIlroy *et al.*, a variable temperature model was developed using petroleum distillates.[6] While the model performed well for predicting chromatograms at various temperatures and F_{Total} levels, only a narrow range of temperatures was considered in model development (*i.e.*, 5 – 35 °C). Thus, the performance of the variable temperature model needs to be evaluated at elevated temperatures more likely to be encountered in a fire. To assess predictive accuracy of the model for such applications, evaporations can be conducted at elevated temperatures, and the experimental chromatograms can be compared to the corresponding predicted chromatograms generated using the refined model. Similar comparisons conducted in this work involving blind samples and burn samples can be performed using the refined model to further assess model performance and predictive accuracy.

While future work is necessary to improve the kinetic model, the results presented in this work demonstrate the utility of the model to generate predicted reference collections to be used during identifications of ignitable liquids. Specifically, the predictive accuracy demonstrated for EIPs is especially applicable for fire debris samples with substrate interferences, highlighted through the use of large-scale burn samples. Overall, the work presented here shows great promise in advancing the field of forensic fire debris analysis and providing forensic laboratories with a tool that can be used to generate reference collections in a time- and cost-efficient manner.

REFERENCES

REFERENCES

1. J.W. McIlroy, A.D. Jones and V.L. McGuffin, Gas Chromatographic Retention Index as a Basis for Predicting Evaporation Rates of Complex Mixtures, Anal. Chim. Acta 852 (2014) 257-266.

2. R. Waddell Smith, R.J. Brehe, J.W. McIlroy and V.L. McGuffin, Mathematically Modeling Chromatograms of Evaporated Ignitable Liquids for Fire Debris Applications, Forensic Chem. 2 (2016) 37-45.

3. N.K. Eklund, B.A. Capistran, V.L. McGuffin and R. Waddell Smith, Improvements in a Kinetic-Based Model to Predict Evaporation of Gasoline, Forensic Chemistry 17 (2020) 100194.

4. H.L. Birks, A.R. Cochran, T.J. Williams and G.P. Jackson, The Surprising Effect of Temperature on the Weathering of Gasoline, Forensic Chem. 4 (2017) 32-40.

5. I.C. Willis, Z. Fan, J.T. Davidson and G.P. Jackson, Weathering of Ignitable Liquids at Elevated Temperatures: A Thermodynamic Model, Based on Laws of Ideal Solutions, to Predict Weathering in Structure Fires, Forensic Chem. 18 (2020) 100215.

6. J. McIlroy, R. Waddell Smith and V. McGuffin, Fixed- and Variable-Temperature Kinetic Models to Predict Evaporation of Petroleum Distillates for Fire Debris Applications, Separations 5 (2018) 47.